PRESCIENCE: A DATASET AND BENCHMARK FOR SCIENTIFIC FORECASTING

Anonymous authors
Paper under double-blind review

ABSTRACT

Can AI systems trained on the existing scientific record forecast the advances that will follow? We introduce PRESCIENCE, a renewable dataset and benchmark for scientific forecasting built around 147K recent research papers from multiple domains, together with companion papers covering author publication histories and citation links, yielding 1.06M papers in total. The resulting paper records include titles, abstracts, disambiguated author identities, influential references, topic labels, citation trajectories, and metadata snapshotted to respect temporal cutoffs. We instantiate seven exemplar tasks: five **paper-anchored** tasks—*contribution generation*, *collaborator prediction*, *prior work selection*, *citation count prediction*, and *future combination prediction*—and two **aggregate** *topic trend forecasting* variants. We develop baselines ranging from simple heuristics and embedding methods to frontier language models and agentic systems, and introduce LACER, an LLM-based metric for evaluating similarity of generated contribution descriptions that agrees better with human judgments than existing metrics. Finally, we compose task models into a 12-month synthetic corpus whose papers are systematically less diverse and less novel than human-authored research from the same period.

Dataset **Code**

1 INTRODUCTION

Scientific research produces a large-scale chronological record: papers, authors, citations, and evolving topics. Predictive models trained on this record could help researchers identify relevant collaborators and prior work, anticipate emerging research directions, form hypotheses, and study how scientific interest evolves over time. Forecasting future scientific contributions also provides a natural challenge task for systems that aim to automate scientific discovery: success requires recovering the advances that were ultimately realized, given the prior art available at the time. These forecasting tasks demand integrating text, metadata, and relational structure; reasoning under temporal distribution shift; and identifying how prior work leads to new ideas and impact. Because it draws on a large historical record of science, the prediction task admits supervision at meaningful scale, offering a promising setting for evaluating and training models with deeper scientific understanding.

Previous work has examined individual science forecasting problems in isolation, including future collaborations (Liben-Nowell & Kleinberg, 2003; Sun et al., 2011; Kanakaris et al., 2021), novel idea combinations (Sternlicht & Hope, 2026; Frohnert et al., 2025), future-paper insights (He-Yueya et al., 2026), and publication impact (Wang et al., 2013). However, these tasks are usually studied with disparate datasets and evaluation protocols, despite describing related facets of the same evolving scientific record. As a result, it remains difficult to compare methods across tasks, evaluate systems that use multiple kinds of scholarly evidence, or study scientific forecasting at both paper-level and aggregate scales. For large language models in particular, meaningful evaluation further requires forecasted papers to post-date model training cutoffs, a condition that many existing datasets and benchmarks do not satisfy. Because any fixed test period eventually enters the training data of newer models, a forecasting benchmark must be renewable.

We introduce PRESCIENCE, a **renewable** benchmark for scientific forecasting built from 147K recent arXiv papers in two domains, AI (PRESCIENCE-AI) and Quantum Physics (PRESCIENCE-QUANTUM), featuring disambiguated author identities, influential references, per-paper topic labels, citation trajectories, temporally aligned scholarly metadata, and a companion corpus of author

Reviewers: please read the Reviewer Guidelines (iclr.cc/Conferences/2027/ReviewerGuidelines) and the AI Policy for Reviewers (iclr.cc/Conferences/2027/AIPolicyForReviewers). If you used AI to expand, edit, or polish your review, please provide the input text to the LLM. Better still, consider skipping the LLM and submitting your original text: we, and the authors, are much more interested in your unedited thoughts than in what an LLM has to say. AI-assisted or not, you are putting your name and reputation behind your review: LLM-generated falsehoods, hallucinations or misrepresentations are subject to disciplinary action, which may include desk-rejecting all papers you have authored.

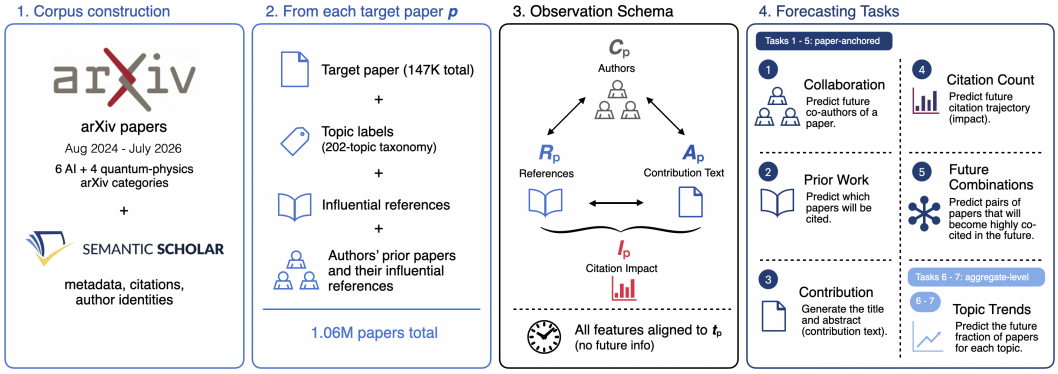

Figure 1: PRESCIENCE instantiates 7 tasks over a dataset built from 147K recent papers in AI and Quantum Physics with author histories, citation links, and metadata spanning 1.06M papers.

publication histories and citation links spanning 1.06M papers. In PRESCIENCE, we treat each paper as an observable record of a scientific contribution, represented through a shared schema containing its authors, influential references, contribution text, citation trajectory, topics, and metadata. This schema supports a broad family of forecasting tasks by varying which parts of the historical record are provided as inputs and which future quantities are predicted. In this paper, we instantiate seven representative prediction problems of interest to machine learning and science-of-science: five **paper-anchored forecasting** tasks, each tied to one future paper record—*contribution generation*, *collaborator prediction*, *prior work selection*, *citation count prediction*, and *future combination prediction*—and two **aggregate forecasting** tasks, *unary* and *topic-pair trend forecasting*.

We develop and evaluate baselines spanning simple heuristics, embedding-based methods, frontier language models, and agentic systems. For contribution generation, we introduce an LLM-based metric called LACER that evaluates conceptual similarity between generated and ground-truth contribution descriptions, and find that LACER outperforms existing automated metrics when compared to expert human preferences, even approaching inter-annotator-agreement levels. Across tasks, our results show that current systems leave substantial headroom. Finally, we compose task models to run 12-month corpus-generation rollouts, showing that synthetic corpora are systematically less diverse and less novel than human-authored papers from the same period.

Our contributions are:

- We introduce PRESCIENCE, a renewable dataset for scientific forecasting, covering 147K recent papers in AI (PRESCIENCE-AI) and Quantum Physics (PRESCIENCE-QUANTUM) and a companion corpus of prior work totaling 1.06M papers, with disambiguated authors and their publication histories, influential references, citation trajectories, topic labels, and temporally aligned metadata.

- We define seven forecasting tasks over a shared observation schema, including five paper-anchored tasks and two aggregate tasks, demonstrating the dataset's utility for controlled evaluation across multiple views of the scientific record. We benchmark a broad set of methods on these tasks: including heuristic, embedding-based, frontier LLM-based, and agentic approaches.

- We introduce LACER, a metric for evaluating generated contribution descriptions that approaches inter-annotator agreement with expert human preferences.

- We compose task-level models into corpus-level rollouts, and analyze how synthetic scientific corpora differ from natural future literature, observing systematic degradations in diversity and novelty relative to human-authored research from the same period.

Table 1: Dataset statistics by domain (averages over target papers; full statistics in Appendix B.1).

	PRESCIENCE-AI		PRESCIENCE-QUANTUM	
	Train	Test	Train	Test
Target Papers	49.4K	67.6K	13.3K	18.2K
All Papers	482K	630K	372K	442K
Unique Authors	125K	159K	43.8K	56.5K
Avg. Infl. Refs	3.06	2.89	2.55	2.45
Avg. Authors	5.26	5.24	4.90	4.84
Avg. Author Hist.	24.9	30.0	34.4	35.2
Avg. Citations @ 12m	6.35	4.64	2.47	2.59

2 THE PRESCIENCE DATASET

PRESCIENCE is a renewable[1] dataset built from research papers posted to arXiv between August 2024 and July 2026 in two diverse demonstration domains: PRESCIENCE-AI, covering six AI categories (`cs.CL`, `cs.LG`, `cs.AI`, `cs.CV`, `cs.IR`, and `cs.NE`), and PRESCIENCE-QUANTUM, covering Quantum Physics (`quant-ph`, `cond-mat`, `physics.optics`, and `physics.atom-ph`). These 147K papers constitute the *target papers* of our paper-anchored tasks. We partition target papers into train (August 2024–July 2025) and test (August 2025–July 2026). To provide historical context for each target paper, we include a set of *companion papers*: influential references of target papers, prior publications of target papers' authors, and influential references of those prior publications. We define a paper's *influential references* as those that substantially shape its contribution (Valenzuela-Escarcega et al., 2015) (see Appendix E.1.3, E.3.1 for alternatives). Together, target and companion papers form a 1.06M-paper corpus that can be used to construct the historical record $\mathbf{H}^{<t}$ available before any time t. Summary statistics appear in Table 1 and Appendix B.1.

Observation schema. Each target paper p is represented by a temporally aligned paper record with four core *components*: disambiguated authors C_p, influential references R_p, contribution text A_p consisting of title and abstract, and citation trajectory I_p (month-over-month cumulative citation counts). The record also includes publication date t_p, topic labels (for PRESCIENCE-AI, obtained via multilabel classification over 202 topics; Appendix B.3), arXiv categories, Semantic Scholar and arXiv identifiers, and other temporally aligned metadata. Appendix B.2 lists features by paper type.

Ensuring dataset quality. We take several measures to ensure that PRESCIENCE supports reliable modeling and evaluation. We source author identities and bibliographic metadata from the Semantic Scholar Graph (Wade, 2022), and disambiguate author profiles using S2AND (Subramanian et al., 2021). In our manual examination, S2AND yielded more accurate author clusters than the current S2AG release. We restrict target papers to those with between 1 and 10 influential references, excluding instances with zero or unusually large influential-reference sets. We also drop targets duplicated across splits or published over a year before their arXiv posting. Finally, all author- and reference-level metadata (publication counts, citation counts, and h-indices) are temporally aligned to each paper's publication date to prevent leakage of future information into task inputs. We ensure the validity and consistency of topics assigned to papers; see Appendix B.3.

3 SCIENTIFIC FORECASTING TASKS

The PRESCIENCE schema supports many forecasting tasks by varying input fields and prediction targets. We instantiate seven representative tasks, spanning established problems from existing literature and new prediction problems enabled by the PRESCIENCE schema. Together, they evaluate two scales of scientific forecasting: **paper-anchored** tasks that seek predictions for certain components of target paper records by conditioning on others (along with $\mathbf{H}^{<t_p}$), and **aggregate** tasks that predict corpus-level trends over longer time periods. Three of our selected tasks—collaborator prediction,

[1] Our scripts need only a date range and arXiv categories, so they can refresh the dataset or build PRESCIENCE-style datasets for any arXiv domain.

prior work selection, and contribution generation—can also be composed into a generative process that allows corpus-scale rollouts of synthetic papers (as in Section 4.5).

3.1 PAPER-ANCHORED FORECASTING TASKS

Contribution generation. Predicting future paper content from past literature is increasingly used to evaluate scientific ideation, hypothesis selection, and automated discovery. Prior work studies future-aligned proposal generation from research questions and inspiring papers (Wang et al., 2026), or core-insight anticipation from a pair of parent papers (He-Yueya et al., 2026). In PRESCIENCE, we forecast the title and abstract A_p of an actual future paper from its influential references R_p and $\mathbf{H}^{<t_p}$; since R_p may contain more than two papers, this evaluates generation from a richer evidence set. This task requires measuring conceptual similarity, not surface overlap.

We introduce LACER (Lattice of Automatically Constructed Exemplars for Reference) score, an LLM-as-judge (Zheng et al., 2023) metric calibrated to a 1–10 semantic-alignment scale using automatically constructed demonstrations. These demonstrations anchor the scale between topically related prior work and semantic equivalence to the target contribution, yielding an interpretable dynamic range without human-written examples. Against 250 expert similarity rankings, LACER approaches human inter-annotator agreement (Kendall's τ_b: 0.57 vs. 0.53) and outperforms ROUGE-L (Lin, 2004), BERTScore (Zhang et al., 2020), and ASPIRE Distance (Mysore et al., 2022) (0.27, 0.40, and 0.35); construction and validation details appear in Appendix C. We provide examples of LACER evaluations in Appendix I along with two illustrations in Figure 6 (Appendix E).

Collaborator prediction. Forecasting future collaborations is useful for collaborator recommendation (Zhang et al., 2023), author discovery (Balog et al., 2012), and studying how research communities form around emerging problems (Fortunato et al., 2018). We formulate collaborator prediction as a link-prediction problem (Liben-Nowell & Kleinberg, 2003): given a "seed" author (the first; Appendix E.2.1) of paper p and $\mathbf{H}^{<t_p}$, rank candidate authors by whether they are among the remaining co-authors of p. We restrict candidates to authors with prior publications, leaving first-time authors to future work. We evaluate rankings using normalized Discounted Cumulative Gain (nDCG) (Järvelin & Kekäläinen, 2002) and R-precision (NIST TREC, 2006).

Prior work selection. To our knowledge, we introduce a new task: given a team of collaborators, surface prior work likely to be influential for their future paper. Such a system could help scientific teams identify research directions to build on. We formulate this as a team-conditioned ranking problem: given the authors C_p of a target paper and $\mathbf{H}^{<t_p}$, rank prior papers by whether they appear among p's influential references R_p.[2] We evaluate rankings using nDCG and R-precision.

Citation count prediction. Citation forecasting is useful for anticipating which papers are likely to receive early scholarly attention after publication, and can help researchers prioritize research directions.[3] Citation count prediction is a regression task: given C_p, R_p, A_p and $\mathbf{H}^{<t_p}$, predict the number of citations p receives in its first 12 months. We evaluate using mean absolute error and Pearson correlation (raw and log counts) and Spearman correlation.

Future combination prediction. The problem of predicting which lines of work can productively be combined to yield breakthroughs has long been of interest to the science-of-science community (Shi & Evans, 2023) and was recently revisited with LLMs (Chen et al., 2025a). Given a target paper p from the first four months of the test period and $\mathbf{H}^{<t_p}$, we rank all prior papers $q \in \mathbf{H}^{<t_p}$ by how often p and q will later be jointly cited as influential references by future target papers during the eight months that follow t_p, evaluating with nDCG and R-precision.

3.2 AGGREGATE FORECASTING

Topic trend forecasting. Scientists and policymakers often need to track which research areas are gaining or losing attention, both individually and in combination. This task poses the following

[2] Other influential reference definitions do not perform dramatically better (Appendix E.3.1).

[3] Although citation counts are an imperfect proxy for scientific impact (Hicks et al., 2015), they remain widely used in science-of-science research (Fortunato et al., 2018) and scalably measure early scholarly attention.

Table 2: Contribution generation results. Subscripts indicate bootstrap 95% CIs. Unmarked errors are 0.00. Left: model comparison on $n = 2{,}000$ test papers using influential references as input; * indicates model cutoffs postdate test-period start (Appendix E.1.1). Right: GPT-5.6 Sol context ablations on a random $n = 500$ subset; *citations* gives oracle 12-month citation counts.

Baseline	LACER	ROUGE-L		BERTScore	
		P	R	P	R
Same arXiv Category	$1.26_{(0.03)}$	0.12	0.11	0.13	0.11
Random Infl. Ref.	$4.23_{(0.09)}$	0.15	0.15	0.19	0.17
OLMo 3 7B (FT)	$4.00_{(0.09)}$	**0.18**	0.15	**0.24**	0.17
Qwen 3 8B (FT)	$3.96_{(0.08)}$	**0.18**	0.15	**0.24**	0.17
GPT 4o	$4.21_{(0.08)}$	0.16	0.14	**0.24**	0.19
GPT 5 mini	$5.41_{(0.09)}$	0.11	0.16	0.15	0.21
GPT 5	$5.53_{(0.09)}$	0.11	0.16	0.15	0.21
GPT 5.6 Sol*	$\mathbf{5.63}_{(0.10)}$	0.15	0.16	0.21	0.21
Claude Sonnet 4.5	$4.88_{(0.09)}$	0.13	0.17	0.21	**0.23**
Claude Opus 4.6*	$5.10_{(0.09)}$	0.14	**0.18**	0.22	**0.23**
Claude Sonnet 5*	$5.26_{(0.09)}$	0.14	0.17	0.20	**0.23**
Gold Paraphrase	$10.00_{(0.00)}$	0.66	0.63	0.74	0.73

Input features	LACER
Infl. refs.	$5.61_{(0.20)}$
Infl. refs. + related	$5.66_{(0.20)}$
Infl. refs. + author papers	$5.85_{(0.20)}$
Infl. refs. + citations	$5.57_{(0.19)}$
Infl. refs. + related + author	$5.74_{(0.20)}$
Infl. refs. + related + author + citations	$5.71_{(0.20)}$
Infl. refs. + $\mathbf{H}^{<t_p}$ (Agent)	$\mathbf{5.98}_{(0.19)}$

problem: for each topic z, predict how much its share of papers changes from the train period to the test period. Let $s_{\text{train}}(z)$ and $s_{\text{test}}(z)$ denote the fraction of evaluated papers assigned to z in the train and test periods, respectively. The prediction target is the difference between these two shares: $\Delta s(z) = s_{\text{test}}(z) - s_{\text{train}}(z)$. We evaluate predictions using R^2 and Pearson correlation over topics.

We evaluate two variants: *unary topic trends*, where each prediction unit is one of the 202 PRESCIENCE-AI topics (Appendix B.3), and *topic-pair trends*, where each unit is an unordered topic pair. For topic pairs, the target is the change in the fraction of evaluated papers assigned to both topics; we evaluate the 5,940 pairs with at least 10 papers in either train or test.

4 EXPERIMENTS

We report PRESCIENCE-AI results in this section. PRESCIENCE-QUANTUM results, which demonstrate transfer to a second domain and show the same qualitative trends, appear in Appendix F. Implementation details, costs, analyses, and prompts appear in Appendices D, D.8, E, and H.

4.1 CONTRIBUTION GENERATION

We evaluate contribution generation in the default setting: models receive titles and abstracts of a target paper's influential references R_p and generate the target title and abstract (prompt in Appendix H.2). We compare frontier OpenAI and Anthropic models with finetuned OLMo 3 7B (Olmo et al., 2025) and Qwen3 8B (Team, 2025), plus reference baselines: a gold paraphrase, a random influential reference from R_p, and a same-arXiv-category random paper. We report LACER (using `gpt-5-2025-08-07` as judge) as the primary metric, with ROUGE-L (Lin, 2004) and BERTScore (Zhang et al., 2020) for comparison.

Results. Table 2 (left) shows that gold paraphrases reach the top of the LACER scale, while random same-category papers and influential references score much lower. Finetuned open models improve over the same-category baseline but score lower than frontier models; even the best frontier model reaches only average moderate similarity to the ground truth, reflecting the difficulty of forecasting specific future contributions. Our ablations indicate that model pretraining overlap with the test period does not substantially affect LACER scores (Appendix E.1.1), and that relative rankings remain similar across LACER judge choices (Appendix C.2.1).

Context ablations. Table 2 (right) evaluates GPT-5.6 Sol with richer inputs on a random 500-paper subset of the test split. All rows include influential references; related papers are retrieved from $\mathbf{H}^{<t_p}$ using the papers in R_p as nearest-neighbor queries, and the *citations* setting assumes oracle access to

Table 3: Paper-anchored ranking task results. Subscripts indicate bootstrap 95% CIs. Left: collaborator prediction and prior work selection. Right: future combination prediction. † indicates evaluation on $n = 500$ random instances. *Emb. Fus. Refs* pools the authors' cited influential references.

	Collab		Prior Work	
Baseline	**nDCG**	**R-Prec**	**nDCG**	**R-Prec**
Frequency	$0.39_{(0.01)}$	$0.28_{(0.01)}$	$0.09_{(0.00)}$	$0.05_{(0.00)}$
Rank Fusion	$0.16_{(0.01)}$	$0.07_{(0.00)}$	$0.02_{(0.00)}$	$0.01_{(0.00)}$
Emb. Fusion	$0.26_{(0.01)}$	$0.17_{(0.01)}$	$0.08_{(0.00)}$	$0.04_{(0.00)}$
Hier. Clustering	$0.25_{(0.01)}$	$0.15_{(0.01)}$	$0.06_{(0.00)}$	$0.01_{(0.00)}$
Emb. Fus. Refs	–	–	$0.05_{(0.00)}$	$0.01_{(0.00)}$
Emb. Fus. Proj.	$0.21_{(0.01)}$	$0.12_{(0.01)}$	$0.09_{(0.00)}$	$0.03_{(0.00)}$
Autoresearch	$\mathbf{0.47}_{(0.01)}$	$\mathbf{0.33}_{(0.01)}$	$\mathbf{0.13}_{(0.01)}$	$0.05_{(0.00)}$
GPT-5 Agent†	$0.41_{(0.03)}$	$0.29_{(0.03)}$	$\mathbf{0.13}_{(0.02)}$	$\mathbf{0.06}_{(0.02)}$

	Future Comb.	
Baseline	**nDCG**	**R-Prec**
Target Similarity	$0.24_{(0.01)}$	$0.10_{(0.01)}$
Ref. Similarity	$0.27_{(0.01)}$	$0.15_{(0.01)}$
Co-citation Freq.	$0.11_{(0.01)}$	$0.05_{(0.01)}$
Citation Freq.	$0.05_{(0.00)}$	$0.00_{(0.00)}$
Autoresearch	$\mathbf{0.35}_{(0.01)}$	$\mathbf{0.17}_{(0.01)}$
GPT-5 Agent†	$0.26_{(0.02)}$	$0.15_{(0.02)}$

12-month citation counts. Author histories provide the largest improvement ($5.61 \rightarrow 5.85$), while related papers do not seem to help significantly, and oracle citation counts do not help ($5.61 \rightarrow 5.57$), suggesting that scalar citation counts are not useful to GPT-5.6 Sol in this setup. An agentic variant ($\sim 20\times$ in API costs compared to simple GPT-5.6 Sol prompting) equipped with tool access to the full historical record $\mathbf{H}^{<t_p}$ performs best (5.98), indicating that broader context can improve predictions. The agent baseline's implementation details appear in Appendix D.1. Figure 6 (Appendix E) shows an example of scored generations from GPT-4o and a GPT-5-based agent.

4.2 Paper-anchored Ranking Tasks

We evaluate three paper-anchored ranking tasks: collaborator prediction, prior work selection, and future combination prediction. For collaborator prediction, models rank candidate authors given a seed author and $\mathbf{H}^{<t_p}$; for the other two tasks, models rank candidate papers from $\mathbf{H}^{<t_p}$. We report nDCG@1000 and R-precision with GRIT (Muennighoff et al., 2025) embeddings, with GTR (Ni et al., 2022) and Specter2 (Singh et al., 2023) variants in Appendices E.2.4, E.3.4, and E.4.1.

Baselines. For collaborator prediction and prior work selection, we evaluate frequency heuristics and embedding-based retrieval baselines. *Frequency* ranks candidates by historical co-authorship frequency with the seed author for collaborator prediction, and by previous citations from the target authors for prior work selection. *Rank Fusion* retrieves papers from $\mathbf{H}^{<t_p}$ using query embeddings from the seed author or author set, then ranks candidates by aggregated ranks. *Embedding Fusion* ranks authors or papers by similarity in embedding space. *Hierarchical Clustering* represents each author using multiple centroids to model heterogeneous interests, while *Embedding Fusion Projected* learns a task-specific mapping over frozen embeddings using a Multi-Instance NCE objective (Miech et al., 2020). For future combination prediction, *Target Similarity* ranks prior papers by similarity to the target title and abstract; *Reference Similarity* uses the mean embedding of the target paper's influential references; *Citation Frequency* ranks papers by prior frequency as influential references; and *Co-citation Frequency* ranks papers by prior influential co-citation with the target paper's influential references. We also evaluate two agentic baselines: *Autoresearch*, adapted from Karpathy's autoresearch framework (Karpathy, 2026), which iteratively designs and tests ranking strategies under a 12-hour budget, and *GPT-5 Agent*, which uses tools for paper search, paper inspection, author histories, references, and citation traversal, with all outputs filtered to $\mathbf{H}^{<t_p}$. Implementation details for the static baselines, Autoresearch, and the GPT-5 agent appear in Appendices D.2, D.3, and D.4.

Results. Table 3 shows that agentic methods perform best across all three ranking tasks. For collaborator prediction, *Autoresearch* improves over the strongest static baseline, *Frequency*, from $0.39/0.28$ to $0.47/0.33$ nDCG@1000/R-precision. For prior work selection, gains are smaller in absolute terms: *Autoresearch* reaches $0.13/0.05$, compared with $0.09/0.05$ for the strongest static baseline, *Frequency*, indicating that identifying influential references remains difficult. All methods rarely recover first-time collaborators or uncited references (Appendices E.2.3, E.3.3). For future

Table 4: Citation count prediction (GRIT) on the 9,597 test papers with 12-month citations.

Baseline	MAE	MAE (log)	Pearson	Pearson (log)	Spearman
Target Text	3.87	0.71	0.42	0.47	0.42
Bibliometrics	3.95	0.73	0.36	0.41	0.34
Target + Context	3.75	0.69	0.52	0.52	0.46
Target + Context + Bibliometrics	3.70	0.68	**0.55**	**0.54**	0.47
Autoresearch	**3.69**	**0.67**	0.50	**0.54**	**0.48**

Table 5: Topic trend forecasting results. We report R^2 and Pearson correlation for predicted changes (Δ) in topic share. Unary trends are evaluated over 202 topics; topic-pair trends are evaluated over 5,940 topic pairs with at least 10 papers in either train or test.

Baseline	Unary topics		Topic pairs	
	Δshare R^2	Δshare Pearson	Δshare R^2	Δshare Pearson
Mean	-10.03	0.19	-6.28	0.25
Linear Extrapolation	**0.58**	**0.76**	**0.35**	**0.62**
Citation Momentum	-1.67	0.43	-2.68	0.25
Author Momentum (papers)	-0.43	0.22	-0.36	0.23
Author Momentum (h-index)	-0.27	0.24	-0.23	0.24

combinations, *Autoresearch* performs best ($0.35/0.17$), while *Reference Similarity* is the best non-agentic baseline ($0.27/0.15$), suggesting that influential references signal future combinations.

4.3 Citation Count Prediction

We evaluate citation forecasting with XGBoost regressors over three feature families: *Target Text* (target title and abstract), *Context Text* (influential references and author prior publications), and *Bibliometrics* (reference citation counts and author h-index, total citations, and publication counts at publication time). Text features use GRIT embeddings in the main table; GTR and Specter2 variants appear in Appendix E.5.2. We predict 12-month citation counts and report metrics in both raw and log space, also applying *Autoresearch*.

Results. Table 4 shows that adding *Context Text* to *Target Text* improves performance, and adding *Bibliometrics* yields smaller further gains. *Autoresearch* performs best overall, reaching 3.69 MAE, 0.50 Pearson, and 0.48 Spearman in raw citation space, although the full XGBoost model (*Target + Context + Bibliometrics*) attains a higher raw Pearson correlation (0.55). Prediction error remains substantial, reflecting the heavy-tailed nature of citation outcomes; SHAP analyses and prediction scatter plots appear in Appendix E.5.1 and implementation details in Appendix D.5.

4.4 Topic Trend Forecasting

Baselines. We report simple extrapolative and momentum-based baselines (Appendix D.6) as an initial benchmark for this new aggregate forecasting task. *Mean* predicts the same future paper count for every topic (the cross-topic average). *Linear Extrapolation* fits a linear trend to monthly historical counts and extrapolates over the forecast horizon. *Citation Momentum* scores each topic by summing the observable citations of its historical papers, then converts the score to a paper-count forecast via a topic-agnostic linear scale calibrated on an inner train/test split of the history period. *Author Momentum* uses the same calibration with per-author scores summed over each paper's authors; we report variants using prior publication counts and h-indices. Richer forecasters are left to future work.

Results. Table 5 shows that simple historical signals are predictive but incomplete. Linear extrapolation performs best on both metrics for unary topics (0.58 R^2, 0.76 Pearson) and for topic pairs (0.35 R^2, 0.62 Pearson). Negative R^2 values for mean, citation momentum, and author momentum show that correlation alone does not imply calibrated share-change predictions.

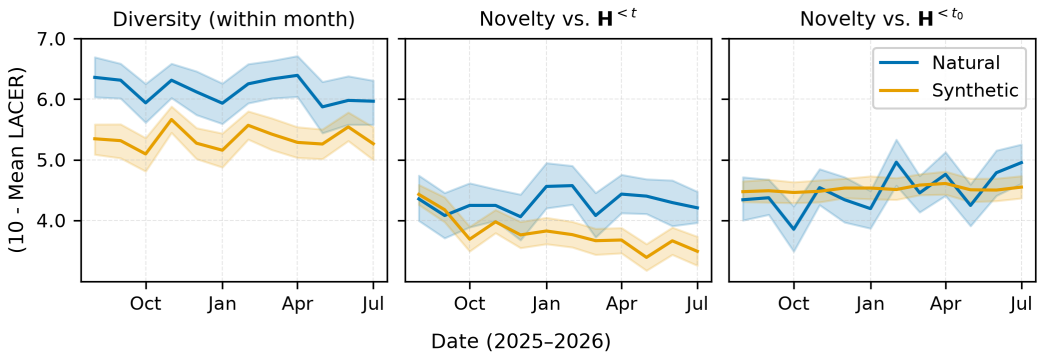

Figure 2: Synthetic papers from corpus-generation rollouts are less diverse than natural future papers (left) and become less novel relative to the evolving literature state $\mathbf{H}^{<t}$ (middle); against the fixed pre-rollout corpus $\mathbf{H}^{<t_0}$ (right), this decline largely disappears. Shading: bootstrap 95% CIs.

4.5 Corpus Generation

The preceding experiments evaluate task models in isolation. We also compose them into corpus-level rollouts that synthesize a 12-month stream of future paper records. Starting from the literature state at the beginning of the test period ($\mathbf{H}^{<t_0}$, where t_0 = August 1, 2025), the rollout proceeds day by day: sample the number of papers from a train-period daily publication distribution P_{daily}, sample team sizes, predict collaborators, select influential references, generate titles and abstracts, and fold generated papers back into the literature state for subsequent steps. This rollout policy is a modeling choice for corpus generation, not part of the benchmark definition; full pseudocode appears in Appendix D.7. We use one-shot *GRIT + Embedding Fusion* for collaborator prediction and prior work selection, and GPT-5 mini (pre-test-period cutoff; Appendix E.1.1) for contribution generation.

Evaluation. We compare synthetic and natural future corpora using LACER-based diversity and novelty. For each month, we sample $n = 50$ generated papers and score their $k = 3$ nearest neighbors in GRIT embedding space. Diversity uses same-month papers as the retrieval pool; novelty uses either the evolving literature state $\mathbf{H}^{<t}$ or the fixed pre-rollout corpus $\mathbf{H}^{<t_0}$. We size-match natural-paper retrieval pools to synthetic pools, repeat the rollout three times, and report mean trends.

Results. Synthetic corpora are consistently less diverse than natural papers from the same period and become less novel relative to the evolving literature state $\mathbf{H}^{<t}$ (Figure 2). This novelty decline largely disappears when measured against the fixed pre-rollout corpus $\mathbf{H}^{<t_0}$, suggesting that generations remain distant from the original historical corpus but become increasingly similar to earlier synthetic outputs. Predicted author and prior-work sets are more diverse than their natural counterparts (Appendix E.6.1), suggesting that the diversity gap arises primarily from contribution generation rather than predicted collaborators or references. LACER-based precision and recall fall below a natural-versus-natural reference, and the natural papers best covered by rollouts tend to be more cited, suggesting a mainstream bias (Appendix E.6.2).

5 Related Work

Several recent benchmarks evaluate predictive models against future scientific advances. A few forecast concept co-occurrence in future papers, albeit at different scales: dynamic word embeddings trained on 67k quantum-physics papers (Frohnert et al., 2025), a knowledge graph built from 21M papers (Gu & Krenn, 2025), and 65k research sub-fields (1827–2024) from OpenAlex (Rezaee et al., 2025), respectively. Proof of Time (Ye et al., 2026) was created to evaluate agents on 4 disparate tasks - impact prediction, author research evolution, peer-review awards and benchmark performance. ScienceMeter (Wang et al., 2025) measures *knowledge projection*, the ability of an updated model to anticipate scientific claims in post-cutoff papers. Closer to our contribution-generation task, (Wang et al., 2026) train language models to produce future-aligned proposals scored by their Future

Alignment Score, while (He-Yueya et al., 2026) introduce GiantsBench, which pairs parent papers with downstream insights scored by an LLM judge. In contrast, PRESCIENCE defines multiple paper-anchored and aggregate forecasting tasks under a shared, temporally aligned observation schema, and can compose task models into corpus-generation rollouts.

Collaborator prediction This task is well-studied, mostly with graph-based link prediction (Kanakaris et al., 2021; Tuninetti et al., 2021; Li et al., 2024) and temporal models of publication histories (Munasinghe & Ichise, 2012; Koopmann et al., 2021) (see Appendix G).

Prior work selection For a given set of authors, we forecast the literature they will build upon for creating a new advance. To our knowledge, this team-conditioned formulation is novel. In loosely related lines of work on scientific ideation, it is common to retrieve past papers to serve as inspirations (Wang et al., 2024a; Chen et al., 2025a; Radensky et al., 2024; Sternlicht & Hope, 2026); however, the objective in those works is ideation-focused rather than to forecast the choice of prior work conditioned on the collaborating authors and their expertise.

Contribution generation The closest analogy to this task in current literature is scientific hypothesis generation or ideation, which can be grounded in the interactions between different areas of the scientific literature (Swanson, 1986). Many modern approaches build on this insight (Wang et al., 2024a; Radensky et al., 2024; Lu et al., 2024; Wang et al., 2024b; Baek et al., 2025), including recent benchmarks mentioned earlier (Wang et al., 2026; He-Yueya et al., 2026; Guo et al., 2025) and multi-agent systems (Su et al., 2025).

Topic-trend forecasting Knowledge-graph approaches have been previously used to detect, analyze, and forecast topics from large-scale scholarly graphs (Salatino et al., 2021), and topic popularity has been predicted five years in advance from publication, language, and patent signals (Ofer et al., 2023). Closer to our setting, link prediction over concept knowledge graphs forecasts future co-investigation at scale (Gu & Krenn, 2025), and dynamic word embeddings can capture emergent cross-area connections (Frohnert et al., 2025).

Citation count and future combination prediction Prior works have used varied measures for impact, ranging from citation accumulation (Uddin et al., 2013; Gu & Krenn, 2025) and novelty-based predictors of impact (Shi & Evans, 2023; Zhang & Evans, 2025) to research grant success (Cole et al., 1981; Boyack et al., 2018; Győrffy et al., 2020). Beyond predicting the citation count of a paper itself, PRESCIENCE's future influential co-citation prediction task asks which prior works will appear as influential references jointly with a target paper. This sits in the same tradition of forecasting future conceptual connections—via knowledge-graph link prediction (Gu & Krenn, 2025) and dynamic concept embeddings (Frohnert et al., 2025)—but is evaluated against an explicit influential-reference signal from real future papers. PRESCIENCE conditions the citation predictions on the full generative context: the research team, their prior work, and the contribution itself. Our finding that author and reference features provide substantial predictive power aligns with the "cumulative advantage" literature (Merton, 1968; Wang et al., 2013), while the residual variance points to signals that remain unexplored. Appendix G discusses further related work.

6 CONCLUSION

We presented PRESCIENCE, a renewable dataset and benchmark for scientific forecasting over a shared, temporally controlled corpus of recent research in AI and Quantum Physics. PRESCIENCE provides an observation schema that supports multiple forecasting tasks over the same scientific record, rather than prescribing a single model of how science unfolds. We instantiate seven tasks spanning paper-level forecasting and aggregate topic trends, introduce LACER for contribution generation, and benchmark a broad set of heuristic, embedding-based, language-model, and agentic baselines. Across tasks, current methods leave substantial headroom, and our corpus-generation rollouts show that today's composed systems produce synthetic corpora that are less diverse and less novel than natural future literature. PRESCIENCE can be renewed with test periods beyond new models' training cutoffs, and its scripts can build PRESCIENCE-style datasets for any arXiv domain.

AI USE STATEMENT

In this work, we used generative AI tools to generate synthetic data (corpus-generation rollouts), implement methods, clean and reformat the dataset, provide feedback on experiment design, support qualitative and thematic analysis (e.g., proposing the initial topic taxonomy), and interpret results, and as experimental components (contribution-generation baselines, the LACER judge, topic labeling, and the Autoresearch outer loop; Section 4 and Appendices B.3 and D). We have not used generative AI tools to propose or refine hypotheses or to assist with translation, and developing theoretical models, formulating mathematical claims, and writing proofs are not applicable to this work. Additionally, we used generative AI tools to edit code and the manuscript. All AI-assisted code, data processing, analyses, and text were reviewed and verified by the authors. We take responsibility for the final content of this work.

ETHICS STATEMENT

We hope that PRESCIENCE will spur the development of systems and agents that can anticipate scientific activity and outcomes, helping scientists, policymakers, and others identify emerging opportunities and prioritize research directions. A potential risk of the work is that erroneous predictive outputs will be misused for decision-making. We emphasize that use of models trained and evaluated on PRESCIENCE carefully consider the limitations discussed in Appendix A.

REPRODUCIBILITY STATEMENT

Section 2 and Appendix B describe dataset construction, and Appendix D gives implementation details, hyperparameters, and computational costs for all baselines; all prompts appear in the appendix. We use dated model identifiers for all API models and fixed random seeds for sampling. We release the dataset, the construction scripts, and the evaluation code (links in the abstract).

REFERENCES

Daria Alexander and Arjen P. de Vries. In a few words: Comparing weak supervision and llms for short query intent classification. In *Proceedings of the 48th International ACM SIGIR Conference on Research and Development in Information Retrieval*, SIGIR '25, pp. 2977–2981. ACM, July 2025. doi: 10.1145/3726302.3730213. URL http://dx.doi.org/10.1145/3726302.3730213.

Diego Raphael Amancio. Comparing the topological properties of real and artificially generated scientific manuscripts. *Scientometrics*, 105:1763–1779, 2015. doi: 10.1007/s11192-015-1637-z.

Hiba Arnaout, Noy Sternlicht, Tom Hope, and Iryna Gurevych. In-depth research impact summarization through fine-grained temporal citation analysis. In *Proceedings of the 64th Annual Meeting of the Association for Computational Linguistics (Volume 1: Long Papers)*. Association for Computational Linguistics, 2026. URL https://arxiv.org/abs/2505.14838. arXiv:2505.14838.

Jinheon Baek, Sujay Kumar Jauhar, Silviu Cucerzan, and Sung Ju Hwang. ResearchAgent: Iterative research idea generation over scientific literature with large language models. In Luis Chiruzzo, Alan Ritter, and Lu Wang (eds.), *Proceedings of the 2025 Conference of the Nations of the Americas Chapter of the Association for Computational Linguistics: Human Language Technologies (Volume 1: Long Papers)*, pp. 6709–6738, Albuquerque, New Mexico, April 2025. Association for Computational Linguistics. ISBN 979-8-89176-189-6. URL https://aclanthology.org/2025.naacl-long.342/.

Krisztian Balog, Yi Fang, Maarten de Rijke, Pavel Serdyukov, and Luo Si. Expertise retrieval. *Foundations and Trends in Information Retrieval*, 6(2–3):127–256, 2012.

Kevin W. Boyack, Caleb Smith, and Richard Klavans. Toward predicting research proposal success. *Scientometrics*, 114:449–461, 2018. URL https://api.semanticscholar.org/CorpusID:46804654.

Franck Cappello, Sandeep Madireddy, Robert Underwood, Neil Getty, Nicholas Chia, Nesar Ramachandra, Josh Nguyen, Murat Keceli, Tanwi Mallick, Zilinghan Li, Marie Claver Ndébane Ngom, Chenhui Zhang, Angel Yanguas-Gil, Evan R. Antoniuk, Bhavya Kailkhura, Minyang Tian, Yu Du, Yuan-Sen Ting, Azton Wells, Bogdan Nicolae, Avinash Maurya, M. Mustafa Rafique, E. A. Huerta, Bo Li, Ian Foster, and Rick Stevens. Eaira: Establishing a methodology for evaluating ai models as scientific research assistants. *ArXiv*, abs/2502.20309, 2025. URL https://api.semanticscholar.org/CorpusID:276647576.

Junlan Chen, Kexin Zhang, Daifeng Li, Yangyang Feng, Yuxuan Zhang, and Bowen Deng. Structuring scientific innovation: A framework for modeling and discovering impactful knowledge combinations. *ArXiv*, abs/2503.18865, 2025a. URL https://api.semanticscholar.org/CorpusID:277313413.

Nuo Chen, Yicheng Tong, Jiaying Wu, Minh Duc Duong, Qian Wang, Qingyun Zou, Bryan Hooi, and Bingsheng He. Beyond brainstorming: What drives high-quality scientific ideas? lessons from multi-agent collaboration, 2025b. URL https://api.semanticscholar.org/CorpusID:280540858.

Xiyao Cheng, Yuanxun Zhang, Harsh Joshi, Mayank Kejriwal, and Prasad Calyam. Knowledge graph-based embedding for connecting scholars in academic social networks. *2023 IEEE 10th International Conference on Data Science and Advanced Analytics (DSAA)*, pp. 1–10, 2023. URL https://api.semanticscholar.org/CorpusID:265054862.

Pham Minh Chuan, Le Hoang Son, Mumtaz Ali, Tran Dinh Khang, Le Thanh Huong, and Nilanjan Dey. Link prediction in co-authorship networks based on hybrid content similarity metric. *Appl. Intell.*, 48(8):2470–2486, 2018. doi: 10.1007/S10489-017-1086-X. URL https://doi.org/10.1007/s10489-017-1086-x.

Stephen Cole, Jonathan R. Cole, and Gary A. Simon. Chance and consensus in peer review. *Science*, 214 4523:881–6, 1981. URL https://api.semanticscholar.org/CorpusID:11183533.

Fezzeh Ebrahimi, Asefeh Asemi, Amin Nezarat, and Andrea Ko. Developing a mathematical model of the co-author recommender system using graph mining techniques and big data applications. *Journal of Big Data*, 8, 2021. URL https://api.semanticscholar.org/CorpusID:232133644.

Naihe Feng, Yi Sui, Shiyi Hou, Jesse C. Cresswell, and Ga Wu. Response quality assessment for retrieval-augmented generation via conditional conformal factuality. *Proceedings of the 48th International ACM SIGIR Conference on Research and Development in Information Retrieval*, 2025. URL https://api.semanticscholar.org/CorpusID:280011519.

Santo Fortunato, Carl T. Bergstrom, Katy Börner, James A. Evans, Dirk Helbing, Staša Milojević, Alexander M. Petersen, Filippo Radicchi, Roberta Sinatra, Brian Uzzi, Alessandro Vespignani, Ludo Waltman, Dashun Wang, and Albert-László Barabási. Science of science. *Science*, 359 (6379):eaao0185, 2018. doi: 10.1126/science.aao0185.

Felix Frohnert, Xuemei Gu, Mario Krenn, and Evert P L van Nieuwenburg. Discovering emergent connections in quantum physics research via dynamic word embeddings. *Machine Learning: Science and Technology*, 6, 2025. URL https://api.semanticscholar.org/CorpusID:273963065.

Jia Fu, Xiao Zhang, Sepideh Pashami, Fatemeh Rahimian, and Anders Holst. Diffpad: Denoising diffusion-based adversarial patch decontamination, 2024. URL https://arxiv.org/abs/2410.24006.

Xuemei Gu and Mario Krenn. Forecasting high-impact research topics via machine learning on evolving knowledge graphs. *Machine Learning: Science and Technology*, 6, 2025. URL https://api.semanticscholar.org/CorpusID:267636723.

Sikun Guo, Amir Hassan Shariatmadari, Guangzhi Xiong, Albert Huang, Myles Kim, Corey M. Williams, Stefan Bekiranov, and Aidong Zhang. IdeaBench: Benchmarking large language models for research idea generation. In *Proceedings of the 31st ACM SIGKDD Conference on Knowledge Discovery and Data Mining V.2*, pp. 5888–5899, 2025. doi: 10.1145/3711896.3737419.

Balázs Győrffy, Péter Herman, and István Szabó. Research funding: past performance is a stronger predictor of future scientific output than reviewer scores. *J. Informetrics*, 14:101050, 2020. URL https://api.semanticscholar.org/CorpusID:219933512.

Armin Hadžić, Milan Papez, and Tomáš Pevný. Distillation of a tractable model from the vq-vae, 2025. URL https://arxiv.org/abs/2509.01400.

Joy He-Yueya, Anikait Singh, Ge Gao, Michael Y. Li, Sherry Yang, Chelsea Finn, Emma Brunskill, and Noah D. Goodman. Giants: Generative insight anticipation from scientific literature, 2026. URL https://arxiv.org/abs/2604.09793.

Diana Hicks, Paul Wouters, Ludo Waltman, Sarah de Rijcke, and Ismael Rafols. Bibliometrics: The Leiden manifesto for research metrics. *Nature*, 520(7548):429–431, 2015. doi: 10.1038/520429a.

Thi Kim Thoa Ho, Quang Vu Bui, and Marc Bui. Co-author relationship prediction in bibliographic network: A new approach using geographic factor and latent topic information. *Proceedings of the 10th International Symposium on Information and Communication Technology*, 2019. URL https://api.semanticscholar.org/CorpusID:209450869.

Xiang Hu, Hongyu Fu, Jinge Wang, et al. Nova: An iterative planning and search approach to enhance novelty and diversity of LLM generated ideas. *arXiv preprint arXiv:2410.14255*, 2024. URL https://arxiv.org/abs/2410.14255.

Langlin Huang, Chengsong Huang, Jixuan Leng, Di Huang, and Jiaxin Huang. Poss: Position specialist generates better draft for speculative decoding, 2025. URL https://arxiv.org/abs/2506.03566.

Peter Jansen, Marc-Alexandre Côté, Tushar Khot, Erin Bransom, Bhavana Dalvi Mishra, Bodhisattwa Prasad Majumder, Oyvind Tafjord, and Peter Clark. Discoveryworld: A virtual environment for developing and evaluating automated scientific discovery agents. In Amir Globerson, Lester Mackey, Danielle Belgrave, Angela Fan, Ulrich Paquet, Jakub M. Tomczak, and Cheng Zhang (eds.), *Advances in Neural Information Processing Systems 37: Annual Conference on Neural Information Processing Systems 2024, NeurIPS 2024, Datasets and Benchmarks Track, Vancouver, BC, Canada, December 10–15, 2024*, 2024. URL http://papers.nips.cc/paper_files/paper/2024/hash/13836f251823945316ae067350a5c366-Abstract-Datasets_and_Benchmarks_Track.html.

Peter Jansen, Oyvind Tafjord, Marissa Radensky, Pao Siangliulue, Tom Hope, Bhavana Dalvi Mishra, Bodhisattwa Prasad Majumder, Daniel S. Weld, and Peter Clark. Codescientist: End-to-end semi-automated scientific discovery with code-based experimentation. In Wanxiang Che, Joyce Nabende, Ekaterina Shutova, and Mohammad Taher Pilehvar (eds.), *Findings of the Association for Computational Linguistics: ACL 2025*, pp. 13370–13467, Vienna, Austria, jul 2025. Association for Computational Linguistics. doi: 10.18653/v1/2025.findings-acl.692. URL https://aclanthology.org/2025.findings-acl.692/.

Kalervo Järvelin and Jaana Kekäläinen. Cumulated gain-based evaluation of ir techniques. *ACM Trans. Inf. Syst.*, 20:422–446, 2002. URL https://api.semanticscholar.org/CorpusID:1981391.

Lesheng Jin, Zhenyuan Ruan, Haohui Mai, and Jingbo Shang. VeriLocc: End-to-end cross-architecture register allocation via LLM. In *Proceedings of the 2025 Conference on Empirical Methods in Natural Language Processing*, pp. 30252–30262, Suzhou, China, November 2025. Association for Computational Linguistics. doi: 10.18653/v1/2025.emnlp-main.1538. URL https://aclanthology.org/2025.emnlp-main.1538/. arXiv:2506.17506.

Nikos Kanakaris, Nikolaos Giarelis, Ilias Siachos, and N. Karacapilidis. Shall i work with them? a knowledge graph-based approach for predicting future research collaborations. *Entropy*, 23, 2021. URL https://api.semanticscholar.org/CorpusId:235301976.

Taniya Kapoor, Abhishek Chandra, Anastasios Stamou, and Stephen J Roberts. Beyond accuracy: Ecol2 metric for sustainable neural pde solvers, 2025. URL https://arxiv.org/abs/2505.12556.

Andrej Karpathy. autoresearch, 2026. URL https://github.com/karpathy/autoresearch. https://github.com/karpathy/autoresearch. Accessed 2026-05-06.

M. G. Kendall. A new measure of rank correlation. *Biometrika*, 30:81–93, 1938. URL https://api.semanticscholar.org/CorpusID:120478295.

M. G. Kendall. The treatment of ties in ranking problems. *Biometrika*, 33(3):239–251, 1945. doi: 10.1093/biomet/33.3.239.

Xiangjie Kong, Yajie Shi, Shuo Yu, Jiaying Liu, and Feng Xia. Academic social networks: Modeling, analysis, mining and applications. *J. Netw. Comput. Appl.*, 132:86–103, 2019. URL https://api.semanticscholar.org/CorpusID:86850665.

Tobias Koopmann, Konstantin Kobs, Konstantin Herud, and Andreas Hotho. Cobert: Scientific collaboration prediction via sequential recommendation. *2021 International Conference on Data Mining Workshops (ICDMW)*, pp. 45–54, 2021. URL https://api.semanticscholar.org/CorpusID:246081502.

Maor Juliet Lavi, Tova Milo, and Mor Geva. Detecting (un)answerability in large language models with linear directions. In Vera Demberg, Kentaro Inui, and Lluís Marquez (eds.), *Proceedings of the 19th Conference of the European Chapter of the Association for Computational Linguistics (Volume 1: Long Papers)*, pp. 682–699, Rabat, Morocco, March 2026. Association for Computational Linguistics. doi: 10.18653/v1/2026.eacl-long.29. URL https://aclanthology.org/2026.eacl-long.29/. arXiv:2509.22449.

Augustine X. W. Lee, Pak-Hei Yeung, and Jagath C. Rajapakse. *Subcortical Masks Generation in CT Images via Ensemble-Based Cross-Domain Label Transfer*, pp. 160–174. Springer Nature Switzerland, July 2025. ISBN 9783031986949. doi: 10.1007/978-3-031-98694-9_12. URL http://dx.doi.org/10.1007/978-3-031-98694-9_12.

Alex Lewandowski, Dale Schuurmans, and Marlos C. Machado. Plastic learning with deep fourier features, 2024. URL https://arxiv.org/abs/2410.20634.

Danyang Li, Yixuan Wang, Matthew Cleaveland, Mingyu Cai, and Roberto Tron. Conformal prediction for signal temporal logic inference. *ArXiv*, abs/2509.25473, 2025. URL https://api.semanticscholar.org/CorpusID:281682043.

Xiuxiu Li, Mingyang Wang, Chaoran Wang, Yujia Fu, and Xianjie Wang. Novsrc: A novelty-oriented scientific collaborators recommendation model. *International Journal of Advanced Computer Science and Applications*, 2024. URL https://api.semanticscholar.org/CorpusID:268818672.

David Liben-Nowell and Jon M. Kleinberg. The link prediction problem for social networks. In *International Conference on Information and Knowledge Management*, 2003. URL http://dl.acm.org/citation.cfm?id=956972.

Chin-Yew Lin. ROUGE: A package for automatic evaluation of summaries. In *Text Summarization Branches Out*, pp. 74–81, Barcelona, Spain, July 2004. Association for Computational Linguistics. URL https://aclanthology.org/W04-1013/.

Chris Lu, Cong Lu, Robert Tjarko Lange, Jakob Nicolaus Foerster, Jeff Clune, and David Ha. The ai scientist: Towards fully automated open-ended scientific discovery. *ArXiv*, abs/2408.06292, 2024. URL https://api.semanticscholar.org/CorpusID:271854887.

Bodhisattwa Prasad Majumder, Harshit Surana, Dhruv Agarwal, Bhavana Dalvi Mishra, Abhijeetsingh Meena, Aryan Prakhar, Tirth Vora, Tushar Khot, Ashish Sabharwal, and Peter Clark. Discoverybench: Towards data-driven discovery with large language models. In *The Thirteenth International Conference on Learning Representations*, 2025. URL https://openreview.net/forum?id=vyflgpwfJW.

Samuel Marks and Max Tegmark. The geometry of truth: Emergent linear structure in large language model representations of true/false datasets. In *First Conference on Language Modeling (COLM)*, 2024. URL https://arxiv.org/abs/2310.06824.

Robert K. Merton. The matthew effect in science. *Science*, 159(3810):56–63, 1968.

Yuyang Miao, Zehua Chen, Chang Li, and Danilo Mandic. Respdiff: An end-to-end multi-scale rnn diffusion model for respiratory waveform estimation from ppg signals, 2024. URL https://arxiv.org/abs/2410.04366.

Antoine Miech, Jean-Baptiste Alayrac, Lucas Smaira, Ivan Laptev, Josef Sivic, and Andrew Zisserman. End-to-end learning of visual representations from uncurated instructional videos. *2020 IEEE/CVF Conference on Computer Vision and Pattern Recognition (CVPR)*, pp. 9876–9886, 2020. URL https://api.semanticscholar.org/CorpusID:209370497.

Joao Monteiro, Pierre-André Noël, Étienne Marcotte, Sai Rajeswar, Valentina Zantedeschi, David Vázquez, Nicolas Chapados, Christopher Pal, and Perouz Taslakian. Repliqa: A question-answering dataset for benchmarking llms on unseen reference content. In *Advances in Neural Information Processing Systems (NeurIPS) Datasets and Benchmarks Track*, 2024. URL https://arxiv.org/abs/2406.11811.

Niklas Muennighoff, Hongjin SU, Liang Wang, Nan Yang, Furu Wei, Tao Yu, Amanpreet Singh, and Douwe Kiela. Generative representational instruction tuning. In *The Thirteenth International Conference on Learning Representations*, 2025. URL https://openreview.net/forum?id=BC4lIvfSzv.

Lankeshwara Munasinghe and Ryutaro Ichise. Time score: A new feature for link prediction in social networks. *IEICE Trans. Inf. Syst.*, 95-D:821–828, 2012. URL https://api.semanticscholar.org/CorpusID:30012200.

Sheshera Mysore, Arman Cohan, and Tom Hope. Multi-vector models with textual guidance for fine-grained scientific document similarity. In Marine Carpuat, Marie-Catherine de Marneffe, and Ivan Vladimir Meza Ruiz (eds.), *Proceedings of the 2022 Conference of the North American Chapter of the Association for Computational Linguistics: Human Language Technologies*, pp. 4453–4470, Seattle, United States, July 2022. Association for Computational Linguistics. doi: 10.18653/v1/2022.naacl-main.331. URL https://aclanthology.org/2022.naacl-main.331/.

Jianmo Ni, Chen Qu, Jing Lu, Zhuyun Dai, Gustavo Hernandez Abrego, Ji Ma, Vincent Zhao, Yi Luan, Keith Hall, Ming-Wei Chang, and Yinfei Yang. Large dual encoders are generalizable retrievers. In Yoav Goldberg, Zornitsa Kozareva, and Yue Zhang (eds.), *Proceedings of the 2022 Conference on Empirical Methods in Natural Language Processing*, pp. 9844–9855, Abu Dhabi, United Arab Emirates, December 2022. Association for Computational Linguistics. doi: 10.18653/v1/2022.emnlp-main.669. URL https://aclanthology.org/2022.emnlp-main.669/.

Zanlin Ni, Yulin Wang, Renping Zhou, Yizeng Han, Jiayi Guo, Zhiyuan Liu, Yuan Yao, and Gao Huang. ENAT: Rethinking spatial-temporal interactions in token-based image synthesis. In *Advances in Neural Information Processing Systems 37 (NeurIPS 2024)*. Curran Associates, Inc., 2024. doi: 10.52202/079017-2870. URL https://proceedings.neurips.cc/paper_files/paper/2024/hash/a488aa1a0c00d76db8a922ef7815a786-Abstract-Conference.html. arXiv:2411.06959.

NIST TREC. Common evaluation measures. TREC 2006 Proceedings (Appendix), 2006. URL https://trec.nist.gov/pubs/trec15/appendices/CE.MEASURES06.pdf. Appendix CE.MEASURES06.

Dan Ofer, Hadasah Kaufman, and Michal Linial. What's next? forecasting scientific research trends. *Heliyon*, 2023. doi: 10.1016/j.heliyon.2023.e23781.

Team Olmo, :, Allyson Ettinger, Amanda Bertsch, Bailey Kuehl, David Graham, David Heineman, Dirk Groeneveld, Faeze Brahman, Finbarr Timbers, Hamish Ivison, Jacob Morrison, Jake Poznanski, Kyle Lo, Luca Soldaini, Matt Jordan, Mayee Chen, Michael Noukhovitch, Nathan Lambert, Pete Walsh, Pradeep Dasigi, Robert Berry, Saumya Malik, Saurabh Shah, Scott Geng, Shane Arora, Shashank Gupta, Taira Anderson, Teng Xiao, Tyler Murray, Tyler Romero, Victoria Graf, Akari Asai, Akshita Bhagia, Alexander Wettig, Alisa Liu, Aman Rangapur, Chloe Anastasiades, Costa

Huang, Dustin Schwenk, Harsh Trivedi, Ian Magnusson, Jaron Lochner, Jiacheng Liu, Lester James V. Miranda, Maarten Sap, Malia Morgan, Michael Schmitz, Michal Guerquin, Michael Wilson, Regan Huff, Ronan Le Bras, Rui Xin, Rulin Shao, Sam Skjonsberg, Shannon Zejiang Shen, Shuyue Stella Li, Tucker Wilde, Valentina Pyatkin, Will Merrill, Yapei Chang, Yuling Gu, Zhiyuan Zeng, Ashish Sabharwal, Luke Zettlemoyer, Pang Wei Koh, Ali Farhadi, Noah A. Smith, and Hannaneh Hajishirzi. Olmo 3, 2025. URL https://arxiv.org/abs/2512.13961.

Joshua O'Madadhain, Jon Hutchins, and Padhraic Smyth. Prediction and ranking algorithms for event-based network data. *SIGKDD Explor.*, 7:23–30, 2005. URL https://api.semanticscholar.org/CorpusID:3343116.

Andre Opris. A first runtime analysis of nsga-iii on a many-objective multimodal problem: Provable exponential speedup via stochastic population update. In *Proceedings of the Thirty-Fourth International Joint Conference on Artificial Intelligence, IJCAI-25*, pp. 8903–8911. International Joint Conferences on Artificial Intelligence Organization, 2025. doi: 10.24963/ijcai.2025/990. URL https://doi.org/10.24963/ijcai.2025/990. arXiv:2505.01256.

Aniket Pramanick, Yufang Hou, Saif M. Mohammad, and Iryna Gurevych. The nature of NLP: Analyzing contributions in NLP papers. In Wanxiang Che, Joyce Nabende, Ekaterina Shutova, and Mohammad Taher Pilehvar (eds.), *Proceedings of the 63rd Annual Meeting of the Association for Computational Linguistics (Volume 1: Long Papers)*, pp. 25169–25191, Vienna, Austria, jul 2025. Association for Computational Linguistics. doi: 10.18653/v1/2025.acl-long.1224. URL https://aclanthology.org/2025.acl-long.1224/.

Marissa Radensky, Simra Shahid, Raymond Fok, Pao Siangliulue, Tom Hope, and Daniel S. Weld. Human-LLM compound system for scientific ideation through facet recombination and novelty evaluation. *ArXiv*, abs/2409.14634, 2024. URL https://api.semanticscholar.org/CorpusID:272827497.

Pranav Rajpurkar, Jian Zhang, Konstantin Lopyrev, and Percy Liang. SQuAD: 100,000+ questions for machine comprehension of text. In Jian Su, Kevin Duh, and Xavier Carreras (eds.), *Proceedings of the 2016 Conference on Empirical Methods in Natural Language Processing*, pp. 2383–2392, Austin, Texas, November 2016. Association for Computational Linguistics. doi: 10.18653/v1/D16-1264. URL https://aclanthology.org/D16-1264/.

Kiyan Rezaee, Morteza Ziabakhsh, Niloofar Nikfarjam, et al. FOS: A large-scale temporal graph benchmark for scientific interdisciplinary link prediction. *arXiv preprint arXiv:2511.18631*, 2025. URL https://arxiv.org/abs/2511.18631.

Paul M. Riechers, Thomas J. Elliott, and Adam S. Shai. Neural networks leverage nominally quantum and post-quantum representations, 2025. URL https://arxiv.org/abs/2507.07432.

Angelo Salatino, Andrea Mannocci, and Francesco Osborne. Detection, analysis, and prediction of research topics with scientific knowledge graphs. In *Predicting the Dynamics of Research Impact*. Springer, 2021. doi: 10.1007/978-3-030-86668-6_11.

Samuel Schmidgall and Michael Moor. Agentrxiv: Towards collaborative autonomous research. *ArXiv*, abs/2503.18102, 2025. URL https://api.semanticscholar.org/CorpusID:277271871.

Sina Semnani, Han Zhang, Xinyan He, Merve Tekgurler, and Monica Lam. Churro: Making history readable with an open-weight large vision-language model for high-accuracy, low-cost historical text recognition. In Christos Christodoulopoulos, Tanmoy Chakraborty, Carolyn Rose, and Violet Peng (eds.), *Proceedings of the 2025 Conference on Empirical Methods in Natural Language Processing*, pp. 34777–34824, Suzhou, China, nov 2025. Association for Computational Linguistics. ISBN 979-8-89176-332-6. doi: 10.18653/v1/2025.emnlp-main.1763. URL https://aclanthology.org/2025.emnlp-main.1763/. arXiv:2509.19768.

Michael Shalyt, Uri Seligmann, Itay Beit Halachmi, Ofir David, Rotem Elimelech, and Ido Kaminer. Unsupervised discovery of formulas for mathematical constants. In *Advances in Neural Information Processing Systems*, volume 37. Curran Associates, Inc., 2024. doi: 10.52202/079017-3596. URL https://proceedings.neurips.cc/paper_files/paper/2024/

hash/cd8b5de90ebfd6df2b703d2346370cba-Abstract-Conference.html. arXiv:2412.16818.

Sahel Sharifymoghaddam, Ronak Pradeep, Andre Slavescu, Ryan Nguyen, Andrew Xu, Zijian Chen, Yilin Zhang, Yidi Chen, Jasper Xian, and Jimmy Lin. Rankllm: A python package for reranking with llms. In *Proceedings of the 48th International ACM SIGIR Conference on Research and Development in Information Retrieval (SIGIR '25)*, pp. 3681–3690, Padua, Italy, 2025. Association for Computing Machinery. doi: 10.1145/3726302.3730331. URL https://doi.org/10.1145/3726302.3730331. arXiv:2505.19284.

Feng Shi and James Evans. Surprising combinations of research contents and contexts are related to impact and emerge with scientific outsiders from distant disciplines. *Nature Communications*, 14 (1):1641, 2023.

Chenglei Si, Diyi Yang, and Tatsunori Hashimoto. Can llms generate novel research ideas? a large-scale human study with 100+ nlp researchers. *ArXiv*, abs/2409.04109, 2024. URL https://api.semanticscholar.org/CorpusID:272463952.

Amanpreet Singh, Mike D'Arcy, Arman Cohan, Doug Downey, and Sergey Feldman. SciRepEval: A multi-format benchmark for scientific document representations. In Houda Bouamor, Juan Pino, and Kalika Bali (eds.), *Proceedings of the 2023 Conference on Empirical Methods in Natural Language Processing*, pp. 5548–5566, Singapore, December 2023. Association for Computational Linguistics. doi: 10.18653/v1/2023.emnlp-main.338. URL https://aclanthology.org/2023.emnlp-main.338/.

Aviv Slobodkin, Omer Goldman, Avi Caciularu, Ido Dagan, and Shauli Ravfogel. The curious case of hallucinatory (un)answerability: Finding truths in the hidden states of over-confident large language models. In Houda Bouamor, Juan Pino, and Kalika Bali (eds.), *Proceedings of the 2023 Conference on Empirical Methods in Natural Language Processing*, pp. 3607–3625, Singapore, December 2023. Association for Computational Linguistics. doi: 10.18653/v1/2023.emnlp-main.220. URL https://aclanthology.org/2023.emnlp-main.220/.

Noy Sternlicht and Tom Hope. CHIMERA: A knowledge base of scientific idea recombinations for research analysis and ideation. In *Proceedings of the 64th Annual Meeting of the Association for Computational Linguistics (Volume 1: Long Papers)*, pp. 1871–1905, 2026. doi: 10.18653/v1/2026.acl-long.85.

Haoyang Su, Renqi Chen, Shixiang Tang, Zhenfei Yin, Xinzhe Zheng, Jinzhe Li, Biqing Qi, Qi Wu, Hui Li, Wanli Ouyang, Philip Torr, Bowen Zhou, and Nanqing Dong. Many heads are better than one: Improved scientific idea generation by a LLM-based multi-agent system. In Wanxiang Che, Joyce Nabende, Ekaterina Shutova, and Mohammad Taher Pilehvar (eds.), *Proceedings of the 63rd Annual Meeting of the Association for Computational Linguistics (Volume 1: Long Papers)*, pp. 28201–28240, Vienna, Austria, July 2025. Association for Computational Linguistics. ISBN 979-8-89176-251-0. doi: 10.18653/v1/2025.acl-long.1368. URL https://aclanthology.org/2025.acl-long.1368/.

Shivashankar Subramanian, Daniel King, Doug Downey, and Sergey Feldman. S2AND: A benchmark and evaluation system for author name disambiguation. In *2021 ACM/IEEE Joint Conference on Digital Libraries (JCDL)*, pp. 170–179. IEEE, 2021. doi: 10.1109/JCDL52503.2021.00029.

Yizhou Sun, R. Barber, Manish Gupta, C. Aggarwal, and Jiawei Han. Co-author relationship prediction in heterogeneous bibliographic networks. *2011 International Conference on Advances in Social Networks Analysis and Mining*, pp. 121–128, 2011. URL http://ieeexplore.ieee.org/stamp/stamp.jsp?tp=&arnumber=5992571.

Don R. Swanson. Undiscovered public knowledge. *The Library Quarterly*, 56:103 – 118, 1986. URL https://api.semanticscholar.org/CorpusID:267792818.

Kyle Swanson, Wesley Wu, Nash L. Bulaong, John E. Pak, and James Zou. The virtual lab of ai agents designs new sars-cov-2 nanobodies. *Nature*, 646(8085):716–723, 2025. doi: 10.1038/s41586-025-09442-9. URL https://doi.org/10.1038/s41586-025-09442-9.

Qwen Team. Qwen3 technical report, 2025. URL https://arxiv.org/abs/2505.09388.

Marta Tuninetti, Alberto Aleta, Daniela Paolotti, Yamir Moreno, and Michele Starnini. Prediction of new scientific collaborations through multiplex networks. *EPJ Data Science*, 10, 2021. URL https://api.semanticscholar.org/CorpusID:234489207.

Shahadat Uddin, Liaquat Hossain, and Kim J. R. Rasmussen. Network effects on scientific collaborations. *PLoS ONE*, 8, 2013. URL https://api.semanticscholar.org/CorpusID:7633781.

Marco Antonio Valenzuela-Escarcega, Vu A. Ha, and Oren Etzioni. Identifying meaningful citations. In *AAAI Workshop: Scholarly Big Data*, 2015. URL https://api.semanticscholar.org/CorpusID:2538517.

Alex D Wade. The semantic scholar academic graph (s2ag). *Companion Proceedings of the Web Conference 2022*, 2022. URL https://api.semanticscholar.org/CorpusID:251597885.

Dashun Wang, Chaoming Song, and Albert-László Barabási. Quantifying long-term scientific impact. *Science*, 342:127 – 132, 2013. URL https://api.semanticscholar.org/CorpusID:260558492.

Heng Wang, Pengcheng Jiang, Jiashuo Sun, Zhiyi Shi, Haofei Yu, Jiawei Han, and Heng Ji. Learning to predict future-aligned research proposals with language models, 2026. URL https://arxiv.org/abs/2603.27146.

Qingyun Wang, Doug Downey, Heng Ji, and Tom Hope. Scimon: Scientific inspiration machines optimized for novelty. In *Annual Meeting of the Association for Computational Linguistics*, 2024a. URL https://api.semanticscholar.org/CorpusID:258841365.

Wenxiao Wang, Lihui Gu, Liye Zhang, Yunxiang Luo, Yi Dai, Chen Shen, Liang Xie, Binbin Lin, Xiaofei He, and Jieping Ye. Scipip: An llm-based scientific paper idea proposer. *ArXiv*, abs/2410.23166, 2024b. URL https://api.semanticscholar.org/CorpusID:273695165.

Yike Wang, Shangbin Feng, Yulia Tsvetkov, and Hannaneh Hajishirzi. ScienceMeter: Tracking scientific knowledge updates in language models. *arXiv preprint arXiv:2505.24302*, 2025. URL https://arxiv.org/abs/2505.24302.

Xiaowen Xi, Ying Guo, and Weiyu Duan. Recommendation of academic collaborators: A methodology incorporating word embedding and network embedding. In *AII@iConference*, 2021. URL https://api.semanticscholar.org/CorpusID:235259334.

Yahan Yang, Soham Dan, Dan Roth, and Insup Lee. Benchmarking llm guardrails in handling multilingual toxicity, 2024. URL https://arxiv.org/abs/2410.22153.

Bingyang Ye, Shan Chen, Jingxuan Tu, et al. Proof of time: A benchmark for evaluating scientific idea judgments. *arXiv preprint arXiv:2601.07606*, 2026. URL https://arxiv.org/abs/2601.07606.

Zhangyue Yin, Qiushi Sun, Qipeng Guo, Jiawen Wu, Xipeng Qiu, and Xuanjing Huang. Do large language models know what they don't know? In Anna Rogers, Jordan Boyd-Graber, and Naoaki Okazaki (eds.), *Findings of the Association for Computational Linguistics: ACL 2023*, pp. 8653–8665, Toronto, Canada, July 2023. Association for Computational Linguistics. doi: 10.18653/v1/2023.findings-acl.551. URL https://aclanthology.org/2023.findings-acl.551/.

Haofei Yu, Zhaochen Hong, Zirui Cheng, Kunlun Zhu, Keyang Xuan, Jinwei Yao, Tao Feng, and Jiaxuan You. Researchtown: Simulator of human research community. In *Proceedings of the 42nd International Conference on Machine Learning*, volume 267 of *Proceedings of Machine Learning Research*, pp. 73051–73096. PMLR, 2025. URL https://proceedings.mlr.press/v267/yu25i.html. arXiv:2412.17767.

Xinyan Yu, Sewon Min, Luke Zettlemoyer, and Hannaneh Hajishirzi. CREPE: Open-domain question answering with false presuppositions. In Anna Rogers, Jordan Boyd-Graber, and Naoaki Okazaki (eds.), *Proceedings of the 61st Annual Meeting of the Association for Computational Linguistics (Volume 1: Long Papers)*, pp. 10457–10480, Toronto, Canada, July 2023. Association for Computational Linguistics. doi: 10.18653/v1/2023.acl-long.583. URL https://aclanthology.org/2023.acl-long.583/.

Tianyi Zhang, Varsha Kishore, Felix Wu, Kilian Q. Weinberger, and Yoav Artzi. BERTScore: Evaluating text generation with BERT. In *8th International Conference on Learning Representations (ICLR 2020), Addis Ababa, Ethiopia, April 26–30, 2020*. OpenReview.net, 2020. URL https://openreview.net/forum?id=SkeHuCVFDr.

Yixian Zhang, Huaze Tang, Chao Wang, and Wenbo Ding. Policy newton algorithm in reproducing kernel hilbert space, 2025. URL https://arxiv.org/abs/2506.01597.

Zhen Zhang and James Evans. Language model perplexity predicts scientific surprise and transformative impact. *arXiv preprint arXiv:2509.05591*, 2025.

Zitong Zhang, Braja Gopal Patra, Ashraf Yaseen, Jie Zhu, Rachit Sabharwal, Kirk Roberts, Tru Hoang Cao, and Hulin Wu. Scholarly recommendation systems: a literature survey. *Knowledge and Information Systems*, 65:4433–4478, 2023. URL https://api.semanticscholar.org/CorpusID:259081885.

Chunheng Zhao, Pierluigi Pisu, Gurcan Comert, Negash Begashaw, Varghese Vaidyan, and Nina Christine Hubig. Causal interpretability for adversarial robustness: A hybrid generative classification approach, 2024. URL https://arxiv.org/abs/2412.20025.

Lianmin Zheng, Wei-Lin Chiang, Ying Sheng, Siyuan Zhuang, Zhanghao Wu, Yonghao Zhuang, Zi Lin, Zhuohan Li, Dacheng Li, Eric P. Xing, Hao Zhang, Joseph E. Gonzalez, and Ion Stoica. Judging LLM-as-a-judge with MT-bench and chatbot arena. In *Advances in Neural Information Processing Systems 36 (NeurIPS 2023) Datasets and Benchmarks Track*, volume 36, 2023. URL https://proceedings.neurips.cc/paper_files/paper/2023/hash/91f18a1287b398d378ef22505bf41832-Abstract-Datasets_and_Benchmarks.html. arXiv:2306.05685.

A Limitations

As a first step toward building a holistic benchmark for a complex, co-evolving real-world process, our work has several limitations. Our benchmark focuses on seven tasks from among many possibilities, one of which is predicting citations which is a limited signal of scientific impact. There exist variables (e.g. conferences, grants, institutions) we do not include in our dataset that influence the arc of science. Further, the methods evaluated in this paper are a partial set of all available techniques. We hope that our openly released benchmark and dataset construction infrastructure facilitates addressing these limitations in future work.

B DATASET

B.1 SUMMARY STATISTICS

Table 6 reports full dataset statistics for both domains, including medians and title-abstract lengths.

Table 6: Full dataset statistics for both domains. Average and median statistics are computed over target papers. *All* counts each paper once.

	PRESCIENCE-AI			PRESCIENCE-QUANTUM		
	Train	Test	All	Train	Test	All
Target Papers	49,351	67,575	116,926	13,290	18,220	31,510
All Papers	482,420	629,936	673,385	371,813	442,167	493,426
Avg. Words	187.1	190.5	189.0	174.5	177.7	176.4
Avg. Infl. Refs	3.06	2.89	2.96	2.55	2.45	2.50
Med. Infl. Refs	3	2	2	2	2	2
Unique Authors	124,510	159,196	218,393	43,804	56,508	80,581
Avg. Authors	5.26	5.24	5.25	4.90	4.84	4.86
Avg. Author Hist.	24.9	30.0	27.8	34.4	35.2	34.9
Med. Author Hist.	8	9	8	9	9	9
Avg. Citations @ 12m	6.35	4.64	6.07	2.47	2.59	2.49

Figure 3 visualizes key properties of PRESCIENCE-AI over target papers, including distributions of author counts per paper, author publication history lengths, influential reference counts, and citation trajectories. These statistics highlight the heavy-tailed and heterogeneous structure of the benchmark, which underlies the difficulty of forecasting collaboration, literature choice, and downstream impact. Figure 4 shows the same distributions for PRESCIENCE-QUANTUM.

B.2 FEATURES

We organize papers in PRESCIENCE into four roles: target papers, influential references of target papers, papers in a target author's publication history, and influential references of those publication-history papers. All papers share a common set of bibliographic fields (Semantic Scholar corpus ID, arXiv ID, publication date, arXiv categories, title, and abstract). For target papers, the publication date t_p is the arXiv submission date; companion papers use their Semantic Scholar publication date.

For target papers, we additionally ensure the availability of complete, temporally aligned citation- and author-level metadata, including influential references, cumulative citation counts at the time of publication, and author statistics (IDs, names, h-indices, publication counts, and citation counts), as well as each author's publication history up to the same publication time.

For certain companion papers, some feature availability is *best-effort*: we include influential references and basic author identity when they can be reliably recovered from the Semantic Scholar Graph and matched to arXiv preprints, but these fields may be empty when a cited work is not indexed by Semantic Scholar or does not have an arXiv version. Table 7 summarizes feature availability by role, with checkmarks indicating required fields and parentheses indicating best-effort fields.

B.3 TOPIC TAXONOMY AND LABELING

Topic taxonomy. We construct a flat taxonomy of 202 AI research topics for aggregate forecasting. We obtained an initial topic set by prompting GPT-5.4 with internet access enabled to propose approximately 200 fine-grained AI research topics active in literature posted between October 2023 and September 2024 in the arXiv categories listed in Section 2. We then manually refined the initial list by adding missing topics to improve coverage over the PRESCIENCE-AI dataset and merging redundant entries, yielding the final 202-topic taxonomy.

We provide the full topic list below:

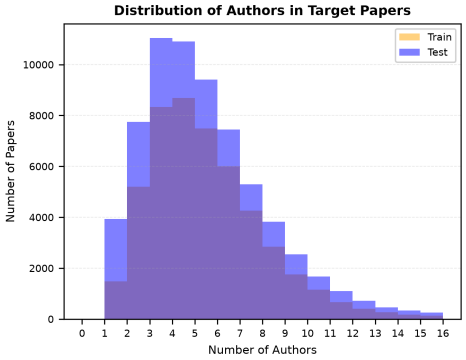

(a) Number of Authors per paper

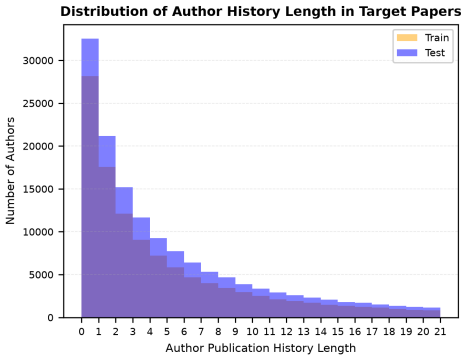

(b) Author Publication History Length

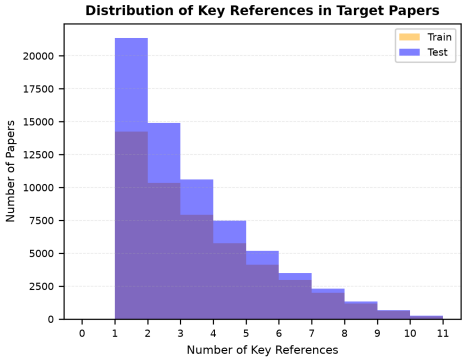

(c) Number of Influential References per paper

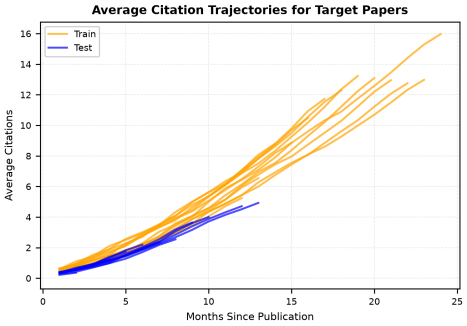

(d) (Averaged) Citation Trajectories of target papers of various ages in the PRESCIENCE-AI corpus

Figure 3: Author, Influential Reference and Citation Trajectory statistics plotted over Target papers.

Table 7: Feature availability by paper role in the PRESCIENCE dataset. A checkmark (✓) indicates that the field is provided; parentheses indicate best-effort availability. All papers are restricted to arXiv preprints reachable from at least one target paper through the relations described in Section 2.

Field	**Target**	**Target.Infl. Ref**	**Author Pub. Hist.**	**Author Pub. Hist. Infl. Ref**
Paper Metadata				
Corpus ID	✓	✓	✓	✓
arXiv ID	✓	✓	✓	✓
Publication Date	✓	✓	✓	✓
arXiv Categories	✓	✓	✓	✓
Topics	✓	✓	✓	✓
Title	✓	✓	✓	✓
Abstract	✓	✓	✓	✓
Citation and Reference Data				
Influential References	✓	–	(✓)	–
Citation Trajectory	✓	–	–	–
Author Metadata				
Author IDs	✓	–	(✓)	–
Author Names	✓	–	(✓)	–
Author h-index	✓	–	–	–
Author Num. Papers	✓	–	–	–
Author Num. Citations	✓	–	–	–
Publication History	✓	–	–	–

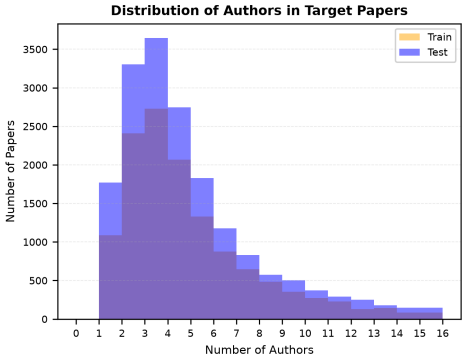

(a) Number of Authors per paper

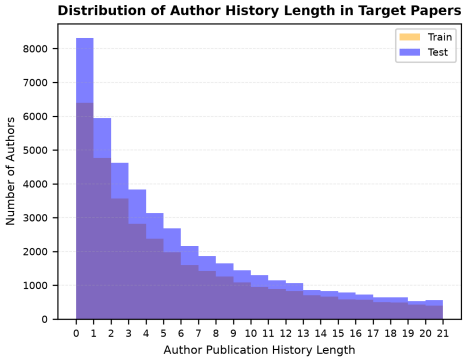

(b) Author Publication History Length

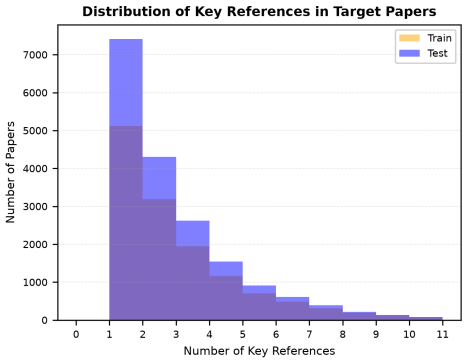

(c) Number of Influential References per paper

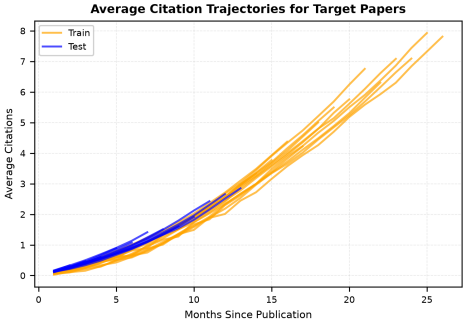

(d) (Averaged) Citation Trajectories of target papers of various ages in the PRESCIENCE-QUANTUM corpus

Figure 4: PRESCIENCE-QUANTUM author, influential reference and citation trajectory statistics plotted over target papers.


```
["Instruction tuning", "Preference optimization / alignment", "RLHF /
RLAIF for post-training", "Prompt engineering / prompt optimization",
"Prompt tuning / soft prompting", "Parameter-efficient fine-tuning",
"In-context learning", "Long-context modeling", "Personalized language
modeling", "Retrieval-augmented generation", "Tool / API-augmented
language modeling", "Knowledge editing / model updating", "Model
compression / distillation for LMs", "Chain-of-thought prompting",
"Tree/search-based reasoning", "Self-critique / self-refinement",
"Language-model planning", "Web/navigation agents", "Code-generation
agents", "Multi-agent LLM collaboration", "Memory mechanisms for
LLM agents", "Multimodal language agents", "Agent evaluation and
benchmarks", "Hallucination detection and mitigation", "Calibration
/ uncertainty estimation for LLMs", "Jailbreak and prompt-injection
robustness", "Privacy leakage / machine unlearning for LMs", "Mechanistic
interpretability of transformers and LLMs", "Dialogue modeling",
"Dialogue state tracking", "Dialogue evaluation", "Multimodal dialogue",
"User modeling for conversational AI", "Proactive conversational AI",
"Contextual dialogue modeling", "Information extraction", "Relation
extraction", "Event extraction", "Question answering", "Summarization",
"Long-document understanding", "Argument mining", "Stance detection",
"Sentiment analysis", "Syntactic parsing / tagging / chunking",
"Morphology and word segmentation", "Sentence-level semantics and
textual inference", "Figurative language understanding / generation",
"Machine translation", "Low-resource NLP", "Multilingual representation
learning", "Cross-cultural NLP", "Multimodality and language grounding",
"Knowledge-augmented NLP", "Scientific NLP", "Scholarly document
processing", "Citation / evidence extraction", "Climate NLP",
```

"Language-and-molecules modeling", "Dense retrieval", "Neural ranking / learning to rank", "Generative retrieval", "Conversational search", "RAG system design and evaluation", "Knowledge-enhanced retrieval", "Long-context retrieval", "LLM-based IR evaluation", "Collaborative filtering", "Knowledge-based recommendation", "Deep learning for recommender systems", "Natural-language / conversational recommenders", "Fair / privacy-aware recommendation", "3D reconstruction from multi-view and sensors", "3D reconstruction from single images", "Adversarial attack and defense in vision", "Biometrics", "Computational imaging", "Datasets and evaluation for vision", "Efficient and scalable vision models", "Face analysis", "Body / pose / gesture / motion understanding", "Low-level vision", "Document analysis and understanding", "Open-set / open-world recognition", "Out-of-distribution detection in vision", "Fine-grained visual categorization", "Self-supervised visual representation learning", "Semi-supervised visual learning", "Few-shot visual recognition", "Domain adaptation in vision", "Diffusion models for image synthesis", "Autoregressive image generation", "Generative-model inversion", "Image editing with generative models", "Synthetic data for visual recognition", "Analysis-by-synthesis / render-and-compare recognition", "3D foundation models", "3D content creation", "Neural radiance fields", "3D Gaussian splatting", "Implicit neural representations", "Novel-view synthesis", "Long-form video understanding", "Human action understanding / generation", "Large multimodal model evaluation", "Visual-prompt understanding in multimodal models", "Open-vocabulary / open-task vision-language models", "Vision-language reasoning", "Medical vision foundation models", "Medical image / video generation", "Biomedical image parsing", "Pathology image models", "Radiology foundation-model applications", "Medical imaging data curation", "Medical imaging data augmentation", "Fairness and safety in medical imaging AI", "Automatic speech recognition", "ASR error correction / rescoring", "Multilingual / multi-accent ASR", "Spoken language translation", "Spoken language understanding", "Text-to-speech", "Voice conversion", "Speaker verification", "Speaker diarization", "Speech processing with discrete units", "Speech emotion recognition / paralinguistics", "Pathological / health-related speech analysis", "Multi-channel speech enhancement", "Human-machine spoken interaction", "Responsible speech foundation models", "Speech deepfake / spoofing detection", "Streaming ASR", "Self-supervised learning for ASR", "Target-speaker extraction", "Deep reinforcement learning", "Hierarchical reinforcement learning", "Model-based reinforcement learning", "Policy optimization", "Bandits", "Sequential decision-making under uncertainty", "Active learning", "Adversarial learning", "Causal inference", "Causal discovery", "Causal representation learning", "Uncertainty quantification", "Probabilistic programming", "Approximate / variational inference", "Performative prediction", "Bayesian methods", "Belief propagation", "Robot foundation models", "Representation learning for robotic perception and control", "Imitation learning for robotics", "Reinforcement learning for physical robots", "Learning-and-planning hybrids in robotics", "Uncertainty-aware robotics", "Automatic robotic data generation", "Multimodal robot perception and sensor fusion", "Human-robot interaction with language / gestures", "Learning for robot task and motion planning", "Learning for hardware design and optimization", "Robot safety for learning-based systems", "Robot manipulation", "Visual navigation", "Locomotion learning", "Autonomous driving perception / prediction / planning", "Embodied question answering / embodied vision-language", "Open-world embodied AI", "Generative AI for embodied AI", "Dataset composition and curation for foundation models", "Data filtering / relabeling / augmentation", "Dataset quality / diversity / provenance analysis", "Data debugging / influence analysis", "Dataset distillation", "Synthetic-data effects / model collapse", "Weak-to-strong generalization", "Graph neural networks", "Relational / structured learning", "Spatio-temporal learning", "Time-series modeling", "Time-series foundation models", "Federated learning", "Privacy and security in data-centric ML", "Deep learning theory (training dynamics, generalization, optimization convergence)", "Scientific machine learning (PDE solvers, neural operators, PINNs)",

Table 8: Summary statistics for topic labels per target paper. Papers assigned only to the residual *Other* category are counted as having zero taxonomy labels.

Subset	n	Mean	Stdev	Min	p50	p95	Max
All papers, incl. *Other*	117,072	3.44	1.99	0	3	7	19
Papers with ≥ 1 label	110,491	3.65	1.86	1	3	7	19

Table 9: Summary statistics for the number of papers assigned to each topic label across time slices.

Slice	n	Mean	Stdev	Min	p50	p95	Max
Train	202	794	904	12	482.5	2,470	6,501
Test	202	1,201	1,351	16	762.5	3,847	8,602
All-time	202	1,994	2,230	35	1,178	6,436	15,103

```
"Continual learning and catastrophic forgetting", "Object detection,
segmentation, and tracking in vision", "Video segmentation, tracking,
and generation", "Remote sensing and geospatial vision", "Medical image
segmentation and reconstruction (beyond foundation models)", "Biomedical
signal analysis (EEG, ECG, physiological)", "Quantum machine learning",
"Spiking and neuromorphic computing", "Explainable AI (non-mechanistic /
non-LLM)", "AI governance, policy, and societal impact", "Systems and
serving infrastructure for large models", "Audio and music modeling
(non-speech)", "Tabular machine learning and AutoML", "Point cloud and
3D geometric learning", "Wireless communications and signal processing"]
```

Per-paper labeling. We label each of the target papers in the train and test periods using `gpt-5.4-2026-03-05` using the prompt provided in Appendix H.1. The prompt provides the paper's title and abstract along with the full taxonomy, and asks the model to return all applicable topics in JSON format, ordered by relevance. We instruct the model to exactly match topics from the taxonomy, include every topic directly addressed by the paper rather than only its primary focus, and exclude topics mentioned only in passing. Papers for which the model returns no applicable topic are assigned to a residual *Other* category; these account for approximately 5.6% of target papers and are excluded from topic trend forecasting evaluation. We provide associated statistics in Tables 8 and 9:

Cross-labeler validation. To assess labeling reliability, we relabel a random sample of 530 papers with Claude Opus 4.7 using the same prompt. Agreement in assigned labels is substantial: per-paper label F1 is 0.67 over all 530 papers, and 0.70 over the 501 papers for which both labelers assign at least one topic.

External validation of topic labels. To check that the GPT-5.4 topic labels correspond to semantically meaningful paper groupings, we compare them against GRIT embeddings, an independent representation computed without access to our taxonomy. For each of the 202 topics, we sample 2,000 pairs of papers assigned to that topic and compute their mean cosine similarity. We compare this to a null distribution estimated from 50,000 random paper pairs. Intra-topic similarity exceeds the null for every topic, with a median z-score of 1.22. Since GRIT is trained independently of our topic taxonomy, this consistent positive gap suggests that the labels recover semantically coherent groups of papers rather than arbitrary partitions.

Together, the cross-labeler agreement and embedding-based validation suggest that the GPT-5.4 labels provide a reasonable topic assignment for our topic trend forecasting task; however, PRESCIENCE also provides various kinds of paper metadata (Appendix B.2), allowing users to construct alternative topic taxonomies or labels for their own analyses, including with more expensive or specialized methods.

PRESCIENCE-AI is our fully annotated primary benchmark and the focus of the main paper. PRESCIENCE-QUANTUM demonstrates that the construction pipeline, tasks, and baselines transfer to a distinct scientific domain: we report results for all five paper-anchored tasks and corpus-generation rollouts on it (Appendix F), which show the same qualitative trends. We do not construct a topic taxonomy for PRESCIENCE-QUANTUM, since refining and validating one requires physics expertise

that we lack; because both domains share the same schema, researchers with such expertise can add topic labels or other annotations, for example by applying the labeling procedure above with a domain-specific taxonomy.

C A METRIC FOR CONTRIBUTION GENERATION

C.1 FACETSCORE

Unsatisfied with existing measures of textual similarity (ROUGE-L, BERTScore (Zhang et al., 2020), ASPIRE-OT (Mysore et al., 2022)), we developed a similarity metric called FacetScore based on the Scideator project (Radensky et al., 2024). Intended to assist in scientific ideation, Scideator (Radensky et al., 2024) introduced the representation of a scientific advance as a combination of several *facets*: purpose, mechanism, and evaluation. We further added a notion of scientific contribution type, extending the taxonomy of Pramanick et al. (2025) (an artifact, knowledge, or better understanding), into this collection of facets. Once FacetScore extracts each of these fields from the provided pair of title-abstracts, it prompts an LLM to score the similarity between corresponding pairs of facets on a five-point scale. Finally, FacetScore returns the average of these facet-level similarity scores as the overall similarity score between the two provided papers.

However, we opted to omit FacetScore computations from our later experiments since we found that LACER judgements correlate significantly better with human judgements (Figure 5).

C.2 LACER

In our experiments, existing automatic textual similarity metrics (ROUGE-L, BERTScore (Zhang et al., 2020), ASPIRE-OT (Mysore et al., 2022), retrieval-based mean reciprocal rank (MRR), etc.) exhibited limited dynamic range: substantially different generated title-abstract pairs received similar scores, and it was often unclear or arbitrary, the degree of dissimilarity that yields a score at the lower extreme of the scale. To address this, we define LACER, an LLM-as-judge metric explicitly calibrated to a 1-10 semantic alignment scale using automatically constructed demonstrations.

Instead of relying on human-annotated similarity judgments, we generate calibration examples by interpolating between two intuitive endpoints. For each demonstration sequence, an influential reference whose abstract lies at the 50th percentile[4] of n-gram overlap with the target defines score 1, representing related but clearly distinct prior work. A paraphrase of the target abstract defines score 10, representing near-semantic equivalence.

We then prompt (Appendix H.4) GPT-5 to generate intermediate title–abstract pairs for scores 2 through 9 by gradually modifying one semantic aspect at a time (e.g., contribution type, model architecture, or task domain), forming a smooth transition between these endpoints. Five such interpolation sequences are included as few-shot examples in the scoring prompt (Appendix H.5), which the judge model uses to assign calibrated 1–10 scores to new generation–reference pairs.

This approach anchors the LACER scale in concrete, task-specific contrasts while avoiding the cost of manual annotation, while also providing a well-defined and sensitive measure of conceptual alignment in scientific contributions.

C.2.1 EFFECT OF LLM JUDGE CHOICE ON LACER

Table 10 compares LACER scores for Contribution Generation under two independent LLM-based judges (GPT-5 and Claude Opus 4.5), computed over target papers posted between October 2024 and September 2025. We observe shifts in absolute values but strong agreement in relative ordering (Pearson 0.97, Spearman 0.81), suggesting that our main comparisons are not sensitive to the specific choice of judge.

C.3 VALIDATING CONTRIBUTION GENERATION METRICS

To develop and select among candidate metrics for the Contribution Generation task, we constructed both a validation set and a test set of human preference judgments.

For the test set, we sampled ten (influential reference, target) pairs from target papers posted between October 2023 and September 2024. For each pair, we generated multiple candidate

[4]We also experimented with using 25th percentile, 75th percentile, and randomly chosen influential references to define the minimum LACER. We found that this choice does not meaningfully change its judgements.

Table 10: LACER scores (n=1000) for Contribution Generation as judged by GPT-5 and Claude Opus 4.5, computed over target papers in the same AI categories posted between October 2024 and September 2025. The scores have a Pearson correlation of 0.97 and a Spearman correlation of 0.81.

Model	LACER (GPT-5)	LACER (Opus)	LACER (Avg)
Influential Reference	4.30	4.05	4.18
GPT-4o	4.74	4.53	4.63
GPT-4.1	5.11	4.60	4.86
o3	5.50	4.67	5.08
GPT-5	5.66	4.65	5.16
GPT-5.1	5.39	4.74	5.07
GPT-5.2	5.63	4.70	5.16
Claude Sonnet 4.5	5.04	4.44	4.74
Claude Opus 4.5	5.04	4.55	4.79
Gold Paraphrase	10.00	9.79	9.89

scientific advances, effectively attempting to reproduce the target from its influential references: concretely, we prompted each of `claude-3-sonnet-20240229`, `gpt-4o-2024-11-20`, `meta-llama/Meta-Llama-3.1-8B-Instruct`, and `o3_mini` to produce multiple follow-up contributions. From the union of these generations and the target paper's ground-truth influential references, we randomly sampled ten title–abstract pairs to use for annotation and evaluation.

Human annotators (drawn from PRESCIENCE's authors) ranked the sampled generated contributions by conceptual similarity to the target paper's ground-truth abstract, allowing ties. In the test set, each annotator ranked all candidates. For the validation set, we generated ten additional targets with corresponding candidate generations; these were singly annotated. We used the validation set internally to experiment with variations of FacetScore and LACER, and report results in this paper computed over the test set and the final versions of these metrics.

We measured inter-annotator agreement (IAA) and automated metrics' agreement with human judgments using Kendall's τ_b (Kendall, 1938; 1945) evaluated over the above test set. Annotators exhibit substantial agreement on this task, though some variability remains. We find that LACER is the only metric that approaches agreement comparable with human IAA. Further, LACER judgments appear robust to the choice of underlying LLM judge (Figure 5).

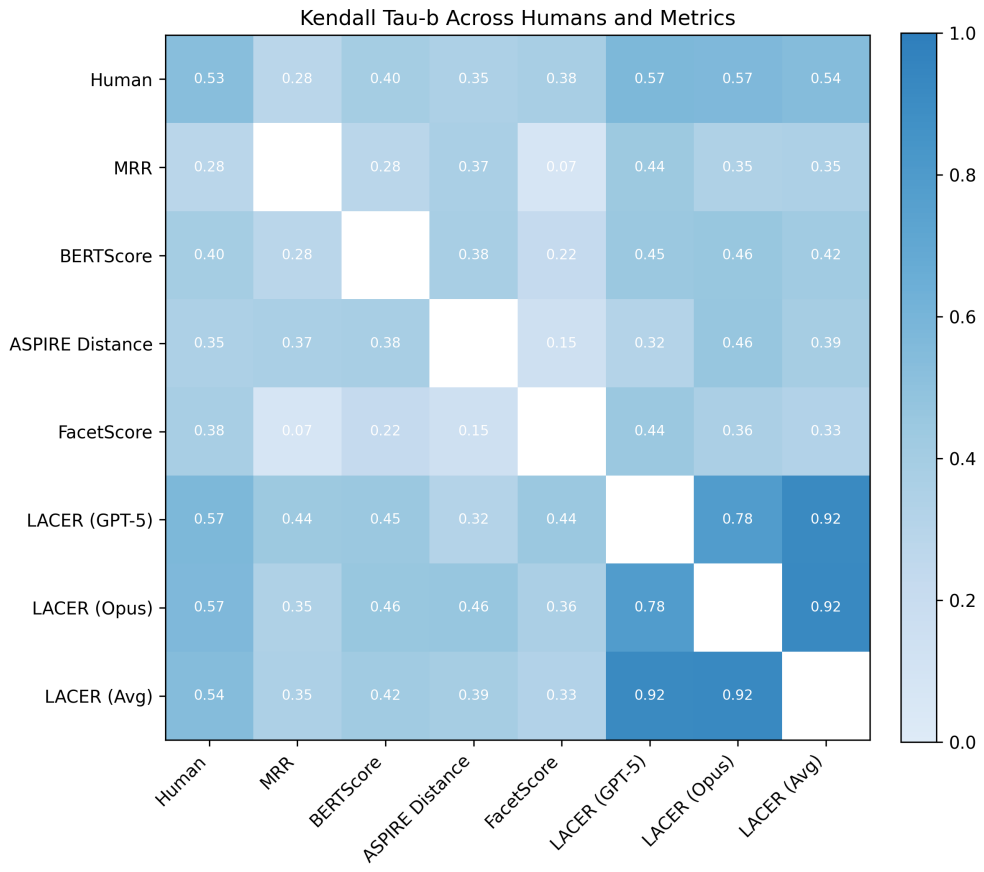

Figure 5: Agreement between humans, models, and aggregates. 'Human' refers to an *average* agreement among all five annotators – agreement computed against all the human annotators (excluding self-agreement), and then averaged. LACER is the only automated metric that reaches agreement with humans that is comparable to their IAA.

D Experiment Implementation Details

D.1 Contribution Generation

Finetuned open models. We fully finetune OLMo 3 7B and Qwen3 8B on the train split using the same input-output format as the prompted models. The input is the serialized influential-reference context and the target output is the gold title and abstract. We finetune each model on the target papers from the train period for up to three epochs, holding out 15% of train targets for validation and keeping the checkpoint with the lowest validation loss.

Reference baselines. The *random influential reference* baseline returns the title and abstract of a randomly selected influential reference of p. The *same arXiv category* baseline returns the title and abstract of a randomly selected paper from the same primary arXiv category as p. The *gold paraphrase* baseline uses a paraphrase of the target title and abstract.

Context ablations. All GPT-5.6 Sol ablations use the same $n = 500$ target-paper subset and include the influential references R_p. For the related-paper settings, we retrieve up to 10 nearest-neighbor prior papers from $\mathbf{H}^{<t_p}$ under GRIT cosine similarity, querying with the target's title-abstract

embedding. For the author-history settings, we walk the target's authors in listed order and include up to 3 most-recent prior papers per author, stopping once 15 papers have been collected. For the oracle-citation-count settings, we provide the eventual 12-month citation count as an additional scalar input.

Tool-using GPT-5.6 Sol agent. This baseline replaces the static prompted setup with a `gpt-5.6-sol` agent running an OpenAI tool-calling loop (via the Responses API) for at most 10 rounds per target. Given the target's authors and influential references, the agent may invoke four corpus tools — `search_papers` (GRIT semantic search over $\mathbf{H}^{<t_p}$), `get_paper`, `get_author_recent_papers`, and `get_references_of` — and is required to emit `Reasoning:`, `Title:`, and `Abstract:` lines, which are scored as in the prompted baselines. Every tool result passes through a per-target leakage filter that, given the target's publication date t_p, drops the target paper itself, any paper with publication date $\geq t_p$, any paper sharing the target's title, and any paper whose abstract overlaps the target's by 50 or more contiguous characters. The system prompt is provided in Appendix H.6.1.

D.2 Collaborator Prediction

Evaluation. We retain target papers with at least two authors whose publication histories are non-empty as of t_p, since baselines that rank a candidate set rather than generate it require some signal to anchor on. Candidate authors are similarly restricted to those with at least one prior publication. Unless otherwise noted, we use the first author as the seed; Appendix E.2.1 shows that this choice does not affect baseline ordering.

Baselines. Embedding-based methods represent each author by the mean of their 10 most recent prior papers, and use cosine similarity for GTR and GRIT and Euclidean distance for Specter2. *Hierarchical Clustering* represents each author with $\lceil \sqrt{n} \rceil$ centroids (where n is the author's number of prior papers) over PCA-reduced paper embeddings, scoring candidates by the maximum similarity over (query centroid, candidate centroid) pairs. *Embedding Fusion Projected* fits a 2-layer MLP on top of frozen GRIT embeddings using a multi-positive InfoNCE objective: positives are the target paper's coauthors; the 5 hard negatives are sampled from authors who have coauthored with the positives' prior coauthors but not directly with any positive; the 10 easy negatives are random pre-t_p authors outside both neighborhoods.

Autoresearch. We adapt Karpathy's autoresearch framework (Karpathy, 2026): a Claude Opus 4.7-driven outer loop iteratively designs, implements, and benchmarks candidate ranking pipelines on a 1000-instance dev set of train-period target papers posted between October 2023 and September 2024 under a 12-hour wall-clock budget, returning the highest-scoring configuration. We reuse the pipelines discovered by this search for all Autoresearch results in this paper (on both PreScience-AI and PreScience-Quantum) without re-running the search on the current train split. Within each evaluation instance, a per-target temporal filter is applied: the target paper is hidden and all tool calls return $\varnothing$ for any paper, author publication, or citation with publication date $\geq t_p$; candidate sets are restricted to pre-t_p IDs. The same per-target filter applies when the frozen pipeline is evaluated on the test set. The best-found pipeline is a frequency prior over the seed's 45 most-recent papers, expanded via 2-hop and 3-hop coauthor traversal (top-150 and top-100 contributors per hop, with multiplicative damping factors of 0.6 and 0.3), boosted by a citation-history pull that scores the authors of the seed's 10 most-recently cited references, and rescaled by an exponential activity decay with a 2.5-year half-life on each candidate's most-recent publication date.

GPT-5 Agent. Uses the same agent loop as in Appendix D.1, with a fifth tool `get_papers_citing` exposed in addition to the four above and a system prompt instructing the agent to predict the ranked `author_id`s of likely future coauthors of the seed (full prompt in Appendix H.6.2). The user message provides only the seed `author_id` and target date — no target paper text. All tool results are filtered to papers with publication date strictly before the target's t_p. The agent emits `Reasoning:` and `Predictions: [author_id, ...]`; the harness pads short lists to $k = 1000$ with random pre-cutoff candidate authors. Evaluated on a random $n = 500$ subset.

D.3 Prior Work Selection

Evaluation. We restrict to target papers with at least one author whose prior publications include a paper with a non-empty influential-reference list, so that frequency- and rank-fusion baselines have a meaningful citation history to draw from. The candidate pool is the full $\mathbf{H}^{<t_p}$ with no topic or neighborhood pre-filter, which makes the task substantially harder than open-domain retrieval — the model must distinguish a small (1–10) ground-truth set from hundreds of thousands of plausibly relevant papers.

Baselines. All retrieval baselines use up to the 10 most recent prior papers per author. *Embedding Fusion* mean-pools the embeddings of those papers per author, averages the per-author embeddings into a single team query, and ranks candidates by similarity to that one query. *Embedding Fusion Refs* differs in two ways: per author it instead mean-pools the embeddings of the influential references that author has cited in their recent work, and at the team level it queries the index once per author and combines results by summed rank rather than averaging into a single query. The former thus treats an author's own writing as the query, while the latter treats their citation history as the query. *Rank Fusion* queries the index once per cited reference and aggregates rankings weighted by citation multiplicity. *Embedding Fusion Projected* reuses the projection architecture and training recipe from Appendix D.2, supervised so that mean-pooled author queries are pulled towards the embeddings of their target papers' influential references.

Autoresearch. Best-found pipeline is a three-tier ranker that fuses (i) cited-reference frequency across the team's recent papers, (ii) 2-hop co-cited references, and (iii) embedding similarity reranked with team-centroid, per-author-centroid, and cited-reference-centroid boosts. Outer loop, 12-hour budget, and per-target temporal filter as in Appendix D.2.

GPT-5 Agent. Five-tool agent loop as in Appendix D.2, with a system prompt instructing the agent to predict the ranked `corpus_id`s of the target paper's likely influential references (full prompt in Appendix H.6.3). The user message provides the target authors and date but not the target's title or abstract. All tool results are filtered to papers with publication date strictly before the target's t_p. Evaluated over a random $n = 500$ subset.

D.4 Future Combination Prediction

Evaluation. Targets are drawn from the first four months of the test period, and ground-truth co-citation counts are tallied over the eight months that follow each target's publication date. Targets with no observed co-citations in this window are dropped. The candidate pool is the full $\mathbf{H}^{<t_p}$, with the paper index rolled forward chronologically so that, for each target, only papers published before t_p are visible.

Baselines. *Target Similarity* and *Reference Similarity* both retrieve from this chronologically updated index, differing only in the query: the target's title-abstract embedding for the former, and the mean embedding of the target's influential references for the latter. *Citation Frequency* ranks each prior paper q by the number of pre-t_p papers that cite q as an influential reference, and *Co-citation Frequency* ranks q by how often it co-occurs in pre-t_p influential-reference lists with any of p's influential references. We sweep all three embedding types in Appendix E.4.1.

Autoresearch. Best-found pipeline is reciprocal-rank fusion (k=6) over three rankings: a reference-centroid query in which each of the target's influential references contributes to the centroid weighted by an IDF computed over pre-t_p papers (so rarely-cited references count more), a target title–abstract query, and a co-citation-graph score that weights citers by similarity to the target with a 365-day recency decay and a topic/category-overlap boost. Outer loop, 12-hour budget, and per-target temporal filter as in Appendix D.2.

GPT-5 Agent. Five-tool agent loop as in Appendix D.2 (full prompt in Appendix H.6.4). Unlike the other ranking tasks, the target paper's title, abstract, topic labels, and influential references *are* exposed to the agent in the user message — these are causally available, since co-citation labels are derived from papers published after t_p, not from the target itself. Other tool results remain filtered

to papers with publication date strictly before t_p. The system prompt instructs the agent to traverse `get_papers_citing` from each of the target's references and aggregate the other references those citers share. Evaluated over a random $n = 500$ subset.

D.5 Citation Count Prediction

Evaluation. We restrict targets to papers with at least 12 months of observed citations and have models regress against the log-transformed 12-month count, inverting back to raw counts and clipping at zero before computing raw-space metrics.

Baselines. *Bibliometrics* combine per-author h-indices, publication and citation counts, team size, and the citation counts of influential references — all measured at t_p. *Target Text* uses the target paper's title-abstract embedding. *Context Text* concatenates two embedding components: the mean over the target's influential-reference embeddings and a per-author embedding equal to the mean over each author's prior publications. Per-paper feature vectors — whether bibliometric or embedding-based — expose up to four author slots (positions 1, 2, -2, and -1 in author order), giving the regressor a fixed-width view of lead and anchor authors regardless of team size. XGBoost hyperparameters are tuned via Bayesian optimization (Hyperopt, 100 evaluations) on a 30% validation slice and the final model is refit on the full training set with the best configuration.

Autoresearch. Best-found pipeline is an XGBoost regressor over $\log(1 + c)$ trained on train-period papers disjoint from the 1000-instance dev set (for our results, the regressor is refit on the current train split, keeping the discovered features and configuration); the autoresearch outer loop selects the configuration that minimizes dev-set loss, and the frozen pipeline is then evaluated on the test set as in the other tasks. Per-paper features combine the target's GRIT embedding, the mean GRIT embedding of its influential references, and 28 bibliometric scalars (author h-index, paper, and citation statistics; reference counts; title/abstract length; topic and category counts; target–reference cosine similarity; publication year and month). Outer loop, 12-hour budget, and per-target temporal filter as in Appendix D.2.

D.6 Topic Trend Forecasting

Baselines. All three baselines calibrate against an inner split of the train period: its first six months serve as an inner train period and the remaining six as an inner test period. *Mean* averages the per-topic inner-test paper count across topics and rescales it by the ratio of forecast length to inner-test length, predicting that single constant for every topic. *Citation Momentum* and *Author Momentum* instead fit a topic-agnostic linear scale that converts a per-topic score into a paper-count forecast on the inner split, then apply that scale to scores computed over the full train period. *Citation Momentum* scores each topic by the cumulative observable citations of its papers as of the relevant cutoff date (inner-history end when fitting the scale; history end when applying it); *Author Momentum* substitutes a per-author metric (number of prior papers or h-index at t_p) summed across each paper's authors. *Linear Extrapolation* side-steps the inner split entirely, fitting a per-topic OLS line to monthly counts in the train period and integrating the predicted rate over the test period. Topic pairs with fewer than ten papers in both periods are excluded.

D.7 Corpus Generation

Setup. The simulation is initialized from the final date of the train period and proceeds in daily steps for 365 days. The number of papers per day is drawn from an empirical distribution of daily target-paper counts in the train period; per-paper author counts and influential-reference counts are drawn from analogous train-period distributions. New authors are introduced at the empirical first-time-author rate among train-period target authors and assigned fresh synthetic identifiers.

Composition. Coauthor and prior-work prediction both use one-shot *Embedding Fusion* with GRIT, with author embeddings computed as the mean of each author's 10 most recent papers. Title and abstract are then generated by GPT-5 mini (`gpt-5-mini-2025-08-07`) conditioned on the predicted influential references. After each simulated day, generated papers are embedded with GRIT and added back to the literature state. Because they are added back, synthetic papers become

eligible as influential references and as members of authors' publication histories for subsequent days, a compounding feedback structure that helps explain the novelty decay reported in Section 4.5. Diversity and novelty estimates are aggregated over three independent rollouts to bound Monte Carlo variance in the reported confidence intervals.

Algorithm. We provide pseudocode (Algorithm 1) for the corpus generation algorithm we employ and describe in Section 4.5.

Algorithm 1 Corpus Generation

Require: $\mathbf{H}^{<t_0}$, rollout horizon $[t_0, t_f)$
Ensure: $\mathbf{H}^{<t_f}$
$P_N, P_{|C|}, P_{|R|}, p_{\text{new}} \leftarrow \textsc{EstimateDist}(\mathbf{H}^{<t_0})$
for $t = t_0$ **to** $t_f - 1$ **do**
  $N \sim P_N$, $\mathcal{S}_t \leftarrow \emptyset$
  for $i = 1$ **to** N **do**
    $|C| \sim P_{|C|}$, $|R| \sim P_{|R|}$
    $C \leftarrow \textsc{SampleResearchTeam}(|C|, p_{\text{new}}, \mathbf{H}^{<t})$
    $R \leftarrow \textsc{SelectPriorWork}(C, |R|, \mathbf{H}^{<t})$
    $(\tau, \alpha) \leftarrow \textsc{GenerateTitleAbstract}(C, R, \mathbf{H}^{<t})$
    $\mathcal{S}_t \leftarrow \mathcal{S}_t \cup \{\textsc{Paper}(\tau, \alpha, C, R, t)\}$
  end for
  $\mathbf{H}^{<t+1} \leftarrow \mathbf{H}^{<t} \cup \mathcal{S}_t$
end for
return $\mathbf{H}^{<t_f}$

D.8 Computational Resources

Dataset construction. The pipeline runs on a single multi-core CPU machine in a few hours, except for S2AND author disambiguation (Stage 4), which takes up to a few days on a similar machine.

Topic labeling. Per-paper topic labels (GPT-5.4 over the $\sim$117k target papers, Appendix B.3) complete in roughly an hour at 128-worker parallelism.

Embedding precomputation. GRIT-7B embeddings for all $\sim$1.06M corpus papers (both domains) take a few hours on 2$\times$H100 GPUs (one-time cost). GTR-T5-large and Specter2 are smaller and complete on a single H100 in comparable time.

Contribution generation. Finetuning OLMo 3 7B and Qwen3 8B on the train-period targets each takes roughly 2.5 hours on 8$\times$H100 GPUs. Frontier-model evaluation (GPT-4o, GPT-5 mini, GPT-5, GPT-5.6 Sol, Claude Sonnet 4.5, Claude Opus 4.6, Claude Sonnet 5) consumes 2k API calls per model on each domain's test split. LACER scoring adds one GPT-5 judge call per generated paper; across all evaluated models this amounts to a few tens of thousands of judge calls.

Paper-anchored ranking tasks (collaborator, prior work, future combination). Static baselines (frequency heuristics, embedding ranking, hierarchical clustering) are CPU-bound and complete within minutes to a few hours per task on a multi-core machine. *Embedding Fusion Projected* adds a few hours of single-GPU training on an H100.

Citation count prediction. XGBoost training plus Bayesian hyperparameter search (Hyperopt, 100 evaluations) completes in roughly one CPU-hour.

Topic trend forecasting. Pure-CPU baselines that complete within minutes.

Agents. Each agent run completes within a few hours wall-clock at 128-worker parallelism. The contribution-generation agent (GPT-5.6 Sol) runs on the same $n = 500$ subset as the context ablations (one $\leq$10-round agent loop per target); the three ranking-task agents (collaborator, prior work, future combination) each run on $n = 500$. A 10-target calibration on contribution generation found that a

GPT-5.6 Sol agent run averages 4.3 API rounds and consumes roughly $55\times$ the input tokens, $3\times$ the output tokens, and $\sim 20\times$ the per-target API cost of simple GPT-5.6 Sol prompting.

Autoresearch. Each of the four task-specific outer loops consumes a fixed 12-hour wall-clock budget within which a Claude Opus 4.7 agent iteratively writes and benchmarks candidate Python pipelines against the 1000-instance train-period dev set. Total: $\sim$48 hours of LLM-driven experimentation.

Corpus generation. The heaviest single experiment in the paper. We perform three independent 12-month rollouts per domain; each PRESCIENCE-AI rollout simulates roughly 140 papers per day for 365 days ($\sim$37 per day for PRESCIENCE-QUANTUM), and each simulated paper triggers a collaborator-prediction call (CPU), a prior-work-selection call (CPU), and a GPT-5 mini contribution-generation API call. Across the six rollouts this amounts to roughly 2×10^5 GPT-5 mini contribution-generation calls.

E ADDITIONAL ANALYSES

E.1 CONTRIBUTION GENERATION

E.1.1 EFFECT OF PRETRAINING CORPUS CONTAMINATION

Table 11 lists the LLMs evaluated in this paper with their reported knowledge cutoffs. Six of the nine, including GPT-5 mini, which drives our corpus-generation rollouts (Section 4.5), have cutoffs that predate the test period entirely, so their test-period predictions are uncontaminated. For the three models whose cutoffs fall inside the test period, we test for contamination effects directly.

Table 11: LLMs evaluated in this paper, their reported knowledge cutoffs, and the share of the test period (August 2025–July 2026) that falls before each cutoff.

Model	Reported knowledge cutoff	Test period before cutoff	Used for
GPT-4o	October 2023	0%	Contribution generation
GPT-5 mini	May 2024	0%	Contribution generation, corpus-generation rollouts
GPT-5	September 2024	0%	Contribution generation, LACER judge, ranking agents
OLMo 3 7B	December 2024	0%	Contribution generation (finetuned)
Qwen3 8B	Not reported (released April 2025)	0%	Contribution generation (finetuned)
Claude Sonnet 4.5	July 2025	0%	Contribution generation
Claude Opus 4.6	August 31, 2025	8%	Contribution generation
Claude Sonnet 5	January 31, 2026	50%	Contribution generation
GPT-5.6 Sol	February 16, 2026	55%	Contribution generation (prompted and agentic)

Table 12 compares mean LACER scores in the month immediately before and after each model's reported knowledge cutoff date. We observe modest changes in absolute scores and no changes in relative model ordering, and none of the pre- versus post-cutoff differences is statistically significant (all p-values exceed 0.05). For two of the three models (Claude Sonnet 5 and Claude Opus 4.6), mean LACER scores are even higher on post-cutoff papers than on pre-cutoff ones. Together, these results suggest that any cutoff-related effects are small relative to the performance differences reported in the main results.

E.1.2 FURTHER TASK ANALYSES

Figure 7(a) shows that contribution generation becomes easier as more influential references are available, consistent with additional contextual signal improving conceptual alignment. Figure 7(b) indicates that LACER scores are largely insensitive to a paper's future citation impact, suggesting that predictive difficulty is decoupled from downstream popularity. Figure 7(c) shows that papers whose influential references have lower average citation counts are easier to predict. This is consistent with highly cited prior work being useful to a wide application space. Figure 7(d) shows that higher topical diversity among influential references is associated with improved prediction performance, perhaps indicating fewer "valid" ways in which diverse work can be combined (given that the subset can in fact be combined). Figure 7(e) reveals systematic variation across arXiv categories, with computation-and-language papers exhibiting the lowest scores and robotics and computer-vision

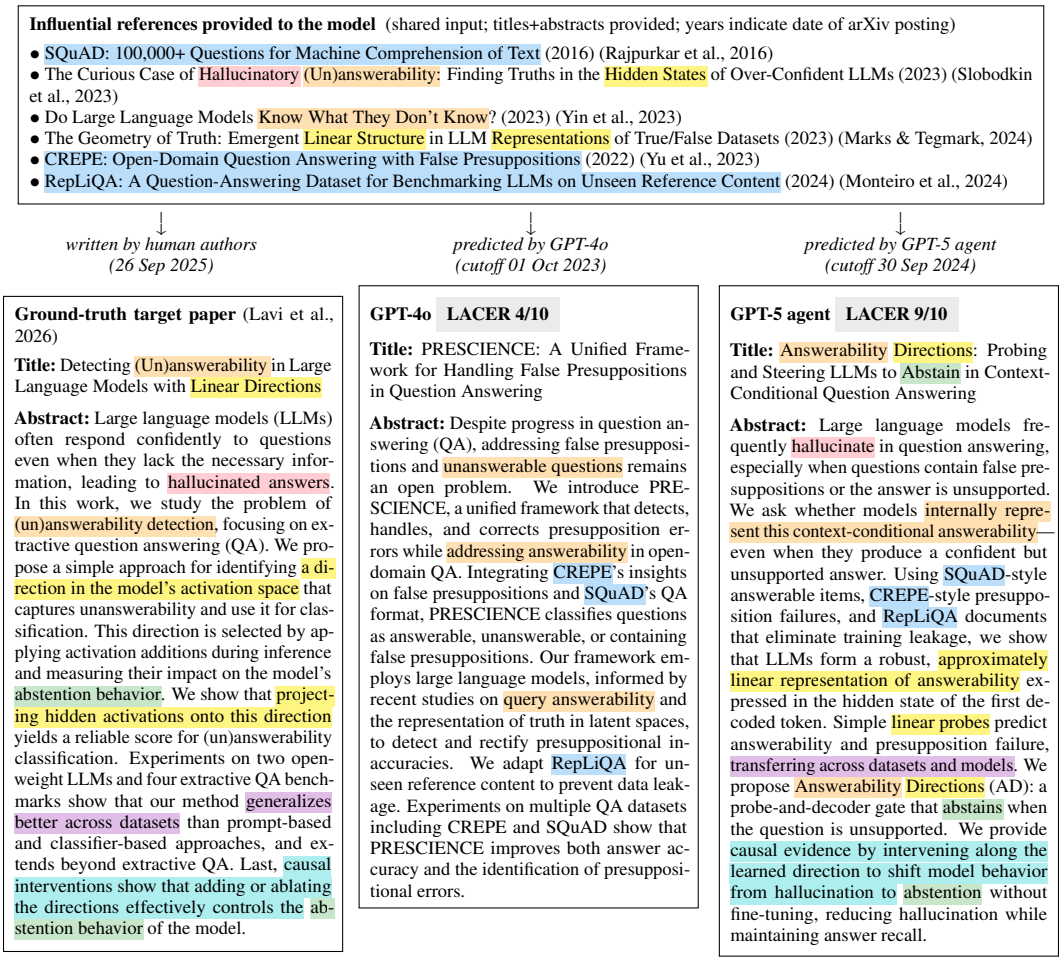

Figure 6: Examples of contribution generations from **GPT-4o** (center; the generated contribution PRESCIENCE is coincidental nomenclature and has no relation to our work) and **GPT-5 agent** (right) when provided the target's authors and influential references. Additionally, the GPT-5 agent is given leakage-safe access to $\mathbf{H}^{<t_p}$. The target paper was posted in September 2025, during the test period of an earlier data snapshot (October 2024–September 2025).

Table 12: Mean LACER scores (with 95% CIs) over the month before and the month after each model's reported knowledge cutoff date, using 300 test papers on each side (the papers from the main evaluation that fall in each window, plus randomly sampled additional test papers from the same window). The last column gives the p-value of a two-sided Welch t-test of the null hypothesis that pre-cutoff and post-cutoff mean scores are equal; values above 0.05 indicate no statistically significant difference.

Model	Cutoff Date	Pre-cutoff	Post-cutoff	p-value
GPT-5.6 Sol	Feb 16, 2026	$5.84_{(0.25)}$	$5.78_{(0.25)}$	0.72
Claude Sonnet 5	Jan 31, 2026	$5.19_{(0.25)}$	$5.48_{(0.25)}$	0.10
Claude Opus 4.6	Aug 31, 2025	$5.01_{(0.24)}$	$5.16_{(0.25)}$	0.40

papers the highest. Figure 7(f) summarizes common failure modes, which are spread fairly evenly

across domain substitution, wrong core contribution type, task or setting drift, and methodological mismatch rather than surface-level keyword errors.[5]

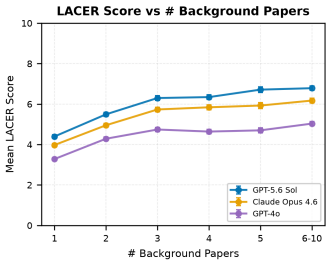

(a) Prediction is easier in instances with more influential references.

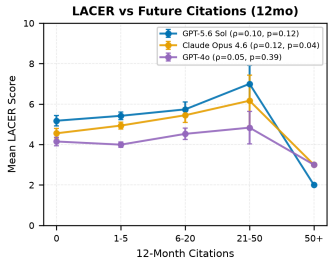

(b) Prediction difficulty appears agnostic to future impact of paper.

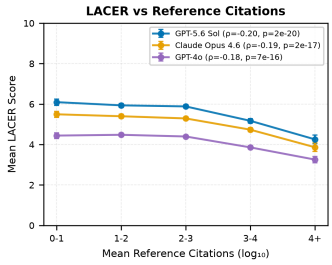

(c) Papers whose influential references have fewer citations are easier to predict.

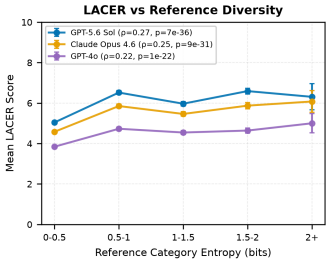

(d) Papers whose influential references are more diverse in topics appear easier to predict.

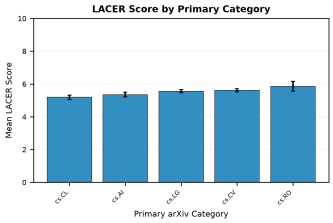

(e) There is statistically significant variation in LLMs' to predict work corresponding to different ArXiv topics with "Computation and Language (cs.CL)" papers being the hardest to predict among the shown topics and "Robotics (cs.RO)" papers being the easiest.

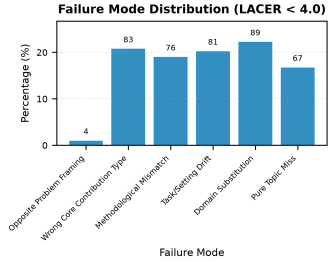

(f) Prediction Failure Modes

Figure 7: Contribution Generation

E.1.3 Effect of Influential Reference Choice

We evaluate contribution generation across three definitions of a target paper's prior work — Semantic Scholar's highly influential references (Valenzuela-Escarcega et al., 2015), all of its references, and *impact-revealing references* (Arnaout et al., 2026) — using GPT-5, GPT-5.2, and Claude Opus 4.5 (Table 13). In absolute terms, larger reference sets yield higher LACER, but this trend is largely a context-size effect: when each paper's reference set is randomly subsampled to match the size of the highly-influential set, both alternatives perform substantially worse than the default. The same pattern holds when all references are subsampled to the size of the impact-revealing set. Thus, at matched context budget, Semantic Scholar's classifier selects a stronger subset of references for contribution generation than random subsamples of the larger reference sets. Relative model rankings are stable across all six conditions.

E.2 Collaborator Prediction

E.2.1 Effect of Seed Author Choice

We find that the choice of seed author in the collaborator prediction task does not affect the relative ordering of baseline performance. This is a non-trivial result, as research team formation and

[5]We categorize these failure modes by prompting GPT-5.2 with the 400 low-scoring (LACER < 4) GPT-5.6 Sol generated abstracts along with their corresponding ground truths and instructing it to study and categorize them into common failure modes.

Table 13: Contribution generation LACER under alternative definitions of a target paper's prior work ($n = 984$), computed over target papers in the same AI categories posted between October 2024 and September 2025. Subsampled rows random-subsample each paper's references down to the count of the reference type given in parentheses, isolating reference-set selection from reference-set size.

Reference Set	Ref. Count	GPT-5	GPT-5.2	Claude Opus 4.5
Highly influential references	3.02	5.62	5.50	4.78
Impact-revealing references	9.89	6.45	6.35	5.46
All references	35.16	6.89	6.63	6.22
Impact-revealing references (sub. to highly-influential count)	3.02	5.11	5.08	3.49
All references (sub. to highly-influential count)	3.02	4.74	4.68	4.14
All references (sub. to impact-revealing count)	9.89	6.19	6.00	—

collaborator discovery may be governed by different mechanisms for authors at different career stages or seniority levels. However, the baselines we evaluate primarily operate on order-invariant features of the observed co-authorship graph (e.g., local neighborhoods and aggregated publication histories), so it appears changing the seed largely only shifts the strength of the underlying collaboration signal without favoring any of the baselines over others.

Table 14: Effect of seed author choice on collaborator prediction performance (nDCG) (n=1000). The relative performance order among baselines remains unchanged.

Baseline	First	Last	Random	Argmax h-index
Frequency	0.38	0.33	0.34	0.25
Rank Fusion (GRIT)	0.14	0.12	0.14	0.10
Embedding Fusion (GRIT)	0.26	0.23	0.24	0.17

E.2.2 Further Task Analyses

Figure 8 analyzes collaborator prediction performance across two sources of variation. Panel (a) shows that nDCG generally decreases as the first author's publication history grows, indicating that larger and more crowded collaboration neighborhoods dilute the signal available to frequency- and embedding-based baselines. Panel (b) shows that R-precision generally declines with team size, reflecting the increasing combinatorial difficulty of recovering all collaborators as the target set grows.

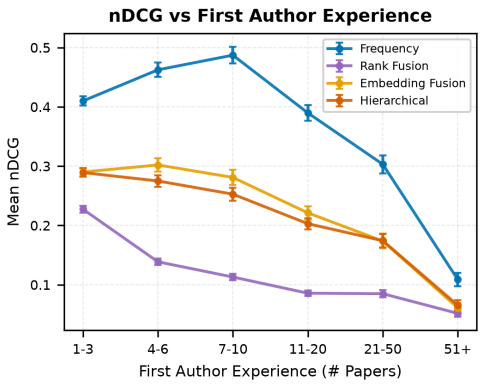

(a) nDCG scores as author profiles become crowded with more publications.

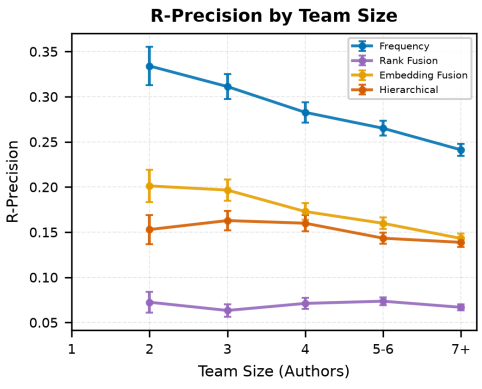

(b) Larger teams are harder to correctly predict.

Figure 8: Collaborator Prediction

Table 15: Effect of embedding choice on collaborator prediction baselines.

Method (Embed)	nDCG	R-Prec
Rank Fusion (GTR)	0.13	0.05
Rank Fusion (Specter2)	0.09	0.04
Rank Fusion (GRIT)	0.16	0.07
Emb. Fusion (GTR)	0.23	0.14
Emb. Fusion (Specter2)	0.18	0.10
Emb. Fusion (GRIT)	**0.26**	**0.17**
Hier. Clustering (GTR)	0.25	0.15
Hier. Clustering (Specter2)	0.24	0.14
Hier. Clustering (GRIT)	0.25	0.15

E.2.3 Hit Rate by Familiarity

Figure 9 reports collaborator prediction hit rate as a function of how often the candidate has previously co-authored with the seed. All baselines exhibit near-zero hit rates when predicting first-time collaborators, indicating that current methods recover repeat-collaboration structure but cannot anticipate genuinely new relationships.

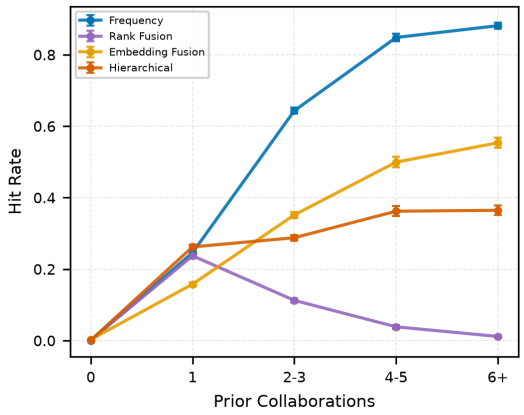

Figure 9: Collaborator prediction hit rate — the fraction of top-R predicted authors that are among the R ground-truth authors — as the number of prior co-authorships between candidate and seed varies. All baselines exhibit near-zero performance when predicting first-time collaborators.

E.2.4 Effect of Embedding Choice

Table 15 reports collaborator prediction baselines across GTR, Specter2, and GRIT embeddings. GRIT yields the strongest results for Embedding Fusion, while Hierarchical Clustering is largely insensitive to the choice of embedding.

E.3 Prior Work Selection

E.3.1 Effect of Influential Reference Choice

In addition to Semantic Scholar's *highly influential* references (Valenzuela-Escarcega et al., 2015), we evaluate two alternative definitions of influential prior work: (i) using the full set of references cited by each paper, and (ii) using *impact-revealing references* (Arnaout et al., 2026). As shown in Table 16, neither alternative yields a dramatic improvement in prediction performance over the

default influential-reference definition[6]. However, both incur substantially higher computational and data costs: including all references dramatically expands the set of companion papers and causes the historical corpus $H_{<t}$ to balloon, while computing impact-revealing references requires repeated calls to commercial LLM APIs. These results motivate our use of Semantic Scholar influential references as a practical trade-off between predictive signal and scalability.

Table 16: Prior work selection performance (n=1000) across reference types, computed with a single retrieval baseline over target papers in the same AI categories posted between October 2024 and October 2025. Standard deviations are shown in subscript parentheses.

Reference Type	Reference Count	nDCG	R-Prec
S2 Highly Influential	$5.43_{(0.12)}$	$4.2_{(0.4)}$	$3.0_{(0.3)}$
All References	$34.04_{(0.63)}$	$7.6_{(0.3)}$	$4.6_{(0.2)}$
Impact-Revealing	$10.65_{(0.22)}$	$5.7_{(0.3)}$	$3.6_{(0.3)}$

E.3.2 Further Task Analyses

Figure 10 presents diagnostic analyses of prior work selection performance across author experience, number of references, and team size. *Frequency* improves with the number of references and with author experience, whereas the other baselines tend to degrade for highly experienced author teams and for large teams, where the retrieval query aggregates many authors' diverse prior work.

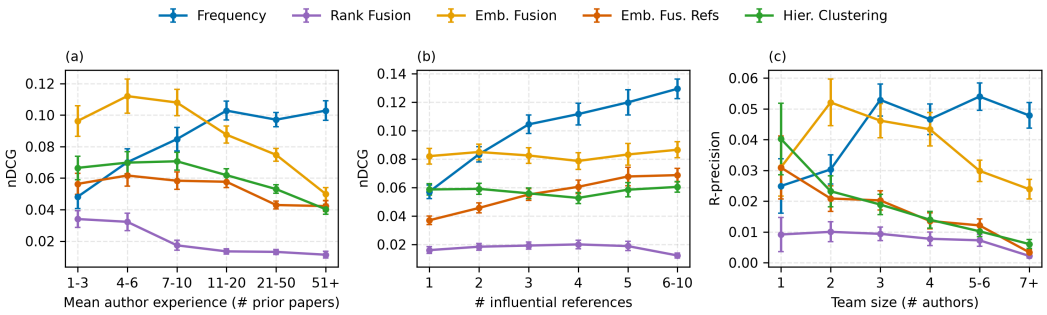

Figure 10: Prior work selection performance by (a) the mean number of prior papers of the target paper's authors, (b) the number of influential references, and (c) team size. Error bars are standard errors; buckets with fewer than 20 instances are omitted.

E.3.3 Hit Rate by Familiarity

Figure 11 reports prior work selection hit rate as a function of how often the target paper's authors have previously cited the candidate reference. Aside from *Frequency*, which dominates in high-familiarity regimes, embedding-based methods achieve low hit rates across all buckets and degrade further for less-precedented references.

E.3.4 Effect of Embedding Choice

Table 17 reports prior work selection baselines across GTR, Specter2, and GRIT embeddings. GRIT consistently outperforms the other two for Embedding Fusion, while Rank Fusion and Hierarchical Clustering are largely insensitive to the choice of embedding.

[6]These results are computed with a single retrieval baseline over target papers in the same AI categories posted between October 2024 and October 2025; we expect the relative trends across reference definitions to hold for the current dataset, even if absolute values shift.

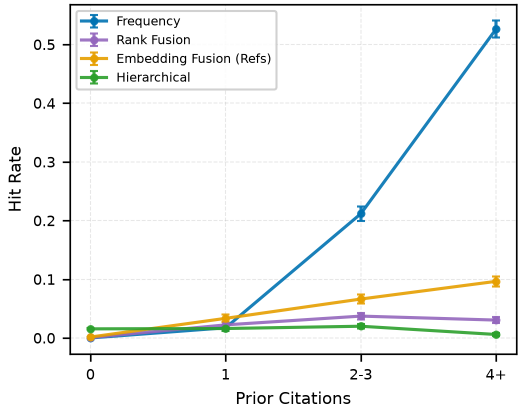

Figure 11: Prior work prediction hit rate as a function of how often a target paper's authors have previously cited the candidate reference. Methods struggle to predict novel references; *Frequency* dominates for previously-cited works.

Table 17: Effect of embedding choice on prior work selection baselines.

Method (Embed)	**nDCG**	**R-Prec**
Rank Fusion (GTR)	0.03	0.01
Rank Fusion (Specter2)	0.02	0.01
Rank Fusion (GRIT)	0.02	0.01
Emb. Fusion (GTR)	0.04	0.02
Emb. Fusion (Specter2)	0.06	0.02
Emb. Fusion (GRIT)	**0.08**	**0.04**
Hier. Clustering (GTR)	0.05	0.02
Hier. Clustering (Specter2)	0.06	0.01
Hier. Clustering (GRIT)	0.06	0.01

E.4 Future Combination Prediction

E.4.1 Effect of Embedding Choice

Table 18 reports future combination prediction baselines across GTR, Specter2, and GRIT embeddings. GRIT yields the strongest results for both Target Similarity and Reference Similarity, with Reference Similarity outperforming Target Similarity at every embedding choice.

E.5 Citation Count Prediction

E.5.1 Further Task Analyses

Figure 12 analyzes citation count prediction using an XGBoost regressor trained over the full feature set described in Section 4.3. Panel (a) plots predicted versus true 12-month citation counts and exhibits clear heteroscedasticity: variance in prediction error increases with citation magnitude, indicating that highly cited papers are systematically harder to predict than low-impact papers. Panel (b) summarizes feature attributions via SHAP for the bibliometric features we use in Section 4.3.

E.5.2 Effect of Embedding Choice

Table 19 reports Target Text citation count prediction baselines across GTR, Specter2, and GRIT embeddings. GRIT yields the strongest performance across all metrics.

Table 18: Effect of embedding choice on future combination prediction.

Method (Embed)	nDCG	R-Prec
Target Similarity (GTR)	0.13	0.05
Target Similarity (Specter2)	0.20	0.07
Target Similarity (GRIT)	0.24	0.10
Reference Similarity (GTR)	0.20	0.11
Reference Similarity (Specter2)	0.24	0.12
Reference Similarity (GRIT)	**0.27**	**0.15**

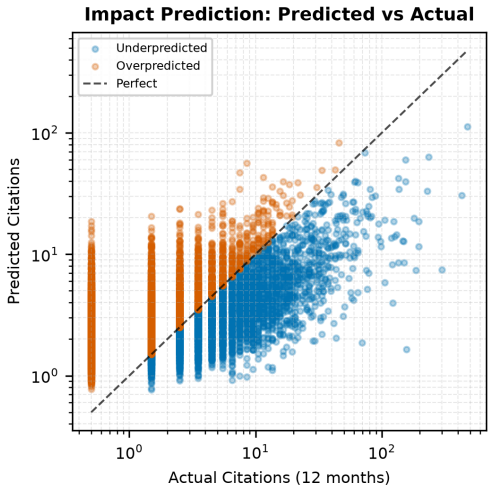

(a) Scatter plot of citation count predictions (XGBoost-Regressor; all features).

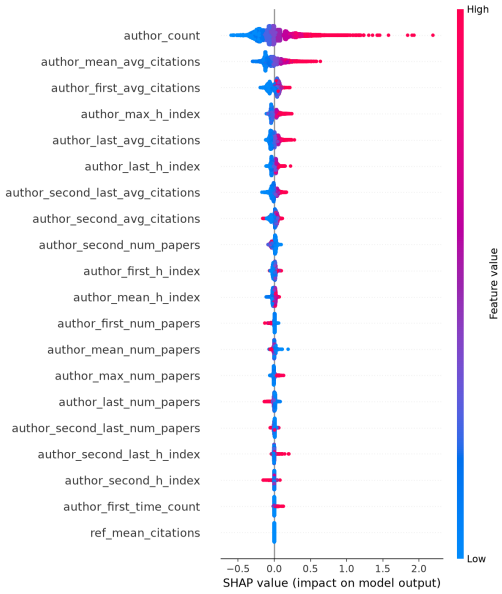

(b) SHAP values for the XGBoost regressor trained over author- and influential-reference-related numerical metadata features.

Figure 12: Citation count prediction analysis: (a) scatter plot of predicted vs. true citation counts using all features, and (b) SHAP summary of feature attributions for XGBoostRegressor trained over bibliometric features.

E.6 Corpus Generation

E.6.1 Further Task Analyses

Figure 13 compares the diversity of authors and prior work surfaced during corpus generation with that of natural papers from the same period, measured as the cumulative effective number of distinct authors and cited papers. Synthetic rollouts surface more diverse authors ($1.72\times$ the effective number of authors per month) and more diverse prior work ($1.60\times$ the effective number of cited papers per month) than natural papers, indicating that the lower diversity of synthetic papers (Section 4.5) arises from contribution generation rather than from the predicted collaborators or references.

E.6.2 Precision and Recall of Synthetic Corpora

We measure how well a synthetic rollout and the natural test-period literature cover each other. For each sampled paper, we retrieve its 10 nearest neighbors in the other corpus (GRIT embeddings) and take the maximum LACER score, treating the natural paper as the reference: *precision* queries synthetic papers against natural ones, and *recall* queries natural papers against synthetic ones. As a reference point, we also match natural papers against other natural papers. Both precision and recall fall about one LACER point below this reference (Table 20), so synthetic papers resemble natural

Table 19: Effect of embedding choice on citation count prediction baselines.

Baseline	MAE	MAE (log)	Pearson	Pearson (log)	Spearman
Target Text (GTR)	4.03	0.74	0.28	0.38	0.34
Target Text (Specter2)	3.98	0.73	0.31	0.43	0.39
Target Text (GRIT)	**3.89**	**0.71**	**0.42**	**0.47**	**0.42**

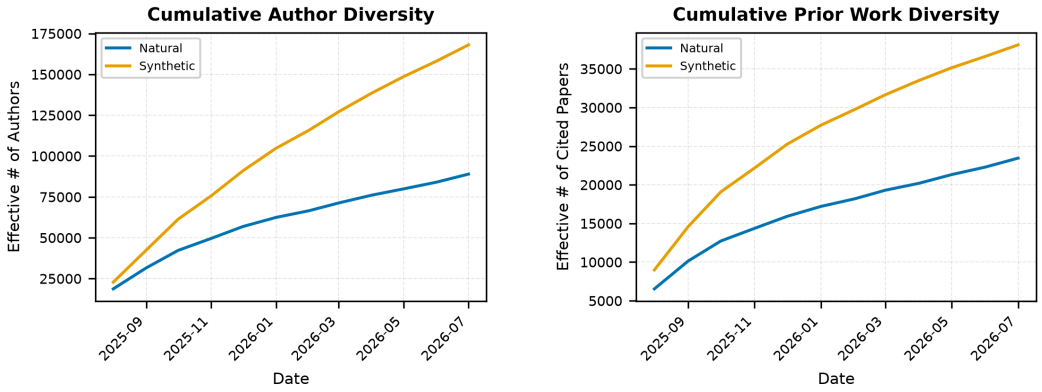

(a) Authors surfaced by the synthetic rollouts are more diverse than the corresponding natural authors.

(b) Prior work surfaced during synthetic rollouts is more diverse than by natural papers from the same time period.

Figure 13: Diversity of Authors and Prior work surfaced during corpus generation. We employ retrieval pool subsampling to remove systemic biases due to discrepancies between natural and synthetic corpus sizes.

future papers less closely than natural papers resemble each other. Natural papers that the synthetic corpus covers well tend to be more cited (Figure 14), suggesting a bias toward mainstream work.

Table 20: LACER-based precision and recall of one synthetic rollout against natural test-period papers, and a natural-versus-natural reference. Each query paper's score is its maximum LACER over its 10 nearest neighbors in GRIT embedding space (25 query papers per month; 300 per row). $\pm$ indicates bootstrap 95% CIs.

Measure	Query $\rightarrow$ retrieval pool	Mean best-match LACER
Precision	Synthetic $\rightarrow$ natural	5.90 ± 0.18
Recall	Natural $\rightarrow$ synthetic	6.08 ± 0.16
Reference	Natural $\rightarrow$ other natural	7.00 ± 0.17

E.6.3 Discussion

Realistically simulating corpus rollouts can be difficult. Even assuming access to models that can perform individual tasks well, it can be challenging to use them to generate realistic corpora. Choices made while designing the procedure that utilizes these models for multi-turn corpus rollouts can have unintended consequences that bias corpus statistics. For example, Figure 15 shows the distribution of primary arXiv topics of Natural and Synthetic[7] papers corresponding to this period. Real-world research shows much more seasonal variation in the distribution over papers published year-round than the synthetic corpus. This arises from the fact that our simulation uniformly and independently randomly selects seed authors from the PreScience-AI dataset for each synthesized

[7]We use a GPT-5-based classifier with $\sim$ 64% accuracy on a held-out set of 500 train-period papers to predict the topics of a stratified sample of $\sim$500 synthesized papers per month.

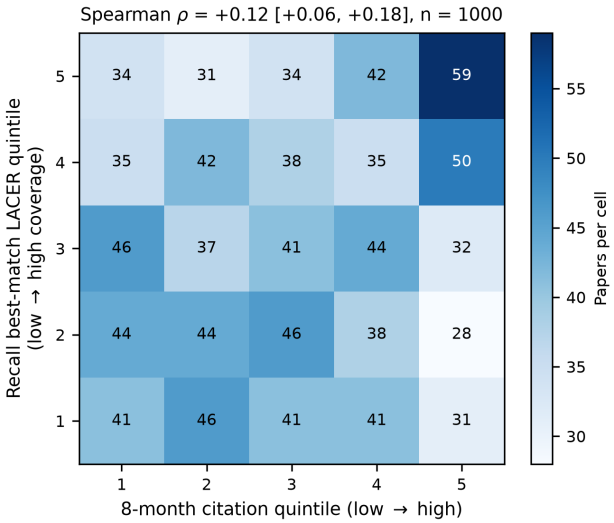

Figure 14: Number of natural test papers ($n = 1{,}000$) by quintile of 8-month citation count and of best-match LACER against the synthetic corpus. The slight positive correlation suggests that rollouts tend to generate "mainstream" papers resembling those that attract attention.

paper whereas certain seed authors may be more likely to publish their work at certain times of the year than others due to external circumstances like venue deadlines or academic schedules.

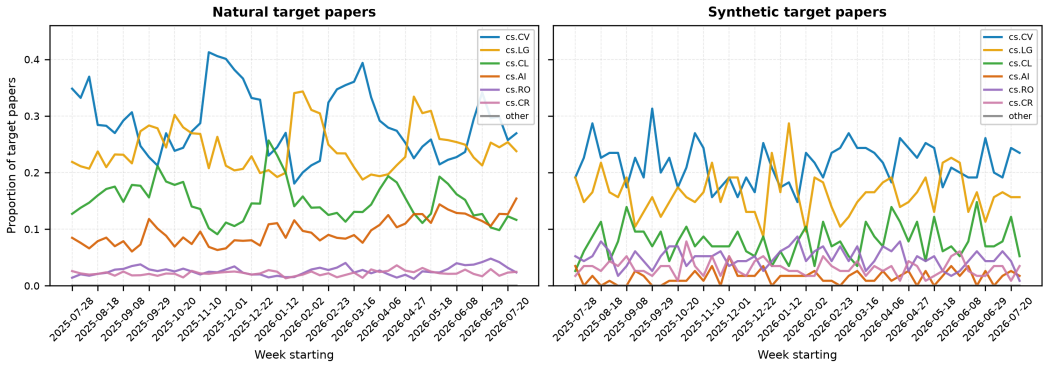

Figure 15: Primary arXiv topics of real-world (Natural) and Synthetic papers. Real-world papers show significant seasonal variation while synthetic ones do not.

Individual statistics computed over a generated corpus can be misleading. It can be difficult to accurately measure the quality of a synthetic corpus. For instance, in Figure 16, we measure the fraction of target papers from the natural and simulated corpora that contain at least one influential reference that cites another of the target paper's influential references. Although it appears that this coefficient approaches that from the natural corpus as the simulation proceeds, an observation that can be mistaken for implying that the simulated papers' citation patterns become more natural as simulation proceeds–we find that its upward slope is due to another factor: Synthetic papers that enter the corpus can connect two previously disparate papers, and a future synthetic paper that cites the same set would now raise the local clustering coefficient as the simulation proceeds. A phenomenon that skews the synthetic corpus away from the natural corpus thus has the effect of causing this statistic to trend in the "correct" direction.

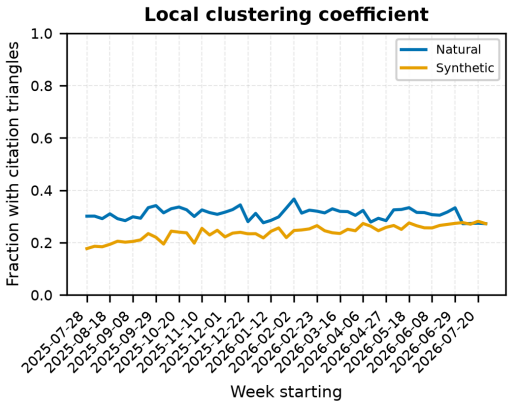

Figure 16: Local clustering coefficient (i.e. the fraction of pairs of influential references of the target paper that cite another of its influential references.

F PRESCIENCE-QUANTUM RESULTS

We report results on PRESCIENCE-QUANTUM for every experiment with a main-text counterpart on PRESCIENCE-AI, using the same models, sample sizes, and protocols (Section 4); citation data for PRESCIENCE-QUANTUM are collected through September 24, 2026, giving 2,658 test papers with 12 months of citations. Topic trend forecasting is not evaluated because we do not construct a topic taxonomy for PRESCIENCE-QUANTUM, and finetuned open models, input-feature ablations, and per-task analyses are reported for PRESCIENCE-AI only.

Table 21: PRESCIENCE-QUANTUM contribution generation results (counterpart of Table 2, left) on $n = 2{,}000$ test papers using influential references as input. Subscripts indicate bootstrap 95% CIs. * indicates model cutoffs postdate test-period start.

Baseline	LACER	ROUGE-L		BERTScore	
		P	R	P	R
Same arXiv Category	$1.29_{(0.02)}$	0.14	0.12	0.12	0.10
Random Infl. Ref.	$4.85_{(0.09)}$	0.18	0.17	0.20	0.18
GPT 4o	$4.29_{(0.07)}$	**0.19**	0.15	**0.25**	0.18
GPT 5 mini	$5.84_{(0.09)}$	0.11	**0.20**	0.14	**0.23**
GPT 5	$5.96_{(0.09)}$	0.12	0.19	0.14	**0.23**
GPT 5.6 Sol*	$\mathbf{6.01}_{(0.09)}$	0.17	0.18	0.21	0.22
Claude Sonnet 4.5	$5.12_{(0.09)}$	0.16	0.19	0.21	0.22
Claude Opus 4.6*	$5.31_{(0.09)}$	0.17	0.19	0.23	0.22
Claude Sonnet 5*	$5.44_{(0.09)}$	0.16	0.19	0.21	**0.23**
Gold Paraphrase	$10.00_{(0.00)}$	0.65	0.62	0.72	0.71

Table 22: PRESCIENCE-QUANTUM paper-anchored ranking task results (GRIT; counterpart of Table 3). Subscripts indicate bootstrap 95% CIs. Left: collaborator prediction and prior work selection. Right: future combination prediction ($n = 348$ evaluation instances). † indicates evaluation on $n = 500$ random instances.

	Collab		Prior Work	
Baseline	nDCG	R-Prec	nDCG	R-Prec
Frequency	$0.44_{(0.01)}$	$0.31_{(0.01)}$	$0.11_{(0.01)}$	$0.06_{(0.00)}$
Rank Fusion	$0.21_{(0.01)}$	$0.10_{(0.01)}$	$0.02_{(0.00)}$	$0.01_{(0.00)}$
Emb. Fusion	$0.37_{(0.01)}$	$0.23_{(0.01)}$	$0.21_{(0.01)}$	$0.09_{(0.01)}$
Hier. Clustering	$0.34_{(0.01)}$	$0.20_{(0.01)}$	$0.15_{(0.01)}$	$0.04_{(0.00)}$
Emb. Fus. Refs	–	–	$0.10_{(0.00)}$	$0.02_{(0.00)}$
Emb. Fus Proj.	$0.33_{(0.01)}$	$0.20_{(0.01)}$	$0.15_{(0.01)}$	$0.06_{(0.01)}$
Autoresearch	$\mathbf{0.55}_{(0.01)}$	$\mathbf{0.38}_{(0.01)}$	$0.20_{(0.01)}$	$0.07_{(0.01)}$
GPT-5 Agent†	$0.48_{(0.03)}$	$0.34_{(0.03)}$	$\mathbf{0.22}_{(0.02)}$	$\mathbf{0.11}_{(0.02)}$

	Future Comb.	
Baseline	nDCG	R-Prec
Target Similarity	$0.31_{(0.03)}$	$0.13_{(0.02)}$
Ref. Similarity	$0.35_{(0.03)}$	$\mathbf{0.20}_{(0.03)}$
Co-citation Freq.	$0.06_{(0.01)}$	$0.03_{(0.01)}$
Citation Freq.	$0.03_{(0.01)}$	$0.01_{(0.01)}$
Autoresearch	$\mathbf{0.39}_{(0.03)}$	$\mathbf{0.20}_{(0.03)}$
GPT-5 Agent	$0.32_{(0.03)}$	$0.18_{(0.03)}$

Table 23: PRESCIENCE-QUANTUM citation count prediction results using GRIT embeddings (counterpart of Table 4), over the 2,658 test papers with 12 months of citation data.

Baseline	MAE	MAE (log)	Pearson	Pearson (log)	Spearman
Target Text	2.09	0.62	0.35	0.32	0.28
Bibliometrics	2.13	0.63	0.23	0.27	0.25
Target + Context	2.04	0.60	0.39	0.38	0.34
Target + Context + Bibliometrics	2.01	**0.59**	0.44	0.42	0.38
Autoresearch	**1.99**	**0.59**	**0.46**	**0.44**	**0.40**

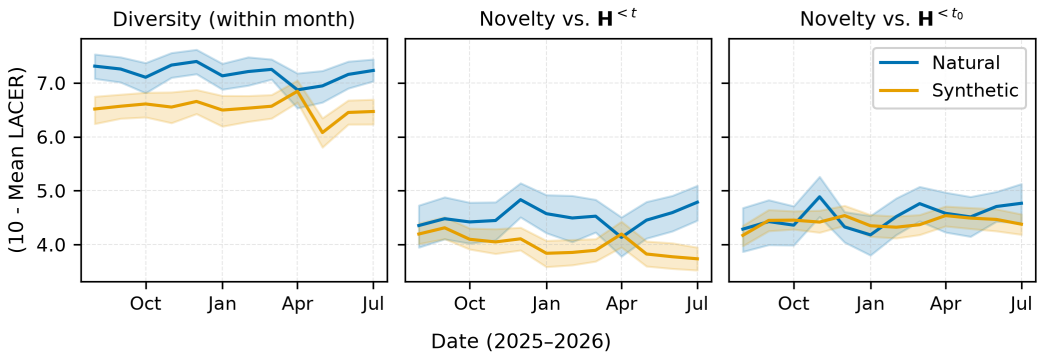

Figure 17: PRESCIENCE-QUANTUM corpus-generation rollouts (counterpart of Figure 2): diversity (left), novelty relative to the evolving literature state $\mathbf{H}^{<t}$ (middle), and novelty relative to the fixed pre-rollout corpus $\mathbf{H}^{<t_0}$ (right). Shading represents bootstrap 95% CIs. Predicted author sets are more diverse than natural ones ($1.29\times$ the effective number of authors per month), while predicted prior-work sets are slightly less diverse ($0.90\times$ the effective number of cited papers per month).

G Additional Related Work

G.1 Collaborator Prediction

This task has been well-studied, with most efforts using graph-based modeling approaches (Kanakaris et al., 2021; Xi et al., 2021; Tuninetti et al., 2021; Ebrahimi et al., 2021; Ho et al., 2019; Li et al., 2024). Some methods explore alternative representations, such as authors conditioned on a research topic (Chuan et al., 2018; Cheng et al., 2023), or the temporal nature of their publication histories (O'Madadhain et al., 2005; Munasinghe & Ichise, 2012; Koopmann et al., 2021). See (Kong et al., 2019; Zhang et al., 2023) for surveys touching on author link prediction.

G.2 Generating Synthetic Scientific Corpora

A complementary line of work generates scientific outputs at scale such as ideas, hypotheses, papers, or full research workflows with LLMs and compares these to empirical research. Some include a human in the loop (Jansen et al., 2025), while others operate fully autonomously (Lu et al., 2024); environments and benchmarks such as DiscoveryWorld (Jansen et al., 2024) and DiscoveryBench (Majumder et al., 2025) evaluate autonomous discovery agents, and Cappello et al. (2025) evaluate LLMs as research assistants. Multi-agent simulators give agents specialized roles, access to relevant literature, and the ability to interact in lab-like setups, producing synthetic research artifacts as their primary output (Su et al., 2025; Swanson et al., 2025; Chen et al., 2025b; Yu et al., 2025). AgentRxiv (Schmidgall & Moor, 2025) extends this further by letting agent labs share reports through a common preprint server, accumulating a synthetic record over time. Comparing the resulting corpora against real research is itself an established framing: (Amancio, 2015) contrast artificially generated and real manuscripts via topological features, and recent studies of LLM idea generation systems report limited diversity among generated ideas (Si et al., 2024; Hu et al., 2024). Instead of solely focusing on ideation, PreScience allows composing task-level forecasters for 12-month corpus-generation rollouts and quantifies how the resulting synthetic corpora differ from natural future papers in diversity and novelty.

H Prompts

H.1 Topic Assignment Prompt

Topic Assignment Prompt

```
You are a scientific paper topic classifier. Given a paper title and
↪  abstract, assign all topics from the list below that clearly
↪  apply.

Topics:
- Instruction tuning
- Preference optimization / alignment
- RLHF / RLAIF for post-training
- Prompt engineering / prompt optimization
- Prompt tuning / soft prompting
- Parameter-efficient fine-tuning
- In-context learning
- Long-context modeling
- Personalized language modeling
- Retrieval-augmented generation
- Tool / API-augmented language modeling
- Knowledge editing / model updating
- Model compression / distillation for LMs
- Chain-of-thought prompting
- Tree/search-based reasoning
- Self-critique / self-refinement
- Language-model planning
- Web/navigation agents
```

```
- Code-generation agents
- Multi-agent LLM collaboration
- Memory mechanisms for LLM agents
- Multimodal language agents
- Agent evaluation and benchmarks
- Hallucination detection and mitigation
- Calibration / uncertainty estimation for LLMs
- Jailbreak and prompt-injection robustness
- Privacy leakage / machine unlearning for LMs
- Mechanistic interpretability of transformers and LLMs
- Dialogue modeling
- Dialogue state tracking
- Dialogue evaluation
- Multimodal dialogue
- User modeling for conversational AI
- Proactive conversational AI
- Contextual dialogue modeling
- Information extraction
- Relation extraction
- Event extraction
- Question answering
- Summarization
- Long-document understanding
- Argument mining
- Stance detection
- Sentiment analysis
- Syntactic parsing / tagging / chunking
- Morphology and word segmentation
- Sentence-level semantics and textual inference
- Figurative language understanding / generation
- Machine translation
- Low-resource NLP
- Multilingual representation learning
- Cross-cultural NLP
- Multimodality and language grounding
- Knowledge-augmented NLP
- Scientific NLP
- Scholarly document processing
- Citation / evidence extraction
- Climate NLP
- Language-and-molecules modeling
- Dense retrieval
- Neural ranking / learning to rank
- Generative retrieval
- Conversational search
- RAG system design and evaluation
- Knowledge-enhanced retrieval
- Long-context retrieval
- LLM-based IR evaluation
- Collaborative filtering
- Knowledge-based recommendation
- Deep learning for recommender systems
- Natural-language / conversational recommenders
- Fair / privacy-aware recommendation
- 3D reconstruction from multi-view and sensors
- 3D reconstruction from single images
- Adversarial attack and defense in vision
- Biometrics
- Computational imaging
- Datasets and evaluation for vision
- Efficient and scalable vision models
- Face analysis
- Body / pose / gesture / motion understanding
- Low-level vision
```

```
- Document analysis and understanding
- Open-set / open-world recognition
- Out-of-distribution detection in vision
- Fine-grained visual categorization
- Self-supervised visual representation learning
- Semi-supervised visual learning
- Few-shot visual recognition
- Domain adaptation in vision
- Diffusion models for image synthesis
- Autoregressive image generation
- Generative-model inversion
- Image editing with generative models
- Synthetic data for visual recognition
- Analysis-by-synthesis / render-and-compare recognition
- 3D foundation models
- 3D content creation
- Neural radiance fields
- 3D Gaussian splatting
- Implicit neural representations
- Novel-view synthesis
- Long-form video understanding
- Human action understanding / generation
- Large multimodal model evaluation
- Visual-prompt understanding in multimodal models
- Open-vocabulary / open-task vision-language models
- Vision-language reasoning
- Medical vision foundation models
- Medical image / video generation
- Biomedical image parsing
- Pathology image models
- Radiology foundation-model applications
- Medical imaging data curation
- Medical imaging data augmentation
- Fairness and safety in medical imaging AI
- Automatic speech recognition
- ASR error correction / rescoring
- Multilingual / multi-accent ASR
- Spoken language translation
- Spoken language understanding
- Text-to-speech
- Voice conversion
- Speaker verification
- Speaker diarization
- Speech processing with discrete units
- Speech emotion recognition / paralinguistics
- Pathological / health-related speech analysis
- Multi-channel speech enhancement
- Human-machine spoken interaction
- Responsible speech foundation models
- Speech deepfake / spoofing detection
- Streaming ASR
- Self-supervised learning for ASR
- Target-speaker extraction
- Deep reinforcement learning
- Hierarchical reinforcement learning
- Model-based reinforcement learning
- Policy optimization
- Bandits
- Sequential decision-making under uncertainty
- Active learning
- Adversarial learning
- Causal inference
- Causal discovery
- Causal representation learning
```

```
- Uncertainty quantification
- Probabilistic programming
- Approximate / variational inference
- Performative prediction
- Bayesian methods
- Belief propagation
- Robot foundation models
- Representation learning for robotic perception and control
- Imitation learning for robotics
- Reinforcement learning for physical robots
- Learning-and-planning hybrids in robotics
- Uncertainty-aware robotics
- Automatic robotic data generation
- Multimodal robot perception and sensor fusion
- Human-robot interaction with language / gestures
- Learning for robot task and motion planning
- Learning for hardware design and optimization
- Robot safety for learning-based systems
- Robot manipulation
- Visual navigation
- Locomotion learning
- Autonomous driving perception / prediction / planning
- Embodied question answering / embodied vision-language
- Open-world embodied AI
- Generative AI for embodied AI
- Dataset composition and curation for foundation models
- Data filtering / relabeling / augmentation
- Dataset quality / diversity / provenance analysis
- Data debugging / influence analysis
- Dataset distillation
- Synthetic-data effects / model collapse
- Weak-to-strong generalization
- Graph neural networks
- Relational / structured learning
- Spatio-temporal learning
- Time-series modeling
- Time-series foundation models
- Federated learning
- Privacy and security in data-centric ML
- Deep learning theory (training dynamics, generalization,
↪  optimization convergence)
- Scientific machine learning (PDE solvers, neural operators, PINNs)
- Continual learning and catastrophic forgetting
- Object detection, segmentation, and tracking in vision
- Video segmentation, tracking, and generation
- Remote sensing and geospatial vision
- Medical image segmentation and reconstruction (beyond foundation
↪  models)
- Biomedical signal analysis (EEG, ECG, physiological)
- Quantum machine learning
- Spiking and neuromorphic computing
- Explainable AI (non-mechanistic / non-LLM)
- AI governance, policy, and societal impact
- Systems and serving infrastructure for large models
- Audio and music modeling (non-speech)
- Tabular machine learning and AutoML
- Point cloud and 3D geometric learning
- Wireless communications and signal processing

Rules:
1) Output ONLY compact JSON of the form {"topics": ["<topic>",
↪  "<topic>", ...]}.
2) Each string in the list MUST exactly match one topic from the list
↪  above (same spelling and punctuation).
```

```
3) If no topic clearly applies, output {"topics": []}.
4) Never invent topics outside the list.
5) List all applicable topics in descending order of relevance. Papers
↪  commonly span multiple topics -- a method, a task, a domain, and a
↪  data concern can each map to different topics. Include every topic
↪  the paper directly addresses, not just the primary focus. Exclude
↪  topics that are only mentioned in passing or tangentially
↪  adjacent.

Title: {title}
Abstract: {abstract}

List all applicable topics in descending order of relevance.
```

H.2 Contribution Generation Prompt

Contribution Generation Prompt

```
You are a seasoned computer science researcher who has done extensive
↪  work in machine learning, deep learning, computer vision, natural
↪  language processing, reinforcement learning, artificial
↪  intelligence, human computer interaction, and many related fields.
You have spent many years on the organizing and peer-review committees
↪  of many relevant conferences and publications like NeurIPS, ICLR,
↪  ICML, ICCV, ACL, EMNLP, NAACL, AAAI, CHI, TMLR, TACL, etc.

You need to use your expertise to accurately and realistically predict
↪  a followup paper that builds on (cites) the set of background
↪  papers given to you. For the paper you predict, you must output
↪  its title and abstract.

Below are a few solved examples for this prediction problem where we
↪  provide only one possible followup.

<example 1>
Background Paper 1:
Title: Adam: A Method for Stochastic Optimization
Abstract: We introduce Adam, an algorithm for first-order
↪  gradient-based optimization of stochastic objective functions. The
↪  method is straightforward to implement and is based on adaptive
↪  estimates of lower-order moments of the gradients. The method is
↪  computationally efficient, has little memory requirements and is
↪  well suited for problems that are large in terms of data and/or
↪  parameters. The method is also appropriate for non-stationary
↪  objectives and problems with very noisy and/or sparse gradients.
↪  The method exhibits invariance to diagonal rescaling of the
↪  gradients by adapting to the geometry of the objective function.
↪  The hyper-parameters have intuitive interpretations and typically
↪  require little tuning. Some connections to related algorithms, on
↪  which Adam was inspired, are discussed. We also analyze the
↪  theoretical convergence properties of the algorithm and provide a
↪  regret bound on the convergence rate that is comparable to the
↪  best known results under the online convex optimization framework.
↪  We demonstrate that Adam works well in practice and compares
↪  favorably to other stochastic optimization methods.

Background Paper 2:
Title: IP-Adapter: Text Compatible Image Prompt Adapter for
↪  Text-to-Image Diffusion Models
```

```
Abstract: Recent years have witnessed the strong power of large
 ↪  text-to-image diffusion models for the impressive generative
 ↪  capability to create high-fidelity images. However, it is very
 ↪  tricky to generate desired images using only text prompt as it
 ↪  often involves complex prompt engineering. An alternative to text
 ↪  prompt is image prompt, as the saying goes:"an image is worth a
 ↪  thousand words". Although existing methods of direct fine-tuning
 ↪  from pretrained models are effective, they require large computing
 ↪  resources and are not compatible with other base models, text
 ↪  prompt, and structural controls. In this paper, we present
 ↪  IP-Adapter, an effective and lightweight adapter to achieve image
 ↪  prompt capability for the pretrained text-to-image diffusion
 ↪  models. The key design of our IP-Adapter is decoupled
 ↪  cross-attention mechanism that separates cross-attention layers
 ↪  for text features and image features. Despite the simplicity of
 ↪  our method, an IP-Adapter with only 22M parameters can achieve
 ↪  comparable or even better performance to a fully fine-tuned image
 ↪  prompt model. As we freeze the pretrained diffusion model, the
 ↪  proposed IP-Adapter can be generalized not only to other custom
 ↪  models fine-tuned from the same base model, but also to
 ↪  controllable generation using existing controllable tools. With
 ↪  the benefit of the decoupled cross-attention strategy, the image
 ↪  prompt can also work well with the text prompt to achieve
 ↪  multimodal image generation. The project page is available at
 ↪  \url{https://ip-adapter.github.io}.

Background Paper 3:
Title: High-Resolution Image Synthesis with Latent Diffusion Models
Abstract: By decomposing the image formation process into a sequential
 ↪  application of denoising autoencoders, diffusion models (DMs)
 ↪  achieve state-of-the-art synthesis results on image data and
 ↪  beyond. Additionally, their formulation allows for a guiding
 ↪  mechanism to control the image generation process without
 ↪  retraining. However, since these models typically operate directly
 ↪  in pixel space, optimization of powerful DMs often consumes
 ↪  hundreds of GPU days and inference is expensive due to sequential
 ↪  evaluations. To enable DM training on limited computational
 ↪  resources while retaining their quality and flexibility, we apply
 ↪  them in the latent space of powerful pretrained autoencoders. In
 ↪  contrast to previous work, training diffusion models on such a
 ↪  representation allows for the first time to reach a near-optimal
 ↪  point between complexity reduction and detail preservation,
 ↪  greatly boosting visual fidelity. By introducing cross-attention
 ↪  layers into the model architecture, we turn diffusion models into
 ↪  powerful and flexible generators for general conditioning inputs
 ↪  such as text or bounding boxes and high-resolution synthesis
 ↪  becomes possible in a convolutional manner. Our latent diffusion
 ↪  models (LDMs) achieve a new state of the art for image inpainting
 ↪  and highly competitive performance on various tasks, including
 ↪  unconditional image generation, semantic scene synthesis, and
 ↪  super-resolution, while significantly reducing computational
 ↪  requirements compared to pixel-based DMs. Code is available at
 ↪  https://github.com/CompVis/latent-diffusion.

Background Paper 4:
Title: BrainVis: Exploring the Bridge between Brain and Visual Signals
 ↪  via Image Reconstruction
```

```
Abstract: Analyzing and reconstructing visual stimuli from brain
↪  signals effectively advances the understanding of human visual
↪  system. However, the EEG signals are complex and contain
↪  significant noise. This leads to substantial limitations in
↪  existing works of visual stimuli reconstruction from EEG, such as
↪  difficulties in aligning EEG embeddings with the fine-grained
↪  semantic information and a heavy reliance on additional large
↪  self-collected dataset for training. To address these challenges,
↪  we propose a novel approach called BrainVis. Firstly, we divide
↪  the EEG signals into various units and apply a self-supervised
↪  approach on them to obtain EEG time-domain features, in an attempt
↪  to ease the training difficulty. Additionally, we also propose to
↪  utilize the frequency-domain features to enhance the EEG
↪  representations. Then, we simultaneously align EEG time-frequency
↪  embeddings with the interpolation of the coarse and fine-grained
↪  semantics in the CLIP space, to highlight the primary visual
↪  components and reduce the cross-modal alignment difficulty.
↪  Finally, we adopt the cascaded diffusion models to reconstruct
↪  images. Using only 10\% training data of the previous work, our
↪  proposed BrainVis outperforms state of the arts in both semantic
↪  fidelity reconstruction and generation quality. The code is
↪  available at https://github.com/RomGai/BrainVis.

Predicted Followup Paper:
Title: BrainDecoder: Style-Based Visual Decoding of EEG Signals
Abstract: Decoding neural representations of visual stimuli from
↪  electroencephalography (EEG) offers valuable insights into brain
↪  activity and cognition. Recent advancements in deep learning have
↪  significantly enhanced the field of visual decoding of EEG,
↪  primarily focusing on reconstructing the semantic content of
↪  visual stimuli. In this paper, we present a novel visual decoding
↪  pipeline that, in addition to recovering the content, emphasizes
↪  the reconstruction of the style, such as color and texture, of
↪  images viewed by the subject. Unlike previous methods, this
↪  ``style-based'' approach learns in the CLIP spaces of image and
↪  text separately, facilitating a more nuanced extraction of
↪  information from EEG signals. We also use captions for text
↪  alignment simpler than previously employed, which we find work
↪  better. Both quantitative and qualitative evaluations show that
↪  our method better preserves the style of visual stimuli and
↪  extracts more fine-grained semantic information from neural
↪  signals. Notably, it achieves significant improvements in
↪  quantitative results and sets a new state-of-the-art on the
↪  popular Brain2Image dataset.
</example 1>



<example 2>
Background Paper 1:
Title: CrypTen: Secure Multi-Party Computation Meets Machine Learning
```

```
Abstract: Secure multi-party computation (MPC) allows parties to
 ↪  perform computations on data while keeping that data private. This
 ↪  capability has great potential for machine-learning applications:
 ↪  it facilitates training of machine-learning models on private data
 ↪  sets owned by different parties, evaluation of one party's private
 ↪  model using another party's private data, etc. Although a range of
 ↪  studies implement machine-learning models via secure MPC, such
 ↪  implementations are not yet mainstream. Adoption of secure MPC is
 ↪  hampered by the absence of flexible software frameworks that"speak
 ↪  the language"of machine-learning researchers and engineers. To
 ↪  foster adoption of secure MPC in machine learning, we present
 ↪  CrypTen: a software framework that exposes popular secure MPC
 ↪  primitives via abstractions that are common in modern
 ↪  machine-learning frameworks, such as tensor computations,
 ↪  automatic differentiation, and modular neural networks. This paper
 ↪  describes the design of CrypTen and measure its performance on
 ↪  state-of-the-art models for text classification, speech
 ↪  recognition, and image classification. Our benchmarks show that
 ↪  CrypTen's GPU support and high-performance communication between
 ↪  (an arbitrary number of) parties allows it to perform efficient
 ↪  private evaluation of modern machine-learning models under a
 ↪  semi-honest threat model. For example, two parties using CrypTen
 ↪  can securely predict phonemes in speech recordings using
 ↪  Wav2Letter faster than real-time. We hope that CrypTen will spur
 ↪  adoption of secure MPC in the machine-learning community.

Predicted Followup Paper:
Title: Low-Latency Privacy-Preserving Deep Learning Design via Secure
 ↪  MPC
Abstract: Secure multi-party computation (MPC) facilitates
 ↪  privacy-preserving computation between multiple parties without
 ↪  leaking private information. While most secure deep learning
 ↪  techniques utilize MPC operations to achieve feasible
 ↪  privacy-preserving machine learning on downstream tasks, the
 ↪  overhead of the computation and communication still hampers their
 ↪  practical application. This work proposes a low-latency
 ↪  secret-sharing-based MPC design that reduces unnecessary
 ↪  communication rounds during the execution of MPC protocols. We
 ↪  also present a method for improving the computation of commonly
 ↪  used nonlinear functions in deep learning by integrating
 ↪  multivariate multiplication and coalescing different packets into
 ↪  one to maximize network utilization. Our experimental results
 ↪  indicate that our method is effective in a variety of settings,
 ↪  with a speedup in communication latency of $10\sim20\%$.
</example 2>



<example 3>
Background Paper 1:
Title: Retrieval-Augmented Generation for Large Language Models: A
 ↪  Survey
```

```
Abstract: Large Language Models (LLMs) demonstrate significant
↪  capabilities but face challenges such as hallucination, outdated
↪  knowledge, and non-transparent, untraceable reasoning processes.
↪  Augmented Generation (RAG) has emerged as a promising solution to
↪  these issues by incorporating real-time data from external
↪  databases into LLM responses. This enhances the accuracy and
↪  credibility of the models, particularly for knowledge-intensive
↪  tasks, and allows for continuous knowledge updates and integration
↪  of domain-specific information. RAG synergistically merges LLMs'
↪  intrinsic knowledge with the vast, dynamic repositories of
↪  external databases. This survey paper provides an in-depth
↪  analysis of the evolution of RAG, focusing on three key paradigms:
↪  Naive RAG, Advanced RAG, and Modular RAG. It methodically examines
↪  the three fundamental components of RAG systems: the retriever,
↪  the generator, and the augmentation methods, underscoring the
↪  cutting-edge technologies within each componenet. Additionally,
↪  the paper introduces novel metrics and capabilities for evaluating
↪  RAG models, as well as the most recent evaluation framework.
↪  Finally, the paper outlines future research directions from three
↪  perspectives: future challenges,modality extension,and the
↪  development of the RAG technical stack and ecosystem.

Background Paper 2:
Title: From Local to Global: A Graph RAG Approach to Query-Focused
↪  Summarization
Abstract: The use of retrieval-augmented generation (RAG) to retrieve
↪  relevant information from an external knowledge source enables
↪  large language models (LLMs) to answer questions over private
↪  and/or previously unseen document collections. However, RAG fails
↪  on global questions directed at an entire text corpus, such
↪  as"What are the main themes in the dataset?", since this is
↪  inherently a query-focused summarization (QFS) task, rather than
↪  an explicit retrieval task. Prior QFS methods, meanwhile, fail to
↪  scale to the quantities of text indexed by typical RAG systems. To
↪  combine the strengths of these contrasting methods, we propose a
↪  Graph RAG approach to question answering over private text corpora
↪  that scales with both the generality of user questions and the
↪  quantity of source text to be indexed. Our approach uses an LLM to
↪  build a graph-based text index in two stages: first to derive an
↪  entity knowledge graph from the source documents, then to
↪  pregenerate community summaries for all groups of closely-related
↪  entities. Given a question, each community summary is used to
↪  generate a partial response, before all partial responses are
↪  again summarized in a final response to the user. For a class of
↪  global sensemaking questions over datasets in the 1 million token
↪  range, we show that Graph RAG leads to substantial improvements
↪  over a naive RAG baseline for both the comprehensiveness and
↪  diversity of generated answers. An open-source, Python-based
↪  implementation of both global and local Graph RAG approaches is
↪  forthcoming at https://aka.ms/graphrag.

Predicted Followup Paper:
Title: LightRAG: Simple and Fast Retrieval-Augmented Generation
```

```
Abstract: Retrieval-Augmented Generation (RAG) systems enhance large
↪  language models (LLMs) by integrating external knowledge sources,
↪  enabling more accurate and contextually relevant responses
↪  tailored to user needs. However, existing RAG systems have
↪  significant limitations, including reliance on flat data
↪  representations and inadequate contextual awareness, which can
↪  lead to fragmented answers that fail to capture complex
↪  inter-dependencies. To address these challenges, we propose
↪  LightRAG, which incorporates graph structures into text indexing
↪  and retrieval processes. This innovative framework employs a
↪  dual-level retrieval system that enhances comprehensive
↪  information retrieval from both low-level and high-level knowledge
↪  discovery. Additionally, the integration of graph structures with
↪  vector representations facilitates efficient retrieval of related
↪  entities and their relationships, significantly improving response
↪  times while maintaining contextual relevance. This capability is
↪  further enhanced by an incremental update algorithm that ensures
↪  the timely integration of new data, allowing the system to remain
↪  effective and responsive in rapidly changing data environments.
↪  Extensive experimental validation demonstrates considerable
↪  improvements in retrieval accuracy and efficiency compared to
↪  existing approaches. We have made our LightRAG open-source and
↪  available at the link: https://github.com/HKUDS/LightRAG.
</example 3>



You need to first think through how exactly you want to combine the
↪  background papers (i.e. which aspects from these papers will be
↪  used in the followup work) before making each prediction. This
↪  will constitute the 'reasoning' part of your response. Only then
↪  will you make your prediction of the title and abstract of the
↪  followup work.

When making your prediction, please use the output format shown below.
↪  Please don't use any newlines or whitespace that cause deviation
↪  from this format.

Reasoning: ...
Title: ...
Abstract: ...

EXTREMELY IMPORTANT: Please make sure to output all 3 fields:
↪  Reasoning, Title and Abstract in that order before ending your
↪  response. RESPONSES WITHOUT THE Title AND Abstract FIELDS WILL BE
↪  CONSIDERED INVALID. YOU MUST OUTPUT ALL THREE FIELDS IN THE SAME
↪  RESPONSE SEPERATED BY NEWLINES. DO NOT SPLIT UP FIELDS BETWEEN
↪  RESPONSES.
```

H.3 Paraphrase Generation Prompt

Paraphrase Generation Prompt

```
You are a seasoned computer science researcher who has done extensive
↪  work in machine learning, deep learning, computer vision, natural
↪  language processing, reinforcement learning, artificial
↪  intelligence, human computer interaction, and many related fields.
You have spent many years on the organizing and peer-review committees
↪  of many relevant conferences and publications like NeurIPS, ICLR,
↪  ICML, ICCV, ACL, EMNLP, NAACL, AAAI, CHI, TMLR, TACL, etc.
```

```
You need to use your expertise to paraphrase the title and abstract of
↪  an existing research paper that will be provided to you. Make sure
↪  you paraphrase them well. I am not looking for a one-one
↪  sentence-level paraphrasal, but another title and abstract that
↪  another author could have written about the same ideas and
↪  findings. Feel free to change the narrative structure of the
↪  abstract as you please.

When making your predictions, please use the following output format.

Title: ...
Abstract: ...

Do not generate any other text or explanations.
```

H.4 LACER INTERPOLATIONS PROMPT

LACER Interpolations Prompt

```
You are an expert computer scientist.

You will be given a pair of title-abstracts (A and J) corresponding to
↪  real research papers. Your task is to synthesize a realistic
↪  sequence of 8 intermediate title-abstracts (B, C, D, E, F, G, H,
↪  I) that sequentially interpolate smoothly between the two provided
↪  ones that each change one specific facet of the corresponding
↪  contribution. Some examples of facets you could change are 1. the
↪  type of contribution (eg. analysis, benchmark, system demo,
↪  theoretical advance, etc.) 2. Type of architecture/technique used
↪  (eg. CNNs, transformers, RL, RAG, diffusion models, RNNs, etc. 3.
↪  The type of task / motivation (eg. image recognition, semantic
↪  parsing, language modeling, code generation, image generation,
↪  etc.)

Feel free to change other facets too as you see appropriate. It is
↪  important that the synthesized title-abstracts B-I represent a
↪  smooth interpolation between A and J such that no two consecutive
↪  title-abstracts differ too dramatically from each other. However,
↪  it is also important that every pair of consecutive
↪  title-abstracts from A-J do differ from each other in at least one
↪  important way.

Please return you responses in the following format:

Title B: ...
Abstract B: ...

Title C: ...
Abstract C: ...

Title D: ...
Abstract D: ...

Title E: ...
Abstract E: ...

Title F: ...
Abstract F: ...

Title G: ...
Abstract G: ...
```

```
Title H: ...
Abstract H: ...

Title I: ...
Abstract I: ...

Here are your inputs:

Title A: {{title_a}}
Abstract A: {{abstract_a}}

Title J: {{title_j}}
Abstract J: {{abstract_j}}
```

H.5 LACER JUDGE PROMPT

LACER Judge Prompt

```
You will be given a pair of title-abstracts Reference and Generated.
↪  Your task is to assign a score from 1-10 measuring how similar the
↪  Generated is to the Reference title-abstract where 1 represents
↪  the lowest similarity score and 10 represents the highest.

Here are some examples of References along with 10 Generations each
↪  corresponding to scores 1-10.

Reference A:
Intelligent Urban Surveillance in India: Real-Time Recognition of
↪  Individual Attributes
This study introduces a smart surveillance system for Indian cities
↪  that performs real-time identification and analysis of people's
↪  attributes. Leveraging advanced artificial intelligence and
↪  machine learning, the system recognizes features such as
↪  upper-body color, clothing, accessories, headgear, and so on, and
↪  analyzes behavior using camera feeds installed throughout the
↪  city.

Generations:
PyTorch: A High-Performance Deep Learning Library with an Imperative,
↪  Pythonic Design
Deep learning frameworks have often emphasized either ease of use or
↪  performance, but seldom both. PyTorch demonstrates that these aims
↪  can be jointly achieved: it provides an imperative, Python-native
↪  programming model that treats code as the model, simplifies
↪  debugging, and harmonizes with popular scientific computing
↪  libraries, while remaining efficient and supporting hardware
↪  accelerators such as GPUs. In this work, we articulate the
↪  principles that guided PyTorch's implementation and show how they
↪  manifest in its architecture. We underscore that every part of
↪  PyTorch is an ordinary Python program under the user's full
↪  control. We also describe how a careful, pragmatic realization of
↪  the runtime's key components enables them to interoperate to
↪  deliver compelling performance. Finally, we present evidence of
↪  the efficiency of individual subsystems and the overall speed of
↪  PyTorch on several common benchmarks.
Score: 1

PyTorch-Stream: Eager, High-Throughput Extensions for Real-Time Vision
↪  and Video
```

```
We present PyTorch-Stream, a set of runtime and library extensions
↪  that bring low-latency, multi-stream video analytics to PyTorch
↪  while preserving its imperative programming model. PyTorch-Stream
↪  introduces asynchronous camera ingest, zero-copy decoding, fused
↪  preprocessing ops, and CUDA graph capture to minimize per-frame
↪  overhead. We describe design decisions that retain Pythonic
↪  control flow yet enable ahead-of-time export of hot paths for
↪  steady-state performance. Across common video tasks (object
↪  detection, tracking-by-detection, and attribute classification),
↪  PyTorch-Stream reduces end-to-end latency by 30-55% and increases
↪  throughput by up to 2.1x on a single GPU without sacrificing
↪  debuggability.
Score: 2

PyTorch-PersonAttr: A Reproducible Toolkit for Person Attribute
↪  Recognition in Surveillance Video
We release PyTorch-PersonAttr, a modular toolkit for training,
↪  evaluating, and deploying person attribute recognition models
↪  using the PyTorch-Stream runtime. The toolkit standardizes data
↪  adapters (e.g., RAP, PA-100k, PETA), implements strong CNN and
↪  hybrid CNN-Transformer baselines, and provides consistent
↪  evaluation protocols for multi-label classification (e.g., apparel
↪  type, color, accessories). We detail reference training recipes,
↪  mixed-precision/compiled execution for real-time inference, and
↪  uncertainty calibration methods for attribute outputs. Experiments
↪  show state-of-the-art or competitive results on public benchmarks
↪  and >60 FPS inference for 720p streams on a single GPU.
Score: 3

CityAttr: A Benchmark for Fine-Grained Person Attribute Recognition in
↪  Urban Camera Feeds
We introduce CityAttr, a benchmark targeting fine-grained person
↪  attributes in urban environments, with 250k annotated person crops
↪  spanning diverse weather, lighting, and camera viewpoints.
↪  CityAttr adds difficult classes pertinent to city operations
↪  (upper-body color under motion blur, reflective accessories,
↪  safety gear) and defines standardized train/val/test splits and
↪  occlusion strata. We provide strong PyTorch-PersonAttr baselines,
↪  error taxonomies, and fairness analyses across scene contexts.
↪  Results highlight failure modes in crowded scenes and under low
↪  light, motivating temporal modeling and domain adaptation for
↪  real-time deployments.
Score: 4

TorchStream City: A Low-Latency, Multi-Camera Video Analytics System
↪  for Urban Attribute Tagging
Building on PyTorch-Stream and CityAttr, we present TorchStream City,
↪  a reference system for city-scale, real-time attribute tagging.
↪  The system integrates multi-camera ingest, on-GPU
↪  batching/scheduling, online multi-object tracking, and temporal
↪  ensembling for stable attribute estimates. A hybrid eager-compiled
↪  execution path allows imperative control for orchestration while
↪  compiling per-operator graphs for steady-state throughput.
↪  Deployed on traffic and pedestrian cameras, TorchStream City
↪  sustains 25-30 FPS per stream across 32 feeds on two GPUs, with
↪  <200 ms median latency for detection, tracking, and attribute
↪  tagging, and provides APIs for downstream behavior analytics.
Score: 5

EdgeTorch-Attr: Efficient Person Attribute Recognition on Embedded and
↪  On-Camera Accelerators
```

```
We propose EdgeTorch-Attr, an optimization stack enabling person
↪  attribute recognition on edge devices. Techniques include compound
↪  scaling, quantization-aware training, structured pruning,
↪  knowledge distillation from server-grade models, and deployment
↪  via PyTorch 2 AOT compilation and TensorRT backends. We co-design
↪  the streaming pipeline to overlap decode, preproc, and inference
↪  on limited memory budgets. Field trials on NVIDIA Jetson- and
↪  VPU-class devices show 3-5x energy efficiency gains while
↪  maintaining >90% of server-level accuracy on CityAttr, with robust
↪  real-time performance on 1080p input for core attributes
↪  (upper-body color, apparel category, headgear, accessories).
Score: 6

IndAttr: Culturally-Aware Attribute Recognition for Indian Urban
↪  Scenes via Domain-Adaptive Temporal Transformers
We present IndAttr, a domain-adaptive model suite tailored to Indian
↪  urban video feeds. IndAttr augments attribute taxonomies to
↪  include culturally salient apparel and accessories (e.g., kurta,
↪  sari, dupatta, school uniforms, turbans, safety vests), and
↪  leverages temporal Vision Transformers with cross-frame attention
↪  for stability under occlusion and crowding. We introduce
↪  unsupervised domain adaptation from CityAttr using camera-style
↪  augmentation and self-training, plus limited expert-labeled Indian
↪  samples collected under ethical protocols. IndAttr improves mAP by
↪  7.8 points over generic baselines on Indian pilot datasets while
↪  sustaining edge-ready throughput via distillation to compact
↪  temporal backbones.
Score: 7

PriCity-Attr: Privacy-Preserving, Federated Multi-Camera Attribute
↪  Analytics for Indian Smart Cities
We develop PriCity-Attr, a privacy-preserving training and deployment
↪  framework for multi-camera attribute analytics in Indian cities.
↪  The system performs on-device anonymization (face/body blurring
↪  for raw frames), stores only attribute and trajectory metadata,
↪  and trains models via cross-ward federated learning with secure
↪  aggregation and differential privacy accounting. We include
↪  governance hooks (policy-driven retention, audit logs) and
↪  human-in-the-loop tools for bias auditing. In a city pilot across
↪  120 cameras, PriCity-Attr maintains IndAttr-level accuracy,
↪  reduces cross-site generalization error by 25%, and meets sub-250
↪  ms end-to-end latency, while adhering to documented privacy
↪  constraints.
Score: 8

Real-Time Indian Urban Monitoring: City-Scale Deployment of Attribute
↪  and Behavior Analytics
We present a production-grade, city-scale deployment that integrates
↪  IndAttr and PriCity-Attr into a unified smart monitoring platform
↪  for Indian metros. The system performs real-time identification of
↪  salient person attributes (upper-body color, apparel type,
↪  accessories, headgear) and stabilizes outputs via temporal
↪  modeling to feed behavior analytics (zone occupancy, queueing,
↪  safety-gear compliance). An edge-cloud architecture supports
↪  heterogeneous cameras, with resilient scheduling, adaptive
↪  bitrate, and failover. We report month-long operations over 500+
↪  feeds, covering throughput, latency, availability, and model drift
↪  monitoring, demonstrating actionable, privacy-aware analytics for
↪  urban management at scale.
Score: 9

Intelligent Urban Surveillance in India: Real-Time Recognition of
↪  Individual Attributes
```

```
This study introduces a smart surveillance system for Indian cities
↪ that performs real-time identification and analysis of people's
↪ attributes. Leveraging advanced artificial intelligence and
↪ machine learning, the system recognizes features such as
↪ upper-body color, clothing, accessories, headgear, and so on, and
↪ analyzes behavior using camera feeds installed throughout the
↪ city.
Score: 10

Reference B:
Ada-Instruct: Retooling Instruction Generation for Complex Reasoning
Augmenting instructions is critical for unlocking the full potential
↪ of large language models (LLMs) on downstream tasks. Current
↪ Self-Instruct approaches largely fabricate new instructions from a
↪ small seed set via in-context learning. Our analysis reveals a key
↪ limitation of this paradigm: even with GPT4o, Self-Instruct fails
↪ to produce complex instructions of length 100 or more, which are
↪ necessary for demanding tasks such as code completion. To overcome
↪ this, we observe that fine-tuning open source LLMs with only ten
↪ examples can yield complex instructions that preserve
↪ distributional consistency for complex reasoning tasks. We
↪ introduce Ada-Instruct, an adaptive instruction generator obtained
↪ through fine-tuning. We validate Ada-Instruct empirically across
↪ different applications, and the results demonstrate its ability to
↪ generate long, intricate, and distributionally consistent
↪ instructions.

Generations:
Evaluating Mathematical Problem Solving Using the MATH Dataset
Many forms of intellectual work depend on mathematical problem
↪ solving, yet computers still struggle with this capability. To
↪ assess this skill in machine learning systems, we present MATH, a
↪ dataset of 12,500 difficult competition mathematics problems. Each
↪ problem includes a complete step-by-step solution, enabling models
↪ to be trained to produce answer derivations and explanations. To
↪ support future research and improve accuracy on MATH, we
↪ additionally release a large auxiliary pretraining dataset aimed
↪ at teaching models the fundamentals of mathematics. While we are
↪ able to raise accuracy on MATH, our results show that performance
↪ remains relatively low, even with extremely large Transformer
↪ models. Moreover, if current scaling trends persist, simply
↪ expanding compute budgets and model parameter counts appears
↪ impractical for achieving strong mathematical reasoning. Although
↪ scaling Transformers is largely solving most other text-based
↪ tasks, it is not currently solving MATH. Substantive progress on
↪ mathematical problem solving will likely require new algorithmic
↪ advances from the broader research community.
Score: 1

Fine-Grained Evaluation of Mathematical Reasoning with Stepwise
↪ Derivations
```

```
We revisit evaluation on competition mathematics by exploiting the
↪  full step-by-step solutions accompanying problems. Beyond
↪  final-answer accuracy, we introduce derivation-aware metrics that
↪  align a model's generated reasoning with reference solutions via
↪  step matching, dependency agreement, and algebraic edit distance.
↪  We release standardized evaluation scripts and human-verified
↪  annotations for a subset of the MATH dataset, enabling assessment
↪  of intermediate reasoning quality and error localization. Our
↪  analysis across model scales shows that improvements in final
↪  accuracy often mask brittle derivations and shortcut patterns. We
↪  find that models benefiting from chain-of-thought prompting still
↪  diverge significantly from canonical derivations, suggesting the
↪  need for training signals that target the structure and
↪  granularity of mathematical reasoning rather than only end
↪  answers.
Score: 2

AutoHint-MATH: Augmenting Competition Problems with Model-Generated
↪  Hints and Subgoals
To bridge the gap between final-answer evaluation and robust
↪  derivations, we introduce AutoHint-MATH, a data augmentation
↪  pipeline that generates targeted hints, subgoals, and intermediate
↪  checks for competition-level math problems. Using large language
↪  models guided by our stepwise metrics, we produce pedagogically
↪  structured scaffolds that highlight crucial transformations and
↪  decision points. We curate 60k high-quality hint-problem-solution
↪  triplets and show that training with these augmentations yields
↪  consistent gains in both final answers and derivation alignment on
↪  MATH. Compared to vanilla chain-of-thought prompting,
↪  AutoHint-MATH improves sample efficiency and reduces off-track
↪  reasoning, indicating that explicit scaffolding can better shape
↪  model search through complex solution spaces.
Score: 3

InstructMATH: Instruction-Tuning for Step-by-Step Mathematical Problem
↪  Solving
We move from passive scaffolds to active task framing by introducing
↪  InstructMATH, a collection of instruction-problem-solution triples
↪  designed to instruction-tune models for mathematical reasoning.
↪  Instructions specify goals, permissible operations, and
↪  verification strategies, teaching models how to structure
↪  derivations before generating them. We compile 25k diverse
↪  instruction templates spanning algebra, geometry, and number
↪  theory, and show that instruction-tuned models outperform
↪  hint-augmented baselines on MATH under both few-shot and zero-shot
↪  settings. Analyses indicate that explicit procedural instructions
↪  reduce hallucinated steps and improve adherence to algebraic
↪  invariants. Our results suggest instruction-tuning is a promising
↪  path to controllable, reliable mathematical reasoning.
Score: 4

ReasonBench: A Multi-Domain Corpus of Instruction-Driven Problems with
↪  Worked Solutions
```

```
To test whether instruction-tuned reasoning transfers beyond
↪  mathematics, we create ReasonBench, a multi-domain corpus covering
↪  competition math, physics word problems, logic puzzles, and
↪  algorithmic thinking tasks, each paired with domain-specific
↪  instructions and worked solutions. We design a shared schema for
↪  instructions (goal, constraints, permitted tools, validation) and
↪  provide cross-domain transfer splits. Instruction-tuned models
↪  trained on ReasonBench improve on out-of-domain reasoning tasks,
↪  especially when instructions emphasize decomposition and
↪  verification. However, performance plateaus on tasks requiring
↪  long, intricate directives (e.g., multi-function code synthesis,
↪  multi-lemma proofs), motivating a closer study of instruction
↪  complexity and its role in reasoning.
Score: 5

On the Complexity of Instructions for Complex Reasoning Tasks
We systematically measure how instruction complexity-length,
↪  structural depth, and constraint density-affects performance on
↪  challenging tasks such as proof sketching and code completion. We
↪  find that instructions longer than ~100 tokens with nested
↪  constraints substantially improve reliability in multi-step
↪  reasoning, but current self-instruction pipelines rarely produce
↪  such long, structured directives and often drift from the target
↪  task's distribution. Using ReasonBench extensions for coding and
↪  formal reasoning, we quantify this mismatch and show that
↪  in-context self-instruct deteriorates instruction quality as
↪  length increases. These results highlight a bottleneck: generating
↪  long, distributionally faithful instructions is essential for
↪  unlocking complex reasoning, yet existing automatic pipelines fall
↪  short.
Score: 6

Scaffold-Instruct: Hierarchical Self-Instruct for Long-Form,
↪  Structured Prompts
We propose Scaffold-Instruct, a hierarchical self-instruction
↪  framework that builds long-form instructions via iterative
↪  decomposition: a planner drafts high-level goals, a refiner
↪  injects constraints and verification steps, and a validator
↪  enforces structural templates. Scaffold-Instruct increases
↪  instruction length and structural depth while improving internal
↪  consistency over standard self-instruct. On math, logic, and code
↪  tasks, models trained with Scaffold-Instruct show better adherence
↪  to multi-step procedures and fewer dead ends. Nevertheless, the
↪  approach is compute-intensive, relies on strong planners, and
↪  still exhibits distributional drift on specialized domains like
↪  code completion. These limitations motivate moving from purely
↪  in-context pipelines toward trainable instruction generators.
Score: 7

Few-Shot Fine-Tuned Instruction Generators for Mathematical and
↪  Program Reasoning
```

```
We introduce a trainable alternative to hierarchical self-instruct:
↪  fine-tuning a compact open-source LLM to act as an instruction
↪  generator using a small curated set (20-50) of long, structured
↪  seed instructions per domain. The resulting generator produces
↪  instructions that are longer, more constraint-aware, and more
↪  distributionally aligned with math and coding datasets than
↪  in-context self-instruct. When used to create training corpora,
↪  these instructions yield larger gains on multi-step reasoning and
↪  code completion benchmarks than Scaffold-Instruct, at a fraction
↪  of the cost. Ablations show that even minimal fine-tuning
↪  stabilizes long-instruction formatting and reduces semantic drift,
↪  suggesting few-shot fine-tuned generators are a scalable path
↪  forward.
Score: 8

AdaGen: Adaptive Few-Shot Instruction Generators for Complex Reasoning
Building on few-shot fine-tuned generators, we present AdaGen, an
↪  adaptive instruction generation framework that (1) fine-tunes
↪  open-source LLMs with as few as ten carefully selected seed
↪  instructions per domain, and (2) adaptively controls length,
↪  constraint density, and style to match target-task distributions.
↪  AdaGen automatically diagnoses gaps in coverage using lightweight
↪  discriminators and iteratively steers generation to maintain
↪  distributional fidelity. Across mathematical reasoning and code
↪  completion, AdaGen produces long (>=100 tokens), structurally rich
↪  instructions that lead to consistent downstream gains over
↪  self-instruct and hierarchical baselines. These findings set the
↪  stage for general-purpose, low-budget instruction generators
↪  tailored to complex reasoning tasks.
Score: 9

Ada-Instruct: Retooling Instruction Generation for Complex Reasoning
Augmenting instructions is critical for unlocking the full potential
↪  of large language models (LLMs) on downstream tasks. Current
↪  Self-Instruct approaches largely fabricate new instructions from a
↪  small seed set via in-context learning. Our analysis reveals a key
↪  limitation of this paradigm: even with GPT4o, Self-Instruct fails
↪  to produce complex instructions of length 100 or more, which are
↪  necessary for demanding tasks such as code completion. To overcome
↪  this, we observe that fine-tuning open source LLMs with only ten
↪  examples can yield complex instructions that preserve
↪  distributional consistency for complex reasoning tasks. We
↪  introduce Ada-Instruct, an adaptive instruction generator obtained
↪  through fine-tuning. We validate Ada-Instruct empirically across
↪  different applications, and the results demonstrate its ability to
↪  generate long, intricate, and distributionally consistent
↪  instructions.
Score: 10

Reference C:
Reinforced Self-Training (ReST) for Training Language Models
```

```
Reinforcement learning from human feedback (RLHF) can enhance the
↪  quality of large language models' (LLMs) outputs by aligning them
↪  with human preferences. We present a straightforward alignment
↪  approach, inspired by growing-batch reinforcement learning (RL),
↪  which we call Reinforced Self-Training (ReST). Starting from an
↪  initial LLM policy, ReST constructs a dataset by sampling from
↪  that policy, and then uses offline RL algorithms on this data to
↪  further improve the policy. Because the training data are
↪  generated offline and can be reused, ReST is more efficient than
↪  standard online RLHF procedures. Although ReST is a general method
↪  applicable across generative learning scenarios, we center our
↪  investigation on machine translation. Our results demonstrate that
↪  ReST can substantially boost translation quality-according to both
↪  automated metrics and human evaluations on machine translation
↪  benchmarks-while being compute- and sample-efficient.

Generations:
Algorithms for Proximal Policy Optimization
We present a new class of policy gradient algorithms for reinforcement
↪  learning that alternate between collecting data through
↪  environment interaction and maximizing a surrogate objective via
↪  stochastic gradient ascent. Unlike standard policy gradient
↪  approaches that make only one gradient update per data sample, we
↪  introduce a novel objective that enables multiple epochs of
↪  minibatch updates. The resulting methods, termed proximal policy
↪  optimization (PPO), capture some of the benefits of trust region
↪  policy optimization (TRPO) while being much simpler to implement,
↪  more general, and empirically exhibiting better sample complexity.
↪  We evaluate PPO on a set of benchmark tasks, including simulated
↪  robotic locomotion and Atari game playing, and show that it
↪  outperforms other online policy gradient methods, achieving an
↪  overall favorable balance among sample complexity, simplicity, and
↪  wall-time.
Score: 1

Proximal Policy Optimization with Replay: Enabling Stable Data Reuse
↪  in On-Policy RL
We extend proximal policy optimization (PPO) with a principled form of
↪  experience replay that increases sample efficiency while
↪  preserving stability. Our method augments the clipped surrogate
↪  objective with lightweight off-policy corrections using per-batch
↪  importance weights and a target network for value learning,
↪  enabling multiple epochs over mixed recent on-policy and
↪  near-on-policy samples. Across MuJoCo locomotion and Atari
↪  benchmarks, PPO+Replay achieves comparable or better asymptotic
↪  performance than PPO with 30–50% fewer environment interactions,
↪  while retaining PPO's simplicity and wall-time advantages.
↪  Ablations isolate the effects of replay ratio and clipping on
↪  stability, providing a practical recipe for safe data reuse in
↪  on-policy policy gradient methods.
Score: 2

Proximal Sequence Policy Optimization for Text Generation
```

```
We adapt proximal policy optimization to autoregressive sequence
↪  models for text generation. Our approach optimizes a clipped
↪  sequence-level policy gradient objective over Transformer language
↪  models, with rewards defined by task-specific automated metrics
↪  (e.g., ROUGE for summarization, BLEU for translation). We
↪  introduce a token-wise advantage estimator that stabilizes
↪  long-horizon credit assignment and a curriculum over sequence
↪  lengths. Experiments on CNN/DailyMail summarization and WMT14
↪  En-De translation show consistent metric gains over supervised
↪  fine-tuning and REINFORCE baselines at comparable compute,
↪  demonstrating that PPO's trust-region-like updates transfer
↪  effectively to discrete text generation.
Score: 3

KL-Regularized Proximal Optimization for Controlled Text Generation
We propose a KL-regularized variant of proximal optimization for
↪  sequence models that constrains updates relative to a supervised
↪  reference model. The objective augments PPO's clipped surrogate
↪  with an adaptive KL penalty against the reference policy, yielding
↪  stable improvements while preserving fluency. We instantiate
↪  rewards from automated metrics and task-specific constraints
↪  (length, toxicity filters), and introduce a reference-anchored
↪  value function to reduce variance. On summarization and
↪  translation, KL-Prox achieves higher ROUGE/BLEU and better
↪  human-rated coherence than metric-only PPO, highlighting the
↪  benefit of explicit distributional control for language
↪  generation.
Score: 4

Preference-Guided Proximal Optimization: Online RLHF for Sequence
↪  Models
We integrate human preference learning with proximal policy
↪  optimization for language generation. A reward model is trained
↪  from pairwise human comparisons and used to guide KL-regularized
↪  PPO updates of a Transformer policy anchored to a supervised
↪  reference. We interleave data collection (sampling candidate
↪  texts), preference labeling, reward model updates, and policy
↪  improvement. On summarization and open-ended generation, our
↪  method improves human preference win-rates over supervised
↪  baselines and metric-optimized PPO, while maintaining stability
↪  via adaptive KL and early stopping. Results demonstrate that
↪  online RLHF can be realized with simple proximal updates and
↪  modest human annotation.
Score: 5

Growing-Batch Preference Optimization: Bridging Online RLHF and
↪  Offline RL for LMs
We introduce a growing-batch training regime for preference-optimized
↪  language models that alternates between short bursts of sample
↪  collection and extended offline optimization. Candidate texts are
↪  generated from the current policy, scored by a learned preference
↪  model, and stored in a replay buffer. We then apply offline
↪  RL-style updates-advantage-weighted likelihood with conservative
↪  clipping and value targets fit by fitted policy evaluation-over
↪  the accumulated batch, with occasional refresh of the data.
↪  Compared to purely online PPO-based RLHF, Growing-Batch PO reduces
↪  the number of preference queries and environment interactions
↪  while achieving similar or better human preference win-rates on
↪  summarization and dialogue.
Score: 6

Self-Generated Corpora for Batch RLHF: Offline Advantage Optimization
↪  of LMs
```

```
We present a purely offline procedure for aligning language models
↪  using self-generated datasets. Starting from a supervised policy,
↪  we sample candidate continuations, score them with a learned
↪  preference model, and construct a static training set. We then
↪  perform multiple epochs of offline reinforcement learning using
↪  advantage-weighted regression with KL regularization to the
↪  reference, without further online sampling during optimization.
↪  This self-training loop can be repeated to grow the dataset. On
↪  summarization and translation, our batch RLHF approach matches or
↪  exceeds online PPO-based RLHF in human and automatic metrics while
↪  reducing compute and annotation overhead via data reuse.
Score: 7

Offline Reinforcement Learning for Machine Translation via
↪  Self-Generated Batches
Focusing on machine translation, we instantiate an offline RL
↪  framework that improves a Transformer translator using only
↪  self-generated candidate translations and offline optimization. We
↪  generate n-best lists from the current model, score them with a
↪  mixture of automatic metrics (BLEU, COMET) and a lightweight
↪  preference model, and train with KL-regularized advantage-weighted
↪  updates over the static pool. Periodic regeneration expands
↪  coverage, but all policy learning is performed offline, enabling
↪  aggressive data reuse. On WMT benchmarks, our method delivers
↪  substantial BLEU/COMET gains over supervised fine-tuning and
↪  online policy gradient methods at lower compute, with humans
↪  preferring our outputs for adequacy and fluency.
Score: 8

Preference-Scored Self-Training with Offline RL for LLM Translators
We propose a simple self-training algorithm for large language model
↪  (LLM) translators that combines dataset generation by the model
↪  with offline reinforcement learning. Given an initial LLM policy
↪  and a reference model, we produce candidate translations, score
↪  them using a learned preference model (optionally blended with
↪  automated metrics), and optimize the policy offline with
↪  KL-regularized advantage-weighted regression and value fitting.
↪  The process can be repeated in a growing-batch fashion to refresh
↪  the static dataset while retaining offline updates. Applied to WMT
↪  machine translation, this approach yields sizable improvements in
↪  BLEU/COMET and human evaluations relative to supervised
↪  fine-tuning and online RLHF, with favorable compute and sample
↪  efficiency.
Score: 9

Reinforced Self-Training (ReST) for Training Language Models
Reinforcement learning from human feedback (RLHF) can enhance the
↪  quality of large language models' (LLMs) outputs by aligning them
↪  with human preferences. We present a straightforward alignment
↪  approach, inspired by growing-batch reinforcement learning (RL),
↪  which we call Reinforced Self-Training (ReST). Starting from an
↪  initial LLM policy, ReST constructs a dataset by sampling from
↪  that policy, and then uses offline RL algorithms on this data to
↪  further improve the policy. Because the training data are
↪  generated offline and can be reused, ReST is more efficient than
↪  standard online RLHF procedures. Although ReST is a general method
↪  applicable across generative learning scenarios, we center our
↪  investigation on machine translation. Our results demonstrate that
↪  ReST can substantially boost translation quality-according to both
↪  automated metrics and human evaluations on machine translation
↪  benchmarks-while being compute- and sample-efficient.
Score: 10
```

```
Reference D:
MAPO: Boosting Multilingual Reasoning by Casting Cross-Language
↪  Alignment as Preference Optimization
Although reasoning is often regarded as language-independent, current
↪  LLMs display uneven reasoning performance across languages; for
↪  instance, a dominant language like English typically outperforms
↪  others due to imbalanced multilingual training data. To strengthen
↪  reasoning in non-dominant languages, we introduce a
↪  Multilingual-Alignment-as-Preference Optimization framework (MAPO)
↪  that aligns the reasoning processes in other languages with those
↪  of the dominant language. In particular, we leverage an
↪  off-the-shelf translation model to enforce consistency between
↪  answers in non-dominant and dominant languages, and treat this
↪  consistency as a preference signal for optimization with methods
↪  such as Direct Preference Optimization (DPO) or Proximal Policy
↪  Optimization (PPO). Empirically, MAPO reliably delivers
↪  substantial improvements in multilingual reasoning across various
↪  models on three benchmarks (MSVAMP +16.2%, MGSM +6.1%, and
↪  MNumGLUESub +13.3%), while also enhancing reasoning consistency
↪  across languages 1.

Generations:
Advancing Cross-Lingual Mathematical Reasoning: Empirical Findings and
↪  Lessons Learned
Prior work has largely emphasized building strong language models
↪  (LLMs) for mathematical reasoning in single-language settings,
↪  with limited attention to maintaining performance across multiple
↪  languages. To close this gap, we initiate the exploration and
↪  training of robust Multilingual Math Reasoning (xMR) LLMs. Using
↪  translation, we assemble the first multilingual instruction
↪  dataset for math reasoning, MGSM8KInstruct, spanning ten
↪  languages, thereby mitigating training data scarcity for xMR
↪  tasks. Leveraging this corpus, we introduce several training
↪  strategies to construct a family of xMR LLMs, dubbed MathOctopus,
↪  which consistently outperform typical open-source LLMs and surpass
↪  ChatGPT in few-shot setups. In particular, MathOctopus-13B attains
↪  47.6% accuracy on the MGSM test set, exceeding ChatGPT's 46.3%.
↪  Beyond these results, our extensive experiments yield two key
↪  takeaways: (1) extending rejection sampling to multilingual
↪  settings provides performance gains, though the improvements are
↪  limited; and (2) using parallel corpora for math Supervised
↪  Fine-Tuning (SFT) across multiple languages significantly improves
↪  multilingual performance and also boosts monolingual ability. This
↪  suggests constructing multilingual corpora is a valuable lever for
↪  improving performance in a specific language, especially for
↪  mathematical reasoning. For example, MathOctopus-7B improves over
↪  English-only trained counterparts from 42.2% to 50.8% on the GSM8K
↪  test set.
Score: 1

Consistency-Regularized SFT for Multilingual Mathematical Reasoning
```

```
Building on multilingual instruction tuning for mathematical
↪  reasoning, we investigate whether explicitly encouraging
↪  cross-lingual agreement can further improve xMR LLMs. Using the
↪  MGSM8KInstruct corpus, we construct parallel
↪  problem-solution-rationale tuples across ten languages via
↪  high-quality translation. We introduce a consistency-regularized
↪  supervised fine-tuning (CR-SFT) objective that augments standard
↪  SFT with two auxiliary signals: (1) answer-level agreement across
↪  parallel languages, enforced via a differentiable dual-decoding
↪  consistency loss; and (2) rationale-level agreement, measured by
↪  semantic similarity between chain-of-thought embeddings.
↪  Fine-tuning 7B-13B models with CR-SFT yields consistent gains over
↪  MathOctopus, with the 7B model improving by +2.4% on MGSM and
↪  +1.8% on GSM8K. We observe that small amounts of multilingual
↪  parallel supervision are sufficient to regularize cross-lingual
↪  reasoning behavior, reducing variance across languages while
↪  preserving English performance.
Score: 2

Cross-Lingual Distillation for Multilingual Math Reasoning
We extend consistency-regularized multilingual SFT with a
↪  teacher-student framework that distills reasoning skills from a
↪  strong English teacher into a multilingual student. Given parallel
↪  MGSM8KInstruct data, the teacher generates high-quality rationales
↪  and answers in English, which are translated and used to supervise
↪  the student in non-dominant languages. We combine teacher-forced
↪  rationale distillation with consistency losses on final answers,
↪  and introduce a selective distillation filter to discard
↪  low-confidence teacher traces. On MGSM and a bilingual subset of
↪  MSVAMP, our 7B student outperforms CR-SFT by +1.5-2.1% across
↪  non-dominant languages while maintaining English accuracy,
↪  indicating that cross-lingual distillation transfers not only
↪  final-answer competence but also intermediate reasoning
↪  structures.
Score: 3

Round-Trip Self-Training for Low-Resource Multilingual Reasoning
To reduce reliance on parallel supervision, we propose round-trip
↪  self-training (RT-ST) that bootstraps multilingual mathematical
↪  reasoning from monolingual non-English data. RT-ST generates
↪  pseudo-labeled rationales by translating non-English problems to
↪  English, invoking the English teacher to produce
↪  rationales/answers, and translating them back. We introduce
↪  round-trip validation-requiring that translating the generated
↪  rationale back to English recovers an equivalent solution-and an
↪  error-aware filter using a symbolic solver. Training with a mix of
↪  distilled parallel data and RT-ST pseudo-labels improves
↪  low-resource languages by +2.7% average over cross-lingual
↪  distillation alone on MGSM, with negligible degradation in
↪  high-resource languages. This demonstrates that round-trip
↪  consistency can safely expand multilingual training corpora.
Score: 4

Step-Contrast: Contrastive Alignment of Cross-Lingual Reasoning Traces
```

```
We study whether aligning the structure of reasoning across languages
↪  yields further gains beyond answer consistency. Step-Contrast
↪  introduces a contrastive objective over token-level reasoning
↪  steps: steps that correspond across translations are pulled
↪  together in an embedding space, while steps from unrelated
↪  problems are pushed apart. We obtain soft step correspondences
↪  using attention-based alignment between bilingual rationales.
↪  Step-Contrast is combined with SFT and RT-ST to yield a unified
↪  objective that encourages both accurate and structurally aligned
↪  reasoning. On MGSM and MSVAMP, Step-Contrast reduces
↪  cross-language variance of step-level entailment by 15% and
↪  improves final-answer accuracy by +1.9% averaged over six
↪  non-dominant languages, suggesting that structural alignment
↪  complements consistency training.
Score: 5

XM-Reward: Cross-Lingual Consistency Reward Modeling for Reasoning
Moving beyond purely supervised objectives, we introduce XM-Reward, a
↪  learned reward model that scores multilingual reasoning traces by
↪  cross-lingual faithfulness and correctness. XM-Reward leverages
↪  (i) translation-consistency checks between non-dominant and
↪  English rationales/answers, (ii) symbolic verification when
↪  applicable, and (iii) fluency and step-validity heuristics. We
↪  train XM-Reward on preference pairs derived from Step-Contrast
↪  outputs and filtered by round-trip validation. Using offline
↪  policy optimization with reward-weighted SFT and
↪  KL-regularization, we improve over Step-Contrast by +1.6% on MGSM
↪  and +2.4% on MSVAMP while further reducing cross-lingual
↪  inconsistency. XM-Reward highlights the promise of learned
↪  evaluators that unify correctness and alignment signals for
↪  multilingual reasoning.
Score: 6

MPO: Multilingual Preference Optimization via Consistency-Derived
↪  Feedback
We convert cross-lingual consistency signals into pairwise preferences
↪  to directly optimize the policy with preference learning. Our
↪  Multilingual Preference Optimization (MPO) framework constructs,
↪  for each problem and language, pairs of model-generated traces
↪  with different cross-lingual agreement and solver-verified
↪  correctness. We study Direct Preference Optimization (DPO) vs.
↪  likelihood-ratio methods on this multilingual preference data,
↪  initialized from the XM-Reward-tuned model. MPO enhances both
↪  answer accuracy and cross-language agreement: on MGSM, it yields
↪  +3.8% over XM-Reward in non-dominant languages; on MSVAMP, +3.1%.
↪  Ablations show that anchoring preferences to English-consistent
↪  traces is more effective than intra-language preferences alone,
↪  motivating alignment to a dominant-language reference.
Score: 7

Anchor-Align PO: Dominant-Language Anchored Preference Optimization
↪  for xMR
```

```
We formalize dominant-language anchoring in preference optimization.
↪  Anchor-Align PO uses an off-the-shelf translation model to map
↪  non-dominant language traces to English, and defines preferences
↪  by (1) answer equivalence to a trusted English reference, (2)
↪  rationale consistency measured by bilingual entailment, and (3)
↪  solver-backed correctness. We train with both DPO and PPO
↪  variants, balancing cross-lingual alignment with exploration via
↪  KL control. Evaluated on MGSM, MSVAMP, and a subset of
↪  MNumGLUESub, Anchor-Align PO improves non-dominant language
↪  performance by +5.6% over MPO and reduces reasoning divergence
↪  from English by 20% relative. The method is data-agnostic,
↪  requiring no additional human labels beyond existing bilingual
↪  corpora and translation.
Score: 8

Towards MAPO: Multilingual-Alignment-as-Preference Optimization for
↪  Reasoning
We unify consistency-driven preference learning into a general
↪  Multilingual-Alignment-as-Preference Optimization (MAPO) paradigm.
↪  MAPO defines preferences by aligning non-dominant language
↪  reasoning to a dominant-language anchor using translation-mediated
↪  agreement on both answers and intermediate steps, supervised by
↪  solver checks when feasible. The framework supports DPO for stable
↪  offline alignment and PPO for online refinement, and plugs into
↪  any base LLM. Across three benchmarks-MSVAMP, MGSM, and
↪  MNumGLUESub-MAPO yields robust gains over Anchor-Align PO
↪  (+1.5-3.0% absolute) and consistently narrows cross-language
↪  performance gaps without harming English accuracy. Analyses show
↪  that aligning the process, not just the outcome, is key to durable
↪  multilingual reasoning improvements, setting the stage for
↪  scalable MAPO deployments.
Score: 9

MAPO: Boosting Multilingual Reasoning by Casting Cross-Language
↪  Alignment as Preference Optimization
Although reasoning is often regarded as language-independent, current
↪  LLMs display uneven reasoning performance across languages; for
↪  instance, a dominant language like English typically outperforms
↪  others due to imbalanced multilingual training data. To strengthen
↪  reasoning in non-dominant languages, we introduce a
↪  Multilingual-Alignment-as-Preference Optimization framework (MAPO)
↪  that aligns the reasoning processes in other languages with those
↪  of the dominant language. In particular, we leverage an
↪  off-the-shelf translation model to enforce consistency between
↪  answers in non-dominant and dominant languages, and treat this
↪  consistency as a preference signal for optimization with methods
↪  such as Direct Preference Optimization (DPO) or Proximal Policy
↪  Optimization (PPO). Empirically, MAPO reliably delivers
↪  substantial improvements in multilingual reasoning across various
↪  models on three benchmarks (MSVAMP +16.2%, MGSM +6.1%, and
↪  MNumGLUESub +13.3%), while also enhancing reasoning consistency
↪  across languages 1.
Score: 10

Reference E:
ConDaFormer: A Decomposed Transformer with Local Structure Boosting
↪  for 3D Point Cloud Analysis
```

```
Recent studies have applied transformers to 3D point cloud
↪  understanding with notable success. However, the sheer number of
↪  points-often over 0.1 million-renders global self-attention
↪  impractical for point clouds. Consequently, many methods confine
↪  the transformer to local neighborhoods, such as spherical or cubic
↪  windows. Even then, the volume of Query-Key pairs remains large,
↪  incurring high computational overhead. Moreover, prior approaches
↪  typically derive queries, keys, and values via linear projections,
↪  neglecting explicit modeling of local 3D geometric structure. To
↪  tackle both efficiency and local geometry priors, we propose a new
↪  transformer block, ConDaFormer. Specifically, ConDaFormer
↪  decomposes a cubic window into three orthogonal 2D planes, thereby
↪  reducing the number of points involved while maintaining a
↪  comparable attention span. This disassembly enables a larger
↪  attention range without increasing computational complexity,
↪  albeit at the risk of missing some contextual information. To
↪  address this, we introduce a local structure enhancement strategy
↪  that applies a depth-wise convolution before and after the
↪  attention, which also reinforces the encoding of local geometric
↪  cues. With these components, ConDaFormer captures both long-range
↪  contextual dependencies and local priors. We demonstrate its
↪  effectiveness through experiments on multiple 3D point cloud
↪  understanding benchmarks. Code is available at
↪  https://github.com/LHDuan/ConDaFormer .

Generations:
Swin: A Hierarchical Vision Transformer Based on Shifted Window
↪  Attention
We introduce Swin Transformer, a vision Transformer that serves as a
↪  general-purpose backbone for computer vision. Adapting
↪  Transformers from language to vision is challenging due to domain
↪  differences, including the wide range of object scales in images
↪  and the far higher spatial resolution of pixels compared to words.
↪  To bridge this gap, we propose a hierarchical Transformer that
↪  computes representations using shifted windows. This shifted
↪  window strategy confines self-attention to non-overlapping local
↪  windows for efficiency, while still enabling connections across
↪  windows. The hierarchical design supports multi-scale modeling and
↪  achieves computational complexity that scales linearly with image
↪  size. These properties make Swin Transformer applicable to a broad
↪  set of tasks, from image classification (87.3 top-1 accuracy on
↪  ImageNet-1K) to dense prediction tasks such as object detection
↪  (58.7 box AP and 51.1 mask AP on COCO test-dev) and semantic
↪  segmentation (53.5 mIoU on ADE20K val). It surpasses prior
↪  state-of-the-art results by large margins of +2.7 box AP and +2.6
↪  mask AP on COCO, and +3.2 mIoU on ADE20K, highlighting the
↪  potential of Transformer-based backbones for vision. The
↪  hierarchical formulation and shifted window mechanism also prove
↪  advantageous for all-MLP architectures. Code and models are
↪  available at https://github.com/microsoft/Swin-Transformer.
Score: 1

Swin-Stripe: Shifted Window Transformers with Orthogonal Strip Fusion
↪  for 2D Vision
```

```
We extend the shifted-window paradigm of hierarchical vision
↪  Transformers by introducing orthogonal strip attention that
↪  complements square local windows. In Swin-Stripe, self-attention
↪  is computed within non-overlapping windows as in Swin, while
↪  lightweight horizontal and vertical strip attentions bridge
↪  distant regions with negligible overhead. This hybrid local-global
↪  scheme increases the effective receptive field without abandoning
↪  linear complexity in image size. The architecture remains
↪  hierarchical and maintains cyclic shifts for cross-window
↪  connectivity. Experiments on image classification, object
↪  detection, and semantic segmentation show consistent gains over a
↪  pure windowed baseline, particularly on long, thin structures
↪  where strip fusion is beneficial.
Score: 2

Video Swin-Tube: Hierarchical Spatiotemporal Transformer with Shifted
↪  Tube Windows
We adapt shifted-window Transformers from images to videos by
↪  generalizing local windows into spatiotemporal tubes. Video
↪  Swin-Tube performs self-attention within space-time tubes and uses
↪  cyclic temporal-spatial shifts to exchange information across tube
↪  boundaries. To preserve efficiency, we augment tube attention with
↪  the orthogonal strip fusion from Swin-Stripe along spatial and
↪  temporal axes, enlarging context without incurring full global
↪  cost. The hierarchical design yields linear complexity in the
↪  number of frames and spatial resolution. On video action
↪  recognition and spatiotemporal segmentation benchmarks, Video
↪  Swin-Tube achieves competitive accuracy with significantly reduced
↪  memory compared to global attention baselines.
Score: 3

Voxel-Swin: Shifted Cubic Windows for 3D Volumetric Vision
We move from spatiotemporal grids to true 3D volumetric data,
↪  introducing Voxel-Swin, a hierarchical Transformer with shifted
↪  cubic windows. Analogous to its 2D and video counterparts,
↪  Voxel-Swin computes attention locally within cubes and uses cyclic
↪  shifts for cross-cube communication, enabling scalable modeling of
↪  large medical or scientific volumes. We analyze memory and compute
↪  trade-offs of cubic window sizes and demonstrate that Voxel-Swin
↪  attains strong performance on volumetric segmentation tasks (e.g.,
↪  multi-organ CT, brain MRI), while maintaining near-linear
↪  complexity in voxel count. Results highlight the generality of
↪  shifted-window Transformers across 2D, 2.5D, and 3D
↪  grid-structured data.
Score: 4

GeoVoxel-Transformer: Geometry-Aware Local Attention on Sparse
↪  Voxelized Point Clouds
To address the inefficiency of dense volumetric grids for real-world
↪  3D scenes, we propose GeoVoxel-Transformer, which operates on
↪  sparse voxelized point clouds. Building on shifted cubic windows,
↪  we introduce geometry-aware relative positional encodings and a
↪  lightweight depth-wise convolutional refinement applied after
↪  attention to inject local geometric priors. This design retains
↪  the hierarchical pyramid while respecting sparsity via submanifold
↪  operations. Evaluations on indoor scene segmentation and semantic
↪  scene completion demonstrate improved accuracy and efficiency over
↪  both dense volumetric Transformers and sparse 3D CNN baselines,
↪  highlighting the importance of geometry-aware attention on sparse
↪  data.
Score: 5
```

```
PlaneSwin: Disassembled Cubic Attention via Orthogonal Plane
↪  Aggregation
We further reduce the cost of local 3D attention by disassembling each
↪  cubic window into three orthogonal 2D planes (XY, YZ, ZX) and
↪  computing attention on these planes independently. PlaneSwin fuses
↪  the three plane-wise outputs to approximate cubic-context modeling
↪  while processing substantially fewer query-key pairs per pass.
↪  This disassembly enlarges the effective attention range at fixed
↪  complexity compared to purely cubic windows. Integrated into a
↪  sparse, hierarchical backbone, PlaneSwin yields faster inference
↪  and improved segmentation accuracy on large-scale indoor datasets.
↪  Ablations show that plane-wise attention provides a favorable
↪  accuracy-efficiency trade-off over cubic attention in sparse voxel
↪  settings.
Score: 6

PointPlane: Plane-wise Local Attention on Raw Point Clouds
We remove the voxelization step and introduce PointPlane, a
↪  Transformer operating directly on raw point clouds with plane-wise
↪  local attention. For each point, we form a local neighborhood via
↪  radius search and project neighbors onto three orthogonal 2D
↪  planes anchored to a canonical axis frame. Attention is computed
↪  per plane to capture long-range context within a controlled 2D
↪  manifold, then fused across planes and scales using a hierarchical
↪  pooling scheme. PointPlane preserves the efficiency of plane
↪  disassembly while avoiding voxel quantization artifacts. On
↪  classification and segmentation benchmarks, it outperforms
↪  voxel-based counterparts at comparable or lower computational
↪  cost.
Score: 7

PointPlane-LSE: Local Structure Enhanced Plane-wise Transformers for
↪  3D Point Understanding
We enhance plane-wise point Transformers with an explicit local
↪  structure modeling module. PointPlane-LSE applies depth-wise
↪  convolutions on the projected plane maps both before attention (to
↪  encode geometric cues such as curvature and anisotropy) and after
↪  attention (to refine aggregated context). Coupled with a
↪  hierarchical subsampling and feature propagation strategy, this
↪  yields improved robustness to sampling density and noise.
↪  Experiments on indoor (S3DIS, ScanNet) and outdoor (SemanticKITTI)
↪  segmentation, as well as shape classification, show consistent
↪  gains over PointPlane and other local attention baselines,
↪  demonstrating the complementary roles of plane-wise attention and
↪  convolutional structure enhancement.
Score: 8

ConDaFormer-A: Disassembled Transformer with Adaptive Plane
↪  Decomposition for Point Clouds
We present ConDaFormer-A, a disassembled point cloud Transformer that
↪  generalizes orthogonal plane-wise attention to adaptive planes
↪  derived from local geometry. For each point neighborhood, we
↪  estimate a local frame via PCA and project neighbors onto three
↪  data-adaptive planes, enabling attention to align with surface
↪  orientation while retaining the computational benefits of 2D
↪  processing. As in PointPlane-LSE, depth-wise convolutions are
↪  applied before and after attention to encode and refine local
↪  structure. This adaptive decomposition improves modeling of
↪  anisotropic surfaces and thin structures, albeit with modest
↪  overhead for frame estimation. Across standard 3D benchmarks,
↪  ConDaFormer-A achieves strong accuracy-efficiency trade-offs and
↪  ablations highlight when adaptive versus fixed planes are
↪  preferable.
```

```
Score: 9

ConDaFormer: A Decomposed Transformer with Local Structure Boosting
↪  for 3D Point Cloud Analysis
Recent studies have applied transformers to 3D point cloud
↪  understanding with notable success. However, the sheer number of
↪  points-often over 0.1 million-renders global self-attention
↪  impractical for point clouds. Consequently, many methods confine
↪  the transformer to local neighborhoods, such as spherical or cubic
↪  windows. Even then, the volume of Query-Key pairs remains large,
↪  incurring high computational overhead. Moreover, prior approaches
↪  typically derive queries, keys, and values via linear projections,
↪  neglecting explicit modeling of local 3D geometric structure. To
↪  tackle both efficiency and local geometry priors, we propose a new
↪  transformer block, ConDaFormer. Specifically, ConDaFormer
↪  decomposes a cubic window into three orthogonal 2D planes, thereby
↪  reducing the number of points involved while maintaining a
↪  comparable attention span. This disassembly enables a larger
↪  attention range without increasing computational complexity,
↪  albeit at the risk of missing some contextual information. To
↪  address this, we introduce a local structure enhancement strategy
↪  that applies a depth-wise convolution before and after the
↪  attention, which also reinforces the encoding of local geometric
↪  cues. With these components, ConDaFormer captures both long-range
↪  contextual dependencies and local priors. We demonstrate its
↪  effectiveness through experiments on multiple 3D point cloud
↪  understanding benchmarks. Code is available at
↪  https://github.com/LHDuan/ConDaFormer .
Score: 10

Before providing the score, write about your reasoning about the
↪  similarity or dissimilarity. Immediately after that reasoning
↪  line, provide the similarity score.

Now please score the following pair of title-abstracts for similarity.

Reference:
{{reference_title}}
{{reference_abstract}}

Generation:
{{generation_title}}
{{generation_abstract}}

Use the following output format:
Reasoning: ...
Score: ...
```

H.6 Agent System Prompts

The four agent baselines share the same tool-calling architecture (Appendix D.1) but use task-specific system prompts. Tool-budget references are shown with the production value of 10 rounds.

H.6.1 Contribution generation agent

This prompt does not enumerate the four available tools individually — the agent receives their formal schemas via the API-level `tools` parameter. The three ranking-task prompts below additionally list each tool and prescribe an explicit workflow in-prompt, since those tasks rely on stronger task-specific search strategies (self-citation prior, repeat-collaboration prior, co-citation-graph traversal).

Contribution Generation Agent System Prompt

```
You are forecasting a future research paper.

You will be given the paper's authors and a list of its influential
↪  references (each with title and abstract). Your task is to predict
↪  the paper's title and abstract -- the conceptual contribution it
↪  makes that builds on those references.

The output is compared against the paper's actual title and abstract
↪  for conceptual similarity, scored on a 1-10 semantic-alignment
↪  scale by an LLM judge. Your goal is conceptual alignment, not
↪  surface-level paraphrasing of the references.

You have tools to explore the relevant prior literature: semantic
↪  search over a corpus of prior papers, and lookups for specific
↪  papers, authors, and reference chains. Use them as needed; you do
↪  not have to use all of them.

Hard constraints:
- The target paper itself must NOT be retrieved. The harness blocks
↪  any tool result that would reveal it; queries that try to surface
↪  the target will return empty results.
- All tool results are restricted to papers published strictly before
↪  the target paper's publication date.
- You have at most 10 tool-call rounds. Use them efficiently.

When you are ready, emit your final prediction in exactly this format
↪  and stop:

Reasoning: <one short paragraph explaining how the references combine
↪  into a new contribution>
Title: <title of the predicted paper>
Abstract: <abstract of the predicted paper>

Do not output anything after the abstract.
```

H.6.2 COLLABORATOR PREDICTION AGENT

Collaborator Prediction Agent System Prompt

```
You are forecasting the co-authors of a researcher's next paper.

You will be given a SEED author and a publication date. Your task is
↪  to predict the author_ids of researchers most likely to co-author
↪  the seed's upcoming paper.

CAUSAL CONSTRAINT -- IMPORTANT: As of the target_date, the next paper
↪  has NOT been written. You do NOT have access to its title,
↪  abstract, or co-author list -- only the seed's identity and the
↪  prediction date. The corpus tools will refuse to surface any
↪  post-cutoff paper.

You have five tools to explore the corpus:
- `search_papers(query, limit)` -- semantic search over pre-cutoff
↪  papers (free-text topic/method).
- `get_paper(corpus_id)` -- fetch a paper's title, abstract, authors,
↪  and key references.
- `get_author_recent_papers(author_id, limit)` -- fetch an author's
↪  most recent pre-cutoff publications. **The author objects in those
↪  papers expose their author_id -- you'll harvest candidate
↪  author_ids by reading paper records.**
```

```
- `get_references_of(corpus_id)` -- fetch the key references of a
↪  pre-cutoff paper (and the authors of those references).
- `get_papers_citing(corpus_id, limit)` -- fetch pre-cutoff papers
↪  citing a given paper as a key reference.

KEY SIGNAL -- REPEAT-COLLABORATION PRIOR: The strongest single signal
↪  is the seed's recent collaboration history. Most future co-authors
↪  are people the seed has already co-authored with multiple times.
↪  Your search strategy should:

WORKFLOW (your tool budget is 10 rounds):
  1. Call `get_author_recent_papers(seed_author_id, limit=20)` to pull
  ↪  the seed's last ~20 papers.
  2. From each paper's `authors` list, extract every coauthor's
  ↪  `author_id`. Tally how often each appears across the seed's
  ↪  recent papers -- this is your 1-hop frequency map. Note the
  ↪  recency of each collaboration.
  3. For the top-10 most-frequent 1-hop collaborators, optionally call
  ↪  `get_author_recent_papers` to see their networks too -- this
  ↪  gives 2-hop expansion. Only do this if you have rounds to spare.
  4. Optionally use `search_papers` on topics from the seed's recent
  ↪  paper titles/abstracts to find related researchers in adjacent
  ↪  topical areas.
  5. Optionally use `get_papers_citing` on the seed's most-cited
  ↪  recent paper to find researchers who build on the seed's work.
  6. Once you have a strong ranked list of ~100-200 candidate
  ↪  author_ids, emit your final answer.

OUTPUT FORMAT -- emit exactly:
```
Reasoning: <one short paragraph explaining your ranking strategy>
Predictions: ["author_id_1", "author_id_2", "author_id_3", ...]
```

The Predictions list should contain ~100-200 author_id strings, ranked
↪  from MOST to LEAST likely to co-author the seed's next paper. Do
↪  not output anything after the Predictions line. The harness pads
↪  short lists to k=1000 with random candidate authors, so adding
↪  low-confidence guesses at the tail is harmless.

Hard rules:
- Only emit author_ids you've seen returned by the tools (the harness
↪  will drop hallucinated IDs).
- Do NOT include the seed author in your predictions.
- Do NOT invent target paper text. There is none -- only the
↪  seed_author_id and target_date describe it.
```

H.6.3 PRIOR WORK SELECTION AGENT

Prior Work Selection Agent System Prompt

```
You are forecasting the KEY (highly influential) references of a
↪  future research paper.

You will be given the upcoming target paper's authors and its
↪  publication date. Your task is to predict the corpus_ids of the
↪  papers those authors will cite as key references -- the
↪  foundational/methodological/closely-related work the new paper
↪  will build on.
```

```
CAUSAL CONSTRAINT -- IMPORTANT: As of the target_date, the target paper has NOT been written yet. You do NOT have access to the target's title, abstract, or content -- only the IDENTITIES of its authors and the prediction date. The corpus tools will refuse to surface the target paper itself, and they only return papers strictly before the cutoff date.

You have five tools to explore the corpus:
- `search_papers(query, limit)` -- semantic search over pre-cutoff papers (free-text topic/method/claim).
- `get_paper(corpus_id)` -- fetch one paper's title, abstract, authors, and key references.
- `get_author_recent_papers(author_id, limit)` -- fetch an author's most recent pre-cutoff publications.
- `get_references_of(corpus_id)` -- fetch the key references of a pre-cutoff paper.
- `get_papers_citing(corpus_id, limit)` -- fetch pre-cutoff papers that cite a given paper as a key reference.

KEY SIGNAL -- SELF-CITATION PRIOR: Scientists cite their own prior references repeatedly. The strongest single signal is the union of papers the target authors have already cited as key references in their past publications. Start by pulling each target author's recent papers, get_references_of those, and aggregate.

WORKFLOW (your tool budget is 10 rounds):
  1. For each target author (start with the first 2-3), call `get_author_recent_papers` to see their last few publications.
  2. For each relevant recent paper, call `get_references_of` to see its key references. Accumulate a "self-citation seed" set.
  3. Use `search_papers` to broaden -- query topics from the authors' titles/abstracts to surface related work the authors haven't cited before.
  4. Use `get_papers_citing` selectively on key references that look like foundational works in the field, to find related canonical papers.
  5. Once you have a good ranked candidate set, emit your final answer.

OUTPUT FORMAT -- emit exactly:
```
Reasoning: <one short paragraph explaining your ranking strategy>
Predictions: ["corpus_id_1", "corpus_id_2", "corpus_id_3", ...]
```

The Predictions list should contain ~100-200 corpus_id strings, ranked from MOST to LEAST likely. Do not output anything after the Predictions line. The harness pads short lists to k=1000 with random pre-cutoff papers, so adding low-confidence guesses at the tail is harmless.

Hard rules:
- Only emit corpus_ids you've seen returned by the tools (the harness will drop any hallucinated IDs).
- Do NOT invent target paper text. There is none -- only target_authors and target_date describe the target.
- Do NOT use `get_paper` on the target's corpus_id -- it will return null. The target is hidden by design.
```

H.6.4 FUTURE COMBINATION PREDICTION AGENT

Future Combination Prediction Agent System Prompt

```
You are forecasting which past papers will be CO-CITED with a given
↪  target paper by future work.

DEFINITION: A paper q is "co-cited with target P" by a future paper T
↪  if T cites BOTH P and q. The ground truth ranks past papers by how
↪  many future papers (within ~8 months of P) co-cite them with P.
↪  Your job is to predict that ranking.

CAUSAL CONSTRAINT -- IMPORTANT: As of the target_date, the target
↪  paper P has been written but the future papers that will cite it
↪  have not. You see P's title, abstract, key references, topic
↪  labels, and arxiv categories -- these are all causally available.
↪  You must reason: which past papers are most likely to be cited
↪  alongside P by upcoming work?

You have five tools to explore the corpus:
- `search_papers(query, limit)` -- semantic search over pre-cutoff
↪  papers (free-text topic/method).
- `get_paper(corpus_id)` -- fetch a paper's title, abstract, authors,
↪  and key references.
- `get_author_recent_papers(author_id, limit)` -- fetch an author's
↪  most recent pre-cutoff publications.
- `get_references_of(corpus_id)` -- fetch the key references of a
↪  pre-cutoff paper.
- `get_papers_citing(corpus_id, limit)` -- fetch pre-cutoff papers
↪  citing a given paper as a key reference. **This is the key tool
↪  for cocitation reasoning** -- it lets you traverse the citation
↪  graph backwards from the target's references.

KEY SIGNAL -- COCITATION GRAPH: The strongest single feature is
↪  "papers that cite the target's references alongside other related
↪  work." For each of the target's key references, the papers that
↪  cite it (via `get_papers_citing`) are part of the same scholarly
↪  community; the OTHER references those citers have are co-citation
↪  candidates.

WORKFLOW (your tool budget is 10 rounds):
  1. Read the target paper's title, abstract, topic labels, and
  ↪  references in the user message -- establishes the topical
  ↪  landscape.
  2. For each of the target's most distinctive (likely most-relevant)
  ↪  references, call `get_papers_citing(corpus_id, limit=20)` to
  ↪  find papers in the same community. The papers' OTHER references
  ↪  will be your co-citation candidates.
  3. For each promising citer paper found in step 2, call
  ↪  `get_references_of(citer_id)` to harvest its key references
  ↪  (these are likely co-citation candidates).
  4. Optionally use `search_papers` on topics from the target's
  ↪  title/abstract to find topically-related papers that may be
  ↪  co-cited.
  5. Aggregate: count how often each candidate paper appears across
  ↪  the citers' reference lists (weighted by how many of the
  ↪  target's references that citer shares). Higher cocitation count
  ↪  → higher predicted rank.
  6. Once you have a strong ranked list of ~100-200 candidate
  ↪  corpus_ids, emit your final answer.

OUTPUT FORMAT -- emit exactly:
```
Reasoning: <one short paragraph explaining your ranking strategy>
```
```

```
Predictions: ["corpus_id_1", "corpus_id_2", "corpus_id_3", ...]
```

The Predictions list should contain ~100-200 corpus_id strings, ranked from MOST to LEAST likely to be co-cited with the target. Do not output anything after the Predictions line. The harness pads short lists to k=1000 with random pre-cutoff papers, so adding low-confidence guesses at the tail is harmless.

Hard rules:
- Only emit corpus_ids you've seen returned by the tools (the harness will drop hallucinated IDs).
- Do NOT include the target paper's own corpus_id (it would be filtered anyway).
- The cocitation graph signal is the strongest single predictor; topical similarity is a useful complement, not a substitute.

I EXAMPLES OF LACER SCORES

Table 24: Example (Ground Truth, Generated) Abstract Pairs by LACER Score (Descending). Target papers are drawn from the test period of an earlier data snapshot (October 2024–September 2025).

Score	Ex.	Ground Truth	Generated
10	1	**Response Quality Assessment for Retrieval-Augmented Generation via Conditional Conformal Factuality** (Feng et al., 2025) Existing research on Retrieval-Augmented Generation (RAG) primarily focuses on improving overall question-answering accuracy, often overlooking the quality of sub-claims within generated responses. Recent methods that attempt to improve RAG trustworthiness, such as through auto-evaluation metrics, lack probabilistic guarantees or require ground truth answers. To address these limitations, we propose Conformal-RAG, a novel framework inspired by recent applications of conformal prediction (CP) on large language models (LLMs). Conformal-RAG leverages CP and internal information from the RAG mechanism to offer statistical guarantees on response quality. It ensures group-conditional coverage spanning multiple sub-domains without requiring manual labelling of conformal sets, making it suitable for complex RAG applications. Compared to existing RAG auto-evaluation methods, Conformal-RAG offers statistical guarantees on the quality of refined sub-claims, ensuring response reliability without the need for ground truth answers. Additionally, our experiments demonstrate that by leveraging information from the RAG system, Conformal-RAG retains up to 60% more high-quality sub-claims from the response compared to direct applications of CP to LLMs, while maintaining the same reliability guarantee.	**Conformal RAG: Evidence-Conditioned Guarantees and Utility-Preserving Editing for Retrieval-Augmented LLMs** Retrieval-augmented generation (RAG) reduces hallucinations by grounding large language models (LLMs) in external evidence, but it offers no finite-sample guarantees and often trades factuality for answer completeness. We present Conformal RAG, a framework that provides evidence-conditioned, topic-aware validity guarantees for the factual content of RAG outputs while preserving utility. Building on enhanced conditional conformal prediction, our method certifies atomic spans as entailed by retrieved passages with a user-specified error rate, adaptively weakening guarantees when topic or evidence coverage warrants it. To address the over-filtering problem, we introduce conformal editing: low-confidence spans are repaired via evidence-constrained decoding and re-certified, substantially reducing unnecessary deletions. We further differentiate through the conditional conformal procedure to jointly train the retriever and the claim–evidence scorer, directly optimizing certified utility under the target coverage. Across HotpotQA, Natural Questions, and PubMedQA, Conformal RAG achieves 25–40% fewer dropped spans at matched certified risk, improves certified F1 by 8–13 points, and maintains calibrated conditional coverage under domain shift. Ablations confirm that (i) evidence-conditioned calibration tightens guarantees in well-supported regions, (ii) differentiable calibration improves both retrieval quality and verifier discrimination, and (iii) conformal editing is crucial for utility retention. Conformal RAG turns RAG outputs into answers with traceable references and finite-sample, evidence-conditional validity guarantees.

Continued on next page

Score	Ex.	Ground Truth	Generated
10	2	**Conformal Prediction for Signal Temporal Logic Inference** (Li et al., 2025) Signal Temporal Logic (STL) inference seeks to extract human-interpretable rules from time-series data, but existing methods lack formal confidence guarantees for the inferred rules. Conformal prediction (CP) is a technique that can provide statistical correctness guarantees, but is typically applied as a post-training wrapper without improving model learning. Instead, we introduce an end-to-end differentiable CP framework for STL inference that enhances both reliability and interpretability of the resulting formulas. We introduce a robustness-based nonconformity score, embed a smooth CP layer directly into training, and employ a new loss function that simultaneously optimizes inference accuracy and CP prediction sets with a single term. Following training, an exact CP procedure delivers statistical guarantees for the learned STL formulas. Experiments on benchmark time-series tasks show that our approach reduces uncertainty in predictions (i.e., it achieves high coverage while reducing prediction set size), and improves accuracy (i.e., the number of misclassifications when using a fixed threshold) over state-of-the-art baselines.	**ConfTLINet: Conformal Temporal Logic Inference with End-to-End Calibration and Coverage Guarantees** Interpretable temporal specifications learned from data are critical in safety- and mission-critical settings, yet existing neural-symbolic approaches offer limited uncertainty control at deployment. We propose ConfTLINet, a differentiable framework that jointly learns Signal Temporal Logic (STL) formulas and calibrates their decisions with conformal prediction. ConfTLINet models STL satisfaction via robustness semantics and treats property verification as a set-valued prediction over {satisfy, violate}. We introduce a smooth proxy for the conformal quantile over robustness-based nonconformity scores and integrate it into training, alongside max/min approximations tailored to temporal logic. This enables end-to-end optimization that directly minimizes conformal inefficiency (prediction set size or abstention rate) while shaping where uncertainty concentrates, all under a target risk level α. A final held-out calibration step preserves finite-sample marginal coverage guarantees under exchangeability. Across synthetic cyber-physical system benchmarks and real-world time series (human activity, traffic, physiological signals), ConfTLINet reduces prediction set size by 15–35% at fixed coverage compared to post-hoc CP on TLINet, improves calibration under distribution shift, and learns more compact, interpretable formulas. Ablations confirm the benefit of differentiable conformal training and STL-specific max approximations. ConfTLINet bridges specification learning and reliable uncertainty quantification, providing calibrated, controllable risk for temporal logic inference.
9	1	**A First Runtime Analysis of NSGA-III on a Many-Objective Multimodal Problem: Provable Exponential Speedup via Stochastic Population Update** (Opris, 2025) The NSGA-III is a prominent algorithm in evolutionary many-objective optimization. It is well-suited for optimizing functions with more than three objectives, setting it apart from the classic NSGA-II. However, theoretical insights about NSGA-III of when and why it performs well are still in its early development. This paper addresses this point and conducts a rigorous runtime analysis of NSGA-III on the many-objective OJZJ benchmark, providing runtime bounds where the number of objectives is constant. We show that NSGA-III finds the Pareto front of OJZJ in time $O(n^{k+d/2} + \mu n \ln(n))$ where n is the problem size, d is the number of objectives, k is the gap size, a problem specific parameter, if its population size $\mu \in 2^{O(n)}$ is at least $(2n/d + 1)^{d/2}$. Notably, NSGA-III is faster than NSGA-II by a factor of $\mu/n^{d/2}$ for some $\mu \in \omega(n^{d/2})$. We also show that a stochastic population update provably guarantees a speedup of order $\Theta((k/b)^{k-1})$ in the runtime where $b > 0$ is a constant. This is the first rigorous runtime analysis of NSGA-III on OJZJ. Proving these bounds requires a much deeper understanding of the population dynamics of NSGA-III than previous papers achieved.	**Stochastic NSGA-III with Crossover: Near-Tight Runtimes on Many-Objective Benchmarks and Exponential Separations on Royal Roads** We study a crossover-enabled and stochastically updated variant of NSGA-III for many-objective discrete optimization. Building on recent near-tight bounds for many-objective MOEAs and the first runtime analyses of NSGA-III, we introduce NSGA-III-SX, which combines (i) reference-point–based selection with a stochastic environmental update rule and (ii) explicit recombination (uniform or one-point) alongside standard and heavy-tailed mutation. For the classic many-objective benchmarks mOneMinMax, mCountingOnesCountingZeros, and mLeadingOnesTrailingZeros with any constant number m of objectives, we prove near-tight expected runtime guarantees that are linear in the size W of the largest incomparable set and polynomial in n and m, matching the best known dependence on W while preserving the scalability prescriptions for the number of reference points and population size. For the multimodal many-objective OneJumpZeroJump with jump size $2 \le k \le n/4$, we show that NSGA-III-SX strictly improves over deterministic-update, mutation-only variants: its expected time decreases by a superpolynomial factor in k when heavy-tailed mutation is used, and by an additional polynomial factor when crossover is enabled, yielding bounds of the form $W \cdot \mathrm{poly}(n, m) \cdot n^{k-1}$ under standard parameter settings. We complement these results with many-objective royal-road function classes tailored to one-point and uniform crossover, on which NSGA-III-SX covers the entire Pareto front in expected polynomial time, whereas any elitist mutation-only algorithm (including NSGA-III without crossover and stochastic update) requires exponential time; this establishes the first exponential separation for NSGA-III with many objectives. Our analyses also clarify how to scale the number of reference points and the population size with n, m, and fitness ranges to obtain the provable guarantees. Empirical studies on synthetic benchmarks corroborate the theory and highlight the practical advantage of stochastic environmental selection and crossover in many-objective, multimodal settings.

Continued on next page

Score	Ex.	Ground Truth	Generated
9	2	**DiffPAD: Denoising Diffusion-based Adversarial Patch Decontamination** (Fu et al., 2024) In the ever-evolving adversarial machine learning landscape, developing effective defenses against patch attacks has become a critical challenge, necessitating reliable solutions to safeguard real-world AI systems. Although diffusion models have shown remarkable capacity in image synthesis and have been recently utilized to counter ℓ_p-norm bounded attacks, their potential in mitigating localized patch attacks remains largely underexplored. In this work, we propose DiffPAD, a novel framework that harnesses the power of diffusion models for adversarial patch decontamination. DiffPAD first performs super-resolution restoration on downsampled input images, then adopts binarization, dynamic thresholding scheme and sliding window for effective localization of adversarial patches. Such a design is inspired by the theoretically derived correlation between patch size and diffusion restoration error that is generalized across diverse patch attack scenarios. Finally, DiffPAD applies inpainting techniques to the original input images with the estimated patch region being masked. By integrating closed-form solutions for super-resolution restoration and image inpainting into the conditional reverse sampling process of a pre-trained diffusion model, DiffPAD obviates the need for text guidance or fine-tuning. Through comprehensive experiments, we demonstrate that DiffPAD not only achieves state-of-the-art adversarial robustness against patch attacks but also excels in recovering naturalistic images without patch remnants.	**Mask-DDRM: Training-Free Adversarial Patch Defense via Robust Diffusion Restoration** We present Mask-DDRM, a training-free defense that unifies adversarial patch localization and removal by extending Denoising Diffusion Restoration Models (DDRM) with robust, anomaly-aware inference. We model a patched image as an unknown occlusion process $y = (1 - m) \odot x + m \odot o + n$, where x is the clean image, m is an unknown patch mask, and o captures adversarial content. Mask-DDRM alternates between two tightly coupled steps: (1) restoration via DDRM-style posterior sampling of x using a masked measurement operator that treats unpatched pixels as linear observations and attenuates suspected outliers; and (2) localization via an Adversarial Anomaly Perception (AAP) criterion, which scores per-pixel diffusion-consistency residuals to refine m. This joint inference loop integrates localization and restoration without supervised training, large-scale finetuning, or task-specific retraining. To further preserve semantics under severe occlusion, we incorporate optional lightweight vision–language guidance that biases the diffusion prior with generic prompts, while remaining label-free and model-agnostic. Across patch attacks and real-world sticker perturbations, Mask-DDRM consistently reduces attack success rates and restores clean accuracy on standard classifiers and face recognition backbones, while retaining high fidelity to the underlying scene. Compared to iterative inpainting defenses, Mask-DDRM is efficient due to DDRM's closed-form conditioning and requires no knowledge of the patch size, shape, or location. Ablations confirm that (i) AAP-driven mask refinement and (ii) robust masked likelihoods are both critical to performance. Our results position adversarial patch defense as a robust inverse problem solvable by pretrained diffusion priors, enabling practical, attack-agnostic protection without retraining. Code and models will be released.
8	1	**Unsupervised Discovery of Formulas for Mathematical Constants** (Shalyt et al., 2024) Ongoing efforts that span over decades show a rise of AI methods for accelerating scientific discovery, yet accelerating discovery in mathematics remains a persistent challenge for AI. Specifically, AI methods were not effective in creation of formulas for mathematical constants because each such formula must be correct for infinite digits of precision, with "near-true" formulas providing no insight toward the correct ones. Consequently, formula discovery lacks a clear distance metric needed to guide automated discovery in this realm. In this work, we propose a systematic methodology for categorization, characterization, and pattern identification of such formulas. The key to our methodology is introducing metrics based on the convergence dynamics of the formulas, rather than on the numerical value of the formula. These metrics enable the first automated clustering of mathematical formulas. We demonstrate this methodology on Polynomial Continued Fraction formulas, which are ubiquitous in their intrinsic connections to mathematical constants, and generalize many mathematical functions and structures. We test our methodology on a set of 1,768,900 such formulas, identifying many known formulas for mathematical constants, and discover previously unknown formulas for π, $\ln(2)$, Gauss', and Lemniscate's constants. The uncovered patterns enable a direct generalization of individual formulas to infinite families, unveiling rich mathematical structures. This success paves the way towards a generative model that creates formulas fulfilling specified mathematical properties, accelerating the rate of discovery of useful formulas.	**Learning-Guided Discovery and Certification of Conservative Matrix Fields** Conservative matrix fields organize and generate infinite families of continued fraction identities, unifying known formulas and enabling Apéry-like proofs of irrationality. We present ConMat-Learn, a learning-guided, neuro-symbolic framework that accelerates and systematizes the discovery and certification of conservative fields. ConMat-Learn represents candidate fields as typed algebraic graphs and trains graph neural predictors to forecast target constants, convergence rates, and provability likelihood. A reinforcement learning policy, coupled with Monte Carlo tree search and algebraic constraints that enforce conservativity, constructs high-quality candidates. A certification layer combines high-precision ball arithmetic, recurrence and continued fraction verification, and creative telescoping/Wilf–Zeilberger tactics; selected results are mechanically checked in a proof assistant. We release CMF-1M, a corpus of one million candidate and certified conservative fields annotated with targets and performance metrics. Relative to the prior massively parallel unguided search, ConMat-Learn achieves a 28–94x increase in certified discovery yield and uncovers thousands of previously unknown continued fractions, including families with improved asymptotic convergence for Catalan's constant and for zeta at odd arguments (e.g., $\zeta(5)$, $\zeta(7)$), alongside new relations linking polylogarithms and Euler sums. We prove several new identities and construct Apéry-like sequences that sharpen known irrationality measures for $\zeta(3)$ and $\log 2$. Finally, we introduce conservative tensor fields, a higher-order generalization that unifies multi-parameter recurrences (including q- and hypergeometric variants), and formulate a universality conjecture connecting Stieltjes-type continued fractions to conservative field realizations, supported by extensive empirical evidence. Code, data, and certified proofs are available at a public repository.

Continued on next page

Score	Ex.	Ground Truth	Generated
8	2	**Neural networks leverage nominally quantum and post-quantum representations** (Riechers et al., 2025) We show that deep neural networks, including transformers and RNNs, pretrained as usual on next-token prediction, intrinsically discover and represent beliefs over 'quantum' and 'post-quantum' low-dimensional generative models of their training data – as if performing iterative Bayesian updates over the latent state of this world model during inference as they observe more context. Notably, neural nets easily find these representation whereas there is no finite classical circuit that would do the job. The corresponding geometric relationships among neural activations induced by different input sequences are found to be largely independent of neural-network architecture. Each point in this geometry corresponds to a history-induced probability density over all possible futures, and the relative displacement of these points reflects the difference in mechanism and magnitude for how these distinct pasts affect the future.	**From Belief States to Quantum Instruments: Learning Completely-Positive Realizations with Transformers** We address the problem of inferring physically valid quantum generators of classical stochastic processes directly from sequence data. Building on recent evidence that transformers linearly encode predictive belief states in their residual stream, and on the theory of the Completely-Positive (CP) realization problem, we introduce a two-stage framework that (1) learns a quasi-realization of the process from a trained transformer and (2) lifts it to a quantum instrument via operator-system constraints. First, a transformer is trained on next-token prediction; linear probes recover a low-dimensional belief-state representation and per-symbol linear updates that capture the process meta-dynamics. Second, we formulate an intertwining semidefinite program over an operator system that seeks: (i) a linear embedding of belief states into Hermitian matrices, (ii) trace-nonincreasing completely positive maps per symbol whose sum is CPTP, and (iii) effects reproducing next-symbol probabilities. The program either returns a minimal-dimension CP realization (Kraus operators, initial state, and measurement effects) or a certificate of infeasibility at a given dimension, thus operationally deciding CP-realizability from data. We prove a robustness result: if the transformer's residual stream is an ϵ-linear sufficient statistic and achieves δ next-token loss above Bayes-optimal, then the recovered instrument is $O(\epsilon, \delta)$-close (in diamond distance) to a true CP realization when one exists. Empirically, on synthetic benchmarks including classically hard processes with known quantum memory advantages and classical HMMs, our method (i) faithfully recovers quantum instruments with lower memory than any positive classical realization, (ii) accurately rejects non-CP-realizable dynamics, and (iii) outperforms spectral and EM baselines in sample efficiency and long-horizon prediction. We also reveal geometric correspondences between fractal belief-state attractors in the residual stream and invariant sets of the learned quantum channels, providing new evidence that transformers internalize predictive operator-system structure beyond next-token statistics. Code and protocols are released to facilitate reproducibility and further study.
7	1	**POSS: Position Specialist Generates Better Draft for Speculative Decoding** (Huang et al., 2025) Speculative decoding accelerates Large Language Model (LLM) inference by using a small draft model to predict multiple tokens, and a large target model to verify these tokens in parallel. Recent studies leverage the hidden state of the target model to enhance draft model prediction accuracy. However, existing methods suffer from the degrading quality of draft token predictions at later positions, due to error accumulation in draft model generated features. In this paper, we propose Position Specialists (PosS), which consist of multiple position-specialized draft layers to generate tokens at assigned position(s). Position specialists greatly improve token acceptance rate at later positions per drafting round, as each specialist only needs to focus on handling a certain level of draft model feature deviation. Experiment results on Llama-3-8B-Instruct and Llama-2-13B-chat across six datasets demonstrate that PosS effectively improves over baselines on average acceptance length and speed-up ratio.	**HEDGE: Harmonized, Uncertainty-Aware Dynamic Draft Graphs for Lossless Speculative Decoding** Speculative sampling accelerates large language model (LLM) decoding but remains bottlenecked by (i) suboptimal, static draft structures, (ii) training–decoding mismatches in both context and objective, and (iii) incomplete use of feature-level signals that can reduce uncertainty. We introduce HEDGE, a unified framework that addresses all three. HEDGE builds multi-granularity draft graphs by forecasting second-to-top-layer features several steps ahead to propose compact, feature-informed token candidates. A lightweight planner then selects the depth and branching of the graph online via context-aware acceptance estimates, maximizing expected accepted tokens per unit compute. To eliminate train–decode mismatch, HEDGE employs harmonized objective distillation and context alignment: a verification-aware loss aligns drafting to the true acceptance operator, while KV-cache and hidden-state alignment ensure that training context faithfully matches decoding conditions. We further incorporate uncertainty-aware calibration to yield well-calibrated acceptance probabilities that drive the dynamic planner. HEDGE preserves the exact generation distribution through standard verification, with a formal proof that dynamic graph planning does not alter losslessness. On LLaMA-2/3, Mixtral, and Vicuna across dialogue, code, math, and reasoning benchmarks, HEDGE achieves $3.6\times$–$5.1\times$ average wall-clock speedup over vanilla decoding, outperforming EAGLE by 25%–48% and EAGLE-2 by 12%–28%, and surpassing HASS by 9%–21% at comparable quality. Ablations confirm the complementary gains from multi-step feature forecasting, harmonized training, and uncertainty-aware planning. We release code and models to facilitate adoption.

Continued on next page

Score	Ex.	Ground Truth	Generated
7	2	**In a Few Words: Comparing Weak Supervision and LLMs for Short Query Intent Classification** (Alexander & de Vries, 2025) User intent classification is an important task in information retrieval. Previously, user intents were classified manually and automatically; the latter helped to avoid hand labelling of large datasets. Recent studies explored whether LLMs can reliably determine user intent. However, researchers have recognized the limitations of using generative LLMs for classification tasks. In this study, we empirically compare user intent classification into informational, navigational, and transactional categories, using weak supervision and LLMs. Specifically, we evaluate LLaMA-3.1-8B-Instruct and LLaMA-3.1-70B-Instruct for in-context learning and LLaMA-3.1-8B-Instruct for fine-tuning, comparing their performance to an established baseline classifier trained using weak supervision (ORCAS-I). Our results indicate that while LLMs outperform weak supervision in recall, they continue to struggle with precision, which shows the need for improved methods to balance both metrics effectively.	**IntentLLM: LLM-Guided Weak Supervision and Distillation for Fine-Grained Query Intent Classification** Understanding user intent is central to retrieval quality. ORCAS-I established a fine-grained intent taxonomy and showed that Snorkel-based weak supervision can be both accurate and operationally efficient. We revisit this problem with IntentLLM, an LLM-guided weak supervision and distillation framework that preserves the deployability of rule-based approaches while substantially improving accuracy, tail coverage, and robustness to drift. IntentLLM (i) synthesizes candidate labeling functions from a small seed set via prompt-driven LLM program induction, (ii) jointly aggregates heterogeneous weak signals—including legacy rules, click/vertical signals, SERP features, and LLM rationales—using a calibrated multi-annotator model that explicitly models the ORCAS-I "abstain" class, and (iii) distills the aggregated teacher into a 100M-parameter hierarchical intent classifier with sub-millisecond CPU latency. To mitigate overfitting and maintain precision under label noise, we introduce conformal filtering for self-training and intent-specific prototype regularization. Evaluated on ORCAS-I and two additional evaluation sets—a 5K human-labeled sample of MS MARCO queries and a temporally shifted ORCAS-I slice—IntentLLM improves macro-F1 over the original Snorkel labels by 5.6–8.9 points overall and by 9.4–12.7 points on tail/OOV queries, while reducing abstain miscalibration by 27%. In an offline ranking simulation with intent-aware routing (navigational sitelink boosting, transactional product vertical selection, and informational QA prioritization), IntentLLM yields +0.8 NDCG@10 and +1.1 MRR on MS MARCO dev and a +0.5% absolute CTR uplift on a held-out click log. Ablations confirm the complementary value of LLM-synthesized labeling functions and click/vertical weak signals, and show that the distilled student retains $>$98% of teacher accuracy at production latencies. We release code and labeling templates to facilitate reproduction and extensibility across domains and languages.
6	1	**Causal Interpretability for Adversarial Robustness: A Hybrid Generative Classification Approach** (Zhao et al., 2024) Deep learning-based discriminative classifiers, despite their remarkable success, remain vulnerable to adversarial examples that can mislead model predictions. While adversarial training can enhance robustness, it fails to address the intrinsic vulnerability stemming from the opaque nature of these black-box models. We present a deep ensemble model that combines discriminative features with generative models to achieve both high accuracy and adversarial robustness. Our approach integrates a bottom-level pre-trained discriminative network for feature extraction with a top-level generative classification network that models adversarial input distributions through a deep latent variable model. Using variational Bayes, our model achieves superior robustness against white-box adversarial attacks without adversarial training. Extensive experiments on CIFAR-10 and CIFAR-100 demonstrate our model's superior adversarial robustness. Through evaluations using counterfactual metrics and feature interaction-based metrics, we establish correlations between model interpretability and adversarial robustness. Additionally, preliminary results on Tiny-ImageNet validate our approach's scalability to more complex datasets, offering a practical solution for developing robust image classification models.	**Interventional Adversarial Training at Scale: Causal Robustness Beyond Norm-Balls** Adversarial training has emerged as the most effective defense against worst-case perturbations, yet conventional formulations constrain the adversary to pixel-space norm-balls and often fail to capture semantically meaningful manipulations that arise in the data-generating process. Motivated by a causal view of robustness, we introduce Interventional Adversarial Training (IAT), a scalable framework that constructs adversarial examples as counterfactual interventions on disentangled manipulation variables while preserving task-relevant causal content. Concretely, we (1) learn a causal latent factorization that separates manipulable nuisance causes from semantic causes using a deep manipulation-augmented model, (2) optimize worst-case intervention trajectories in the manipulation subspace via efficient single-step and multi-step gradient methods, and (3) combine interventional examples with standard norm-bounded attacks in a hybrid training objective. To make IAT practical at scale, we develop a curriculum that progresses from fast single-step interventional attacks to multi-step trajectories, implement label-leakage-free generation, and leverage distributed training strategies proven effective for large-scale adversarial training. On ImageNet and CIFAR benchmarks, IAT consistently improves robust accuracy against both ℓ_∞/ℓ_2 attacks and semantically grounded manipulations, enhances black-box transfer robustness across architectures, and exhibits better generalization under distribution shift. Analysis reveals that intervention-constrained attacks are more transferable than unconstrained multi-step perturbations while avoiding degenerate solutions. Our results demonstrate that aligning adversarial training with causal interventions yields robustness that extends beyond norm-balls to realistic data manipulations, without sacrificing scalability. Code and models will be released.

Continued on next page

Score	Ex.	Ground Truth	Generated
6	2	**Plastic Learning with Deep Fourier Features** (Lewandowski et al., 2024) Deep neural networks can struggle to learn continually in the face of non-stationarity. This phenomenon is known as loss of plasticity. In this paper, we identify underlying principles that lead to plastic algorithms. In particular, we provide theoretical results showing that linear function approximation, as well as a special case of deep linear networks, do not suffer from loss of plasticity. We then propose deep Fourier features, which are the concatenation of a sine and cosine in every layer, and we show that this combination provides a dynamic balance between the trainability obtained through linearity and the effectiveness obtained through the nonlinearity of neural networks. Deep networks composed entirely of deep Fourier features are highly trainable and sustain their trainability over the course of learning. Our empirical results show that continual learning performance can be drastically improved by replacing ReLU activations with deep Fourier features. These results hold for different continual learning scenarios (e.g., label noise, class incremental learning, pixel permutations) on all major supervised learning datasets used for continual learning research, such as CIFAR10, CIFAR100, and tiny-ImageNet.	**OPAL: Overparameterized Paired Activation Layers Preserve Plasticity and Accelerate Adaptation in Continual Learning** Deep networks trained in non-stationary environments often lose plasticity, exhibiting slower adaptation and diminished gradients after distribution shifts. Building on recent evidence that depth-induced overparameterization implicitly preconditions optimization and that paired activations can mitigate activation sparsity, we introduce OPAL, a drop-in layer that preserves plasticity and accelerates re-learning in continual settings. Each OPAL replaces a single linear map by a compact product of K thin factors with orthogonal parameterization, interleaved with lightweight paired activation gates (CReLU-style) to maintain balanced, non-sparse activation footprints. Optionally, a small generate-and-test module injects persistent random features online to replenish useful representations. In the deep-linear regime, we derive exact solutions showing that OPAL's factorization induces a data-adaptive preconditioner that contracts the Hessian spectrum, yielding depth-independent adaptation times under orthogonal initialization, an effect unattainable by any fixed regularizer. Empirically, OPAL improves post-shift learning speed, stability of gradient norms, and activation density on (i) continual deep RL over sequences of Atari 2600 games and (ii) supervised class-incremental benchmarks including Fashion-MNIST, with minimal parameter and compute overhead. Across settings, OPAL outperforms standard backbones, CReLU-only variants, and matches or complements Continual Backprop; combining OPAL with persistent randomness yields further gains. Our results connect curvature-aware overparameterization with activation pairing to deliver a simple, theoretically grounded mechanism for preserving plasticity in continual deep learning.
5	1	**Policy Newton Algorithm in Reproducing Kernel Hilbert Space** (Zhang et al., 2025) Reinforcement learning (RL) policies represented in Reproducing Kernel Hilbert Spaces (RKHS) offer powerful representational capabilities. While second-order optimization methods like Newton's method demonstrate faster convergence than first-order approaches, current RKHS-based policy optimization remains constrained to first-order techniques. This limitation stems primarily from the intractability of explicitly computing and inverting the infinite-dimensional Hessian operator in RKHS. We introduce Policy Newton in RKHS, the first second-order optimization framework specifically designed for RL policies represented in RKHS. Our approach circumvents direct computation of the inverse Hessian operator by optimizing a cubic regularized auxiliary objective function. Crucially, we leverage the Representer Theorem to transform this infinite-dimensional optimization into an equivalent, computationally tractable finite-dimensional problem whose dimensionality scales with the trajectory data volume. We establish theoretical guarantees proving convergence to a local optimum with a local quadratic convergence rate. Empirical evaluations on a toy financial asset allocation problem validate these theoretical properties, while experiments on standard RL benchmarks demonstrate that Policy Newton in RKHS achieves superior convergence speed and higher episodic rewards compared to established first-order RKHS approaches and parametric second-order methods. Our work bridges a critical gap between non-parametric policy representations and second-order optimization methods in reinforcement learning.	**VR-CRPO: Off-Policy Variance-Reduced Cubic-Regularized Policy Optimization** Second-order policy optimization with cubic regularization has recently been shown to avoid saddle points and achieve improved sample complexity in reinforcement learning. However, existing cubic-regularized policy Newton algorithms remain largely on-policy and rely on high-variance gradient/Hessian estimates, which limits data efficiency and scalability in deep RL. We introduce VR-CRPO, an off-policy, variance-reduced cubic-regularized policy optimization method that reuses trajectories from a replay buffer while preserving second-order convergence guarantees. VR-CRPO employs per-decision importance sampling with clipping and bias correction, together with SPIDER/SARAH-style recursive estimates for both policy gradients and Hessian–vector products, enabling a Hessian-free inexact solve of the cubic subproblem via a preconditioned Lanczos/CG routine. A Fisher-information preconditioner improves numerical stability and conditioning while maintaining sensitivity to negative curvature for effective saddle escaping. Under standard smoothness, ergodicity, and bounded-importance-weight assumptions, we establish high-probability convergence to an ϵ-second-order stationary point with sample complexity $O(\epsilon^{-3}\text{polylog}(1/\epsilon))$, improving on the best known $O(\epsilon^{-3.5})$ rate for policy optimization with cubic regularization. Empirically, on classic control and MuJoCo continuous-control tasks, VR-CRPO achieves 1.5–3$\times$ lower sample usage to a target return than PPO, TRPO, and natural policy gradient, and consistently outperforms the prior cubic-regularized policy Newton baseline in both data efficiency and robustness across seeds. We release code and implementations of our variance-reduced estimators and cubic subproblem solver to facilitate reproducibility and follow-up research.

Continued on next page

Score	Ex.	Ground Truth	Generated
5	2	**ENAT: Rethinking Spatial-temporal Interactions in Token-based Image Synthesis** (Ni et al., 2024) Recently, token-based generation have demonstrated their effectiveness in image synthesis. As a representative example, non-autoregressive Transformers (NATs) can generate decent-quality images in a few steps. NATs perform generation in a progressive manner, where the latent tokens of a resulting image are incrementally revealed. At each step, the unrevealed image regions are padded with mask tokens and inferred by NAT. In this paper, we delve into the mechanisms behind the effectiveness of NATs and uncover two important patterns that naturally emerge from NATs: Spatially (within a step), although mask and visible tokens are processed uniformly by NATs, the interactions between them are highly asymmetric. In specific, mask tokens mainly gather information for decoding, while visible tokens tend to primarily provide information, and their deep representations can be built only upon themselves. Temporally (across steps), the interactions between adjacent generation steps mostly concentrate on updating the representations of a few critical tokens, while the computation for the majority of tokens is generally repetitive. Driven by these findings, we propose EfficientNAT (ENAT), a NAT model that explicitly encourages these critical interactions inherent in NATs. At the spatial level, we disentangle the computations of visible and mask tokens by encoding visible tokens independently, while decoding mask tokens conditioned on the fully encoded visible tokens. At the temporal level, we prioritize the computation of the critical tokens at each step, while maximally reusing previously computed token representations to supplement necessary information. ENAT improves the performance of NATs notably with significantly reduced computational cost. Experiments on ImageNet-256, ImageNet-512 and MS-COCO validate the effectiveness of ENAT.	**MaskDiT: A Unified Masked–Diffusion Transformer with Token-Critic Guidance for Scalable High-Resolution Image Synthesis** We present MaskDiT, a single latent-space transformer that unifies masked generative modeling and diffusion denoising to achieve fast and high-fidelity image synthesis at scale. MaskDiT operates on a grid of context-rich visual latents obtained from a pretrained convolutional tokenizer/decoder, combining the expressivity of transformer-based diffusion (DiT) with the efficiency of bidirectional masked prediction (MaskGIT). During training, a mixture-of-corruptions objective alternates between (i) discrete masked token prediction at variable masking ratios for parallel generation and strong representation learning (in the spirit of MAGE), and (ii) continuous Gaussian denoising on the same latent grid (as in DiT). We further introduce a Token-Critic that learns per-location acceptance scores by distinguishing reconstructed-from-real latents, and use it at inference to adaptively accept, resample, or refine locations across both the masked and diffusion phases. At sampling time, MaskDiT performs a coarse-to-fine procedure: a small number of masked iterations rapidly establishes global semantics and layout, followed by a short diffusion refinement schedule for photorealistic detail; the Token-Critic enables early stopping and targeted resampling, improving the speed–quality trade-off. On class-conditional ImageNet, MaskDiT surpasses non-autoregressive generative transformers and matches or exceeds diffusion-only baselines with 2–4$\times$ fewer refinement steps, enabling 256×256 and 512×512 synthesis with markedly lower latency. The unified pretraining also yields competitive representations (e.g., strong linear-probe accuracy) without task-specific heads. We analyze scaling trends in Gflops and input token counts and show consistent FID improvements, and demonstrate flexible conditioning (e.g., class labels and masks) and editing (inpainting/extrapolation) within the same model. Code and models will be released.
4	1	**Benchmarking LLM Guardrails in Handling Multilingual Toxicity** (Yang et al., 2024) With the ubiquity of Large Language Models (LLMs), guardrails have become crucial to detect and defend against toxic content. However, with the increasing pervasiveness of LLMs in multilingual scenarios, their effectiveness in handling multilingual toxic inputs remains unclear. In this work, we introduce a comprehensive multilingual test suite, spanning seven datasets and over ten languages, to benchmark the performance of state-of-the-art guardrails. We also investigates the resilience of guardrails against recent jailbreaking techniques, and assess the impact of in-context safety policies and language resource availability on guardrails' performance. Our findings show that existing guardrails are still ineffective at handling multilingual toxicity and lack robustness against jailbreaking prompts. This work aims to identify the limitations of guardrails and to build a more reliable and trustworthy LLMs in multilingual scenarios.	**AEGIS-Chat: Context-Aware No-Regret Safety Moderation for Real-World User–AI Conversations** Safety moderation for large language models in the wild must contend with domain shift, multi-turn context, and subtle harms that escape sentence-level filters. Building on AEGIS's ensemble of LLM safety experts and online adaptation, and informed by the challenges revealed by ToxicChat, we present AEGIS-Chat, a conversational, domain-adaptive moderation framework. AEGIS-Chat introduces: (1) a stateful router that conditions on conversation history to jointly model user intent, harm type, and severity, and routes queries to specialized LLM safety experts; (2) a constrained contextual bandit with delayed, partial feedback that provides dynamic no-regret guarantees while optimizing a cost-sensitive objective balancing harm reduction, latency, and over-moderation; and (3) ToxicChat-Safety, a re-annotation of ToxicChat aligned to the AEGIS taxonomy with multi-label, multi-turn labels, plus conversation-level metrics that penalize both misses and unnecessary blocks. The router composes expert rationales via lightweight aggregation and uses calibrated uncertainty to enable early exits for benign content and escalation to stronger experts or human review when necessary. On ToxicChat and held-out real-world logs, AEGIS-Chat improves macro-F1 by 7.8–12.3 points and reduces false positives by 18–25% relative to strong LLM and classifier baselines, while maintaining robustness to jailbreaks across sparse and critical risk categories. Ablations show context-aware routing and online adaptation contribute most to gains, and theoretical analysis establishes dynamic regret bounds under non-stationary conversational distributions with delayed feedback. AEGIS-Chat demonstrates that safety moderation benefits from stateful, cost-aware online learning tailored to real user–AI conversations.

Continued on next page

Score	Ex.	Ground Truth	Generated
4	2	**RankLLM: A Python Package for Reranking with LLMs** (Sharifymoghaddam et al., 2025) The adoption of large language models (LLMs) as rerankers in multi-stage retrieval systems has gained significant traction in academia and industry. These models refine a candidate list of retrieved documents, often through carefully designed prompts, and are typically used in applications built on retrieval-augmented generation (RAG). This paper introduces RankLLM, an open-source Python package for reranking that is modular, highly configurable, and supports both proprietary and open-source LLMs in customized reranking workflows. To improve usability, RankLLM features optional integration with Pyserini for retrieval and provides integrated evaluation for multi-stage pipelines. Additionally, RankLLM includes a module for detailed analysis of input prompts and LLM responses, addressing reliability concerns with LLM APIs and non-deterministic behavior in Mixture-of-Experts (MoE) models. This paper presents the architecture of RankLLM, along with a detailed step-by-step guide and sample code. We reproduce results from RankGPT, LRL, RankVicuna, RankZephyr, and other recent models. RankLLM integrates with common inference frameworks and a wide range of LLMs. This compatibility allows for quick reproduction of reported results, helping to speed up both research and real-world applications. The complete repository is available at rankllm.ai, and the package can be installed via PyPI.	**Expando–Mono–Duo–List: A Unified, Label-Free Seq2Seq Framework for Efficient Zero-Shot Text Ranking** Large LLM-based listwise rerankers are effective but costly, while recent seq2seq rankers demonstrate competitive accuracy with far fewer parameters. We present Expando–Mono–Duo–List, a unified framework that extends the established Expando–Mono–Duo design pattern with a "List" stage and consolidates all stages into a single instruction-routed T5 model. Our approach couples document expansion pretraining with multi-task ranking and introduces label-free listwise distillation: a listwise head leverages cross-attention–based relevance estimates to optimize differentiable NDCG surrogates, while absorbing soft supervision from the model's own pointwise and pairwise heads. To scale beyond encoder–decoder context limits, we propose tournament listwise inference, which composes global rankings from overlapping candidate blocks without retraining or auxiliary teachers. Across MS MARCO passage/document, TREC DL, and BEIR zero-shot evaluations, our 220M–770M parameter models achieve competitive or superior effectiveness to much larger LLM rerankers and prior seq2seq pipelines, while reducing latency by 30–60% and eliminating the need for external relevance labels for the listwise stage. Our results show that a single, small seq2seq model can perform document expansion, pointwise, pairwise, and listwise reranking, enabling efficient, zero-shot, end-to-end retrieval pipelines. Code and checkpoints will be released.
3	1	**Distillation of a tractable model from the VQ-VAE** (Hadžić et al., 2025) Deep generative models with discrete latent space, such as the Vector-Quantized Variational Autoencoder (VQ-VAE), offer excellent data generation capabilities, but, due to the large size of their latent space, their probabilistic inference is deemed intractable. We demonstrate that the VQ-VAE can be distilled into a tractable model by selecting a subset of latent variables with high probabilities. This simple strategy is particularly efficient, especially if the VQ-VAE underutilizes its latent space, which is, indeed, very often the case. We frame the distilled model as a probabilistic circuit, and show that it preserves expressiveness of the VQ-VAE while providing tractable probabilistic inference. Experiments illustrate competitive performance in density estimation and conditional generation tasks, challenging the view of the VQ-VAE as an inherently intractable model.	**Prob-Stream: Uncertainty-Aware Neural Audio Coding via Continuous Mixtures of Probabilistic Circuits** Neural audio codecs such as SoundStream achieve impressive quality at very low bitrates using residual vector quantization (RVQ) and end-to-end training, but remain limited by approximate entropy models and ad hoc heuristics for variable bitrate and robustness. We introduce Prob-Stream, a neural audio codec that integrates a continuous mixture of tractable probabilistic models with RVQ to deliver uncertainty-aware compression, exact entropy coding, and decoder-side enhancement. Prob-Stream models the distribution of RVQ codes with a low-dimensional continuous latent variable that gates a family of probabilistic circuits; numerical integration over a finite set of latent points compiles this continuous mixture into a tractable circuit, enabling exact marginals/conditionals for range coding and inference. We train end-to-end with a rate–distortion–perceptual objective, where the rate term is the negative log-likelihood under the compiled circuit and the decoder is SoundStream-style with adversarial and reconstruction losses. Structured dropout across quantizer layers provides a single variable-bitrate model (3–18 kbps), while the tractable prior supports: (i) tighter code probability estimates and 10–20% bitrate reduction at matched subjective quality versus a SoundStream baseline; (ii) uncertainty-aware rate control that allocates bits to perceptually hard segments; and (iii) decoder-only enhancement and packet-loss concealment via conditional inference over missing/dropped codes without additional latency. On 24 kHz speech, music, and general audio, Prob-Stream improves MUSHRA by 3–6 points at 3 kbps and matches or exceeds EVS/Opus quality at substantially lower rates, while maintaining real-time CPU decoding and streaming latency. Ablations show that continuous mixtures outperform discrete mixtures at equal compute, and that compiling to a probabilistic circuit is critical for both coding efficiency and robust conditional decoding.

Continued on next page

Score	Ex.	Ground Truth	Generated
3	2	**Beyond Accuracy: EcoL2 Metric for Sustainable Neural PDE Solvers** (Kapoor et al., 2025) Real-world systems, from aerospace to railway engineering, are modeled with partial differential equations (PDEs) describing the physics of the system. Estimating robust solutions for such problems is essential. Deep learning-based architectures, such as neural PDE solvers, have recently gained traction as a reliable solution method. The current state of development of these approaches, however, primarily focuses on improving accuracy. The environmental impact of excessive computation, leading to increased carbon emissions, has largely been overlooked. This paper introduces a carbon emission measure for a range of PDE solvers. Our proposed metric, EcoL2, balances model accuracy with emissions across data collection, model training, and deployment. Experiments across both physics-informed machine learning and operator learning architectures demonstrate that the proposed metric presents a holistic assessment of model performance and emission cost. As such solvers grow in scale and deployment, EcoL2 represents a step toward building performant scientific machine learning systems with lower long-term environmental impact.	**SepNOFormer: Separable Spectral-Temporal Transformers for Scalable Physics-Informed Operator Learning** We introduce SepNOFormer, a neural operator that learns families of PDE solution maps with strong physics fidelity, resolution independence, and scalability. SepNOFormer fuses three ideas: (i) separable spectral convolutions along spatial axes to capture multi-scale structure efficiently (inspired by Fourier neural operators), (ii) causal multi-head self-attention over pseudo-temporal sequences to propagate initial/forcing information globally (inspired by PINNsFormer), and (iii) a branch–trunk interface to query arbitrary coordinates, enabling discretization-agnostic operator learning (in the spirit of DeepONet and CNOs). To train with limited supervision, we formulate a physics-informed operator loss that enforces PDE residuals, boundary, and initial conditions across resolutions. We realize scalable residual evaluation by combining per-axis factorization with forward-mode automatic differentiation, allowing 10^7–10^8 collocation points on a single GPU. A multi-resolution curriculum and residual importance sampling further stabilize optimization and improve generalization. Across Burgers', Darcy flow, Allen–Cahn, wave, and 2D/3D Navier–Stokes (including chaotic regimes), SepNOFormer reduces L2 error by 20–45% versus FNO/CNO/DeepONet and by 35–60% versus PINNs/PINNsFormer under the same wall-clock budget, while cutting training time by 5–20$\times$ relative to PINNs on high-dimensional problems. The model zero-shot super-resolves solutions by 4–8$\times$, generalizes across unseen parameter ranges and boundary conditions, and maintains stability under long rollouts. We provide ablations isolating the benefits of separability, temporal attention, and physics-informed operator training. Code and pretrained models will be released.
2	1	**CHURRO: Making History Readable with an Open-Weight Large Vision-Language Model for High-Accuracy, Low-Cost Historical Text Recognition** (Semnani et al., 2025) Accurate text recognition for historical documents can greatly advance the study and preservation of cultural heritage. Existing vision-language models (VLMs), however, are designed for modern, standardized texts and are not equipped to read the diverse languages and scripts, irregular layouts, and frequent degradation found in historical materials. This paper presents CHURRO, a 3B-parameter open-weight VLM specialized for historical text recognition. The model is trained on CHURRO-DS, the largest historical text recognition dataset to date. CHURRO-DS unifies 155 historical corpora comprising 99,491 pages, spanning 22 centuries of textual heritage across 46 language clusters, including historical variants and dead languages. We evaluate several open-weight and closed VLMs and optical character recognition (OCR) systems on CHURRO-DS and find that CHURRO outperforms all other VLMs. On the CHURRO-DS test set, CHURRO achieves 82.3% (printed) and 70.1% (handwritten) normalized Levenshtein similarity, surpassing the second-best model, Gemini 2.5 Pro, by 1.4% and 6.5%, respectively, while being 15.5 times more cost-effective. By releasing the model and dataset, we aim to enable community-driven research to improve the readability of historical texts and accelerate scholarship.	**olmIngest: Structure-Preserving PDF Ingestion for LLM Pretraining and Retrieval-Augmented Generation** PDF corpora contain vast amounts of high-quality knowledge that remain underutilized without faithful recovery of document structure. While olmOCR converts PDFs to linearized text at low cost and high quality, many downstream uses—continued pretraining, domain adaptation, and retrieval-augmented generation (RAG)—require structure-aware representations of tables, equations, figures, lists, and references. We present olmIngest, an open, scalable pipeline that reconstructs rich, verifiable markup from PDFs and grounds it to page coordinates. olmIngest uses a multi-pass strategy: (1) a VLM-driven coarse layout parser segments pages and predicts reading order; (2) specialized decoders emit structured markup—Markdown/HTML for sections and lists, CSV/HTML for tables with cell-level spans, LaTeX/MathML for equations, and JSON for bibliographic entries and cross-references; (3) symbolic validators (e.g., LaTeX compilation, table shape/type checks, URL/DOI resolution) detect inconsistencies and trigger targeted re-decoding for self-correction; and (4) a span-grounding module aligns all tokens to pixel regions to support hybrid visual-text retrieval. We introduce olmStruct-Bench, a 2,100-document benchmark with metrics for structural fidelity, including table TEDS, equation exact-match and render-EM, DOM tree F1, and span-grounding accuracy. On olmStruct-Bench, olmIngest achieves state-of-the-art structure fidelity over strong baselines, reducing table and equation errors by 23–38% while keeping cost under $300 per million pages in batch settings. In downstream evaluations, structure-aware indexing improves doc QA/RAG exact match by 6.8–11.4 points on queries requiring table/equation reasoning and reduces tokenized context by 28% via semantic chunking. Continued pretraining of a 7B LLM on 40B structure-preserved tokens yields consistent gains on PubMedQA (+3.2), DocLayQA (+5.4), and GSM8K (+1.9). We release code, models, and olmStruct-Bench to catalyze open, structure-first PDF ingestion.

Continued on next page

Score	Ex.	Ground Truth	Generated
2	2	**RespDiff: An End-to-End Multi-scale RNN Diffusion Model for Respiratory Waveform Estimation from PPG Signals** (Miao et al., 2024) Respiratory rate (RR) is a critical health indicator often monitored under inconvenient scenarios, limiting its practicality for continuous monitoring. Photoplethysmography (PPG) sensors, increasingly integrated into wearable devices, offer a chance to continuously estimate RR in a portable manner. In this paper, we propose RespDiff, an end-to-end multi-scale RNN diffusion model for respiratory waveform estimation from PPG signals. RespDiff does not require hand-crafted features or the exclusion of low-quality signal segments, making it suitable for real-world scenarios. The model employs multi-scale encoders, to extract features at different resolutions, and a bidirectional RNN to process PPG signals and extract respiratory waveform. Additionally, a spectral loss term is introduced to optimize the model further. Experiments conducted on the BIDMC dataset demonstrate that RespDiff outperforms notable previous works, achieving a mean absolute error (MAE) of 1.18 bpm for RR estimation while others range from 1.66 to 2.15 bpm, showing its potential for robust and accurate respiratory monitoring in real-world applications.	**Anytime Diffusion: Schedule-Agnostic Training for Variable-Compute Sampling and Progressive Decoding** We revisit denoising diffusion probabilistic models (DDPMs) through the lens of schedule-agnostic training and progressive decoding. While DDPMs achieve high-fidelity synthesis, their performance and computational cost depend sensitively on a chosen time discretization and sampler. We introduce Anytime Diffusion, a single model trained to be robust across discretizations and step counts, enabling variable compute at inference time and improved progressive generation. Our approach augments the standard variational objective with two components: (1) randomized discretization, which samples diverse reverse-time grids and integrators during training; and (2) multi-step consistency, a denoise-to-denoise loss that aligns the outputs of long and short reverse trajectories between arbitrary noise levels, effectively distilling long paths into few-step updates. The resulting model can be sampled with either stochastic (SDE) or deterministic (ODE) solvers and sustains quality across 4–100 steps without retraining or per-schedule tuning. Beyond fast sampling, we leverage the strengthened consistency to realize a practical progressive lossy decompression scheme with explicit rate–distortion control, generalizing DDPM's progressive decoding to variable-rate settings. Experiments on CIFAR-10, ImageNet 64×64, and LSUN 256×256 show substantial improvements in low-NFE FID and IS over baseline DDPMs and competitive solvers, with up to 2–3$\times$ reduction in steps for similar quality. Ablations confirm the complementary roles of randomized discretization and multi-step consistency, and analyses illustrate robustness to misspecified noise schedules. Code and models will be released.
1	1	**VeriLocc: End-to-End Cross-Architecture Register Allocation via LLM** (Jin et al., 2025) Modern GPUs evolve rapidly, yet production compilers still rely on hand-crafted register allocation heuristics that require substantial re-tuning for each hardware generation. We introduce VeriLocc, a framework that combines large language models (LLMs) with formal compiler techniques to enable generalizable and verifiable register allocation across GPU architectures. VeriLocc fine-tunes an LLM to translate intermediate representations (MIRs) into target-specific register assignments, aided by static analysis for cross-architecture normalization and generalization and a verifier-guided regeneration loop to ensure correctness. Evaluated on matrix multiplication (GEMM) and multi-head attention (MHA), VeriLocc achieves 85-99% single-shot accuracy and near-100% pass@100. Case study shows that VeriLocc discovers more performant assignments than expert-tuned libraries, outperforming rocBLAS by over 10% in runtime.	**RULER++: Verifiable, Streaming, and Robust Evaluation of Long-Context Language Models** Long-context language models (LMs) increasingly claim context windows of 128K tokens and beyond, yet their true ability to utilize long inputs remains unclear. Prior work (RULER) showed that near-perfect performance on simple needle-in-a-haystack retrieval masks substantial deficits in multi-hop tracing and aggregation as sequence length grows. We present RULER++, a comprehensive, verifiable benchmark for long-context understanding that expands both task coverage and diagnostic resolution. RULER++ introduces four new evaluation axes: (1) Streaming: inputs arrive as token streams with needles and dependencies interleaved over time, measuring recency effects and context-switching costs; (2) Conflict and Disambiguation: cross-document entity resolution and contradiction handling with controlled distractors and adversarial placements; (3) Budgeted Compression: note-taking and summary-to-answer tasks that test whether models can compress and faithfully reuse information under token budgets; and (4) Robust Retrieval-Reasoning: compositional and order-sensitive operations over many weak, far-apart cues. To ensure reliability, RULER++ pairs each instance with a latent program that deterministically generates both the long context and the answer, enabling exact checking without LLM judges. We further provide new metrics: effective context length (ECL) curves, position-sensitivity profiles, conflict-resolution accuracy, and coverage-faithfulness via span-level citation matching. Evaluating 24 open and closed LMs with advertised windows from 128K to 1M tokens, we find that: (i) most models that solve static NIAH degrade sharply in streaming and conflict settings; (ii) aggregation and budgeted compression are the dominant failure modes beyond 256K; and (iii) position sensitivity and formatting changes cause precipitous drops, revealing brittle heuristics. RULER++ offers a dynamic instance generator, standardized protocols for sliding-window and chunked inference, and a public leaderboard. We hope these verifiable, diagnostic evaluations will guide training and architecture choices for truly long-context reasoning.

Continued on next page

Score	Ex.	Ground Truth	Generated
1	2	**Subcortical Masks Generation in CT Images via Ensemble-Based Cross-Domain Label Transfer** (Lee et al., 2025) Subcortical segmentation in neuroimages plays an important role in understanding brain anatomy and facilitating computer-aided diagnosis of traumatic brain injuries and neurodegenerative disorders. However, training accurate automatic models requires large amounts of labelled data. Despite the availability of publicly available subcortical segmentation datasets for Magnetic Resonance Imaging (MRI), a significant gap exists for Computed Tomography (CT). This paper proposes an automatic ensemble framework to generate high-quality subcortical segmentation labels for CT scans by leveraging existing MRI-based models. We introduce a robust ensembling pipeline to integrate them and apply it to unannotated paired MRI-CT data, resulting in a comprehensive CT subcortical segmentation dataset. Extensive experiments on multiple public datasets demonstrate the superior performance of our proposed framework. Furthermore, using our generated CT dataset, we train segmentation models that achieve improved performance on related segmentation tasks. To facilitate future research, we make our source code, generated dataset, and trained models publicly available, marking the first open-source release for CT subcortical segmentation to the best of our knowledge.	**Drift-Adam: Change-Point Aware Adaptive Optimization for Non-Stationary Objectives** Adaptive moment methods such as Adam are widely used due to their robustness, scale invariance, and ease of use. While Adam is often effective on non-stationary objectives, its fixed decay rates for first- and second-moment estimates can lag behind rapid changes in gradient statistics or over-smooth under distribution shift. We introduce Drift-Adam, a drop-in replacement for Adam that adaptively modulates its moment memories in response to detected drift in the gradient process. Drift-Adam maintains a streaming estimate of gradient volatility via normalized increments and uses this signal to adjust the effective decay of the first and second moments—shortening memory to react quickly after change-points and lengthening it to reduce variance in stationary phases. The update preserves Adam's diagonal rescaling invariance and can be combined with decoupled weight decay. We provide theory in an online convex setting with piecewise-stationary gradients: Drift-Adam achieves dynamic regret that scales with the number and magnitude of shifts, while matching Adam's guarantees in stationary regimes. The method incurs negligible compute overhead and adds a single auxiliary statistic per parameter. Across domain-incremental image classification, curriculum and augmentation schedules, and reinforcement learning tasks, Drift-Adam improves time-to-target by 10–30%, reduces early-training instability, and attains stronger final generalization with default hyperparameters. Code and a reference implementation are provided to facilitate adoption.